Modelling of Spatiotemporal EEG and ERP Brain Data for Dynamic Pattern Recognition and Brain State Prediction using Spiking Neural Networks: Methods and Applications in Psychology

Zohreh Doborjeh

A thesis submitted to

Auckland University of Technology

In fulfilment of the requirements for the degree of

Doctor of Philosophy (PhD)

2019

School of Engineering, Computer and Mathematical Sciences

Abstract

Interest in understanding neuropsychological mechanisms of human behaviour has spurred an eruption of innovative methods to measure and interpret brain activities across different fields and sectors. This includes Spatiotemporal Brain Data (STBD), such as Electroencephalogram (EEG), Event-Related Potential (ERP), Functional Magnetic Resonance Imaging (fMRI), and Magnetic Resonance Imaging (MRI) as well as sophisticated analytical methods involving statistical and experimental psychology based-techniques. Despite the rapid development of brain imaging techniques and state-of-the-art analytical tools, methods that can accurately explain dynamic patterns from spatiotemporal data in relation to brain activities are limited. Multivariate STBD is intrinsically complex as it contains both time and space dimensions that represent the patterns of cognitive processes in the brain. Analysis of STBD is a challenging task, as temporal features may manifest complex interactions that may also change dynamically over time. Most the extant analytical techniques create models by separately processing the *spatial* and *temporal* information. They also lack biological plausibility as well as model's interpretability. To overcome these limitations when dealing with spatiotemporal data, this thesis aims to develop and apply brain-inspired analytics for both dynamic pattern recognition and pattern prediction in two different types of neuroimaging data: EEG and ERP, using Spiking Neural Network (SNN) method. EEG was recorded in a study measuring the effect of mindfulness on individual well-being, while ERP was recorded when individuals were presented with marketing-related products. SNN is one of the most promising recent trends in artificial intelligence research which uses

algorithms loosely modelled on the behaviour of the human brain to recognise patterns from sets of streaming data. It incorporates both *spatial* and *temporal* characteristics of data into a computational model.

In this thesis, the pattern recognition phase includes the design of an SNN-based methodology for mapping, modelling, visualising and classifying of human brain activity patterns, measured as EEG and ERP spatiotemporal data. The pattern prediction phase involves investigation of the dynamic trajectories in the SNN models of the EEG and ERP for early prediction of the brain responses at different mental states.

In the case of neuromarketing, a brain-inspired SNN architecture is designed that tracks brain responses to marketing familiar and unfamiliar logos on the *millisecond* timescale even before conscious thoughts are formed. The results shed light on the early spikes in brain activity that correspond to stimuli awareness. This was supported by capturing the activation time and spiking intensity of neural areas involved in perceiving of familiar and unfamiliar marketing stimuli. The results suggested that familiar logos elicited more widespread brain responses than unfamiliar logos. The differences between SNN models of familiar and unfamiliar were most prominent around 200 milliseconds, but variations in brain activity could be picked up as early as 100 milliseconds after a familiar logo was shown. This resulted in obtaining a high classification accuracy of 83% which represents an average improvement of 40% when compared with conventional machine learning methods such as Support Vector Machine (SVM), Multilayer Perceptron (MLP) and Multilayer Regression (MLR). The model might be further developed to recognise patterns of choice behaviour, and as such could be used to direct marketing strategies.

In the case of mindfulness training, a brain-inspired SNN architecture is designed for investigating neural activity as a function of depression and response to mindfulness in a

nonclinical population. Investigating both spatial and temporal patterns has led to "identifying improved brain functions as a result of intervention" and "neural activation patterns that predict treatment response at the individual-levels. The SNN models identified which areas of the brain contributed to an increase in EEG (after the intervention) and also how did it happen over time. Findings support the SNN approach in distinguishing brain states associated with depression and responsiveness to mindfulness training. This study conducted in the hope of furthering our understanding of typical and disordered brains, with the overall goal to facilitate personalised approaches to intervention.

Overall, this thesis expands the field of cognitive science and artificial intelligence on three main empirical contributions: as a generic framework for dynamic pattern recognition and prediction in EEG and ERP; as a model of consumers' behaviour for detection and prediction of preference; and as a mental wellbeing application for detection and prediction of brain responses to an intervention. Future contributions are also directed into two main marketing and health-related applications.

Table of Content

Abstract I

List of Figures I

List of Tables V

List of Abbreviations I

Attestation of Authorship III

Acknowledgements IV

Chapter 1 Introduction 1

1.1 Rational and Significance of the Study 1

1.2 Aims of the Study and Research Questions 4

1.3 Thesis Structure 6

1.4 Scientific contribution 9

1.5 Chapter Summary 11

Chapter 2 Review on EEG and ERP, and Analytical Methods 12

2.1 Introduction 12

2.2 The Human Brain and the Information Processing System 12

2.3 Review of EEG Data Used for the Study of Cognitive Activity 16

2.4 Review of ERP Data for the Study of Cognitive Activity 20

2.5 Analytical Methods for EEG and ERP STBD 24

2.6 Chapter Summary 33

Chapter 3 Spiking Neural Networks 34

3.1 Introduction 34

3.2 Brain-inspired Spiking Neural Networks 34

3.3 Chapter Summary 43

Chapter 4 Methodological Design 44

4.1 Introduction 44

4.2 A Method for Dynamic Pattern Recognition and Knowledge Representation from EEG and ERP Data based on brain-inspired SNN 45

4.3 A Method for Predictive Modelling of EEG and ERP Data to Predict Future Brain States 47

4.4 SNN Model Evaluation through Leave One Cross Validation 50

4.5 Applying the Designed SNN Methods for Real-Life Scenarios in Psychology 52

4.6 Chapter Summary 54

4.7 Contribution 55
Chapter 5 Study 1 in Psychology - Neuromarketing 56
5.1 Introduction 56
5.2 Neuromarketing and the role of sub-conscious marketing stimuli processing in Consumers' Preferences 56
5.3 Experimental Design 59
5.4 Results 64
5.5 Discussion 82
5.6 Chapter Summary 87
5.7 Contribution 88
Chapter 6 Study 2 in Psychology - Mindfulness Training 89
6.1 Introduction 89
6.2 Mindfulness Training and Brain Mental States 89
6.3 Method and Experimental design 92
6.4 Results 96
6.5 Discussion 113
6.6 Chapter Summary 120
6.7 Contribution 121
Chapter 7 Conclusion and Recommendations for Future Work 122
7.1 Introduction 122
7.2 Overview of the Thesis 122
7.3 Key Findings in Psychology 124
7.4 Empirical and Theoretical Contributions 127
7.5 Limitations of the Thesis 130
7.6 Future Direction and Implications 131
References 135
Appendix A 145
Appendix B 147
Appendix C 159

List of Figures

Figure 1-1. A bird's eye view of the relationships between the different components of interest of this thesis.....8

Figure 2-1. The neuron's structure.....15

Figure 2-2. The flow of an action potential across the axon of a neuron, including the action of Na+ and K+ gated ion channels. The figure is originally from Human Brain Book (Carter, 2014) and has been slightly modified here. 15

Figure 2-3. EEG recordings that show electrical charges resulted from the activity of brain cells. 18

Figure 2-4. EEG band frequency corresponding to signals recorded from an electrode and filtered signals into five bands including: delta, theta, alpha, beta and gamma.....19

Figure 2-5. An example of topographic mapping of brain activity under different mental activities obtained using Neuroguide software (Thatcher, 2008). (a) when subjects dealing with target stimuli; (b) when subjects dealing with non-target stimuli; and (c) when subjects dealing with neutral stimuli.....20

Figure 2-6 Experimental protocol of ERP data collection.....23

Figure 2-7. Event Related Potential (ERP) waveforms across 1100 millisecond epoch after stimuli presentation. ERP waveforms consist of a series of positive and negative voltage deflections with a peak amplitudes that is corresponding to a set of main underlying components as shown in different colours: Green colour: Early ERP component (including N100, P100, P200 and N200); Blue: P300 (the most common component across studies); and Pink: Late ERP Component (related to the cognitive processing of the stimulus).....23

Figure 2-8. Analytical methods for STBD, summarised in two aspects: statistical and AI-based methods.....24

Figure 2-9. A diagram of a simple ANN with three input neurons, three hidden layers, and one output neuron.....30

Figure 3-1 a) Structure of a biological neuron which receives input information across axon terminals and processes it; (b) Picture of a simulated artificial spiking neuron with the model of Leaky-Integrate-Fire (LIF); (c) Functionality of LIF model using an input spike sequence (upper spike train), the output emitted spikes (middle spike train) and the changes of post-synaptic potential. 36

Figure 3-2. The NeuCube SNN architecture, which contains several modules: input spike-time data encoding; a 3D SNN reservoir for unsupervised learning; a SNN classification/regression module using RO and STDP for supervised learning; gene regulatory network (GRN) as a system parameter optimisation model (optional and not used in the current thesis).....37

Figure 3-3. An example of encoding EEG data into sequence of positive (black) and negative spikes (red) using the TBR algorithm that is the format of the input data into the SNN architecture. The image shows 500 EEG data time points of electrode CZ from one subject. 38

Figure 4-1. (a) An example of sequentially activated areas in a clusters of neurons (circles) as a trajectory of deep-learned patterns in the SNN models showing changes of spiking activity every 50 millisecond; (b) The connections of the trained SNN models. 48

Figure 4-2. The trajectory of functional pathway as deep knowledge, representing a sequence of four events at times t1 …,t4 that are executed as 4 large cortical locations in a sequence of 4 aggregated time segments. 49

Figure 4-3. The connectivity of SNN models trained on two conditions (a and b) measured by EEG data. (c) the differences in connectivity between the SNN models (a) and (b) reflecting the spatiotemporal differences between mental state condition. 49

Figure 4-4. Iterative SNN modelling through the leave-one-out method. For n samples, the SNN model is initialised n times, and trained by a fold of different (n-1) samples. Then the trained model is cross-validated by the hold-out sample. 51

Figure 5-1. The SNN architecture performs as follows: encoding EEG data as spike sequences; mapping of these sequences into a 3D SNN model created with the use of a brain template; unsupervised learning of the spike sequences in the SNN model; supervised learning and classification of the learned patterns in a SNN classifier. 62

Figure 5-2. Grand average ERP waveforms of all participants across 800-milliseconds epoch after familiar versus unfamiliar marketing stimuli presentation. Peak amplitudes correspond to the P100, N100 and P200 components of ERPs across the EEG channels located at posterior areas of the brain (O1, O2, P3 and P4 channels). Black line = familiar logos; red line = unfamiliar logos. 67

Figure 5-3. A pareto chart showing distribution of early ERP (P1, P2 and N1) components across five sites of the brain (Frontal, Temporal, Central, Parietal and Occipital) for both familiar and unfamiliar stimuli that represented in descending order by bars. The left vertical axis is the mean amplitude values. The right vertical axis is the cumulative percentage of the total values of the variables. It shows early ERP components are mostly distributed with higher amplitudes across the posterior regions of the brain (Occipital and Parietal-highlighted in yellow color) in compared with other sites of the brain (highlighted in pink color). 68

Figure 5-4. Clustering of EEG channels into five sites for both hemisphere (left and right) with respect to their topological information including: Left Frontal (Fp1 and F3); Right Frontal (Fp2 and F2); Left Central (C3); Right Central (C4); Left Temporal (F7, T3 and T5); Right Temporal (F8, T4 and T6); Left Parietal (P3); Right Parietal (P4); Left Occipital (O1); and Right Occipital (O2). 69

Figure 5-5. The mean amplitude values of early ERP components (P1, P2 and N1) towards familiar and unfamiliar stimuli at Frontal, Parietal, Central, Temporal and Occipital. Green line corresponding to the unfamiliar stimuli and blue line representing the familiar stimuli. 70

Figure 5-6. Neuronal connections created during learning in the SNN models, reflecting the dynamic patterns of EEG data corresponding to different epoch lengths: (a) 100ms, (b) 150ms and (c) 200ms after presentation of familiar marketing logos. Excitatory connections are represented by blue lines, while inhibitory ones are in red. The thicker the line, the greater the enhancement of the connection captured after the learning process. Neurons in the SNN models are labelled by eight brain areas from the Talairach template: Temporal (pink), Parietal (light-blue), Frontal (yellow-green), Sub-lobar (orange), Cerebellar (light yellow), Limbic (green), Pituitary (blue) and Occipital (red). The connection weights are averaged and reported for each SNN model. For a clear visualisation, we only visualised the connection weight greater than 0.08. The pictures show that familiar stimuli result in a higher connectivity and higher connection weights at average. 74

Figure 5-7. Neuronal connections created during learning in the SNN models, reflecting the dynamic patterns of EEG data corresponding to different epoch lengths: (a) 100ms, (b) 150ms and (c) 200ms after presentation of unfamiliar marketing logos. Excitatory connections are represented by blue lines, while inhibitory ones are in red. The thicker the line, the greater the enhancement of the connection captured after the learning process. Neurons in the SNN models are labelled by eight brain areas from the Talairach template: Temporal (pink), Parietal (light-blue), Frontal (yellow-green), Sub-lobar (orange), Cerebellar (light yellow), Limbic (green), Pituitary (blue) and Occipital (red). The connection weights are averaged and reported for each SNN model. For a clear visualisation, we only visualised the connection weight greater than 0.08. The pictures show that familiar stimuli result in a higher connectivity and higher connection weights at average. 75

Figure 5-8 Clusters of active neurons (spiking) in the 3D SNN models are illustrated for every 50ms while learning from the input EEG data streams of (a) familiar logos and (b) unfamiliar ones. The value A refers to the number of active neurons at each time frame. 77

Figure 5-9. Spatiotemporal patterns of activities in the trained SNN models shown as trajectories of 4 aggregated stages (t1=50, t2=100, t3=150 and t4=200ms) during learning in the SNN models for (a) familiar logos versus (b) unfamiliar logos. In fact, the time for a deep-learning step in the SNN model is a millisecond, and the actual activation trajectories (chains) in the SNN are 200 neuronal clusters long, but here the activity of only 4 steps of learning are visualised. 79

Figure 5-10 the levels of spike activation 79

Figure 6-1. A block diagram of the methodology, consisting of: encoding EEG data into spike sequences; a brain-inspired 3D SNN structure for data mapping; learning; visualisation in 3D SNN; and output classification of patterns. 94

Figure 6-2. SNN connectivity trained on EEG samples that measured at T1 (before MT) and T2 (after MT), related to (a) non-depressed group (ND), (b) responsive-depressed group (D^+) and (c) unresponsive-depressed group (D^-). 99

Figure 6-3. Differences between the connectivity in the trained SNN models of T1 (prior to MT) and T2 (post-training) in (a) non-depressed (ND) group, (b) responsive-depressed (D+) group, and (c) unresponsive-depressed (D-) group. The connections in each neural cluster represent the areas of main changes in the EEG data at post-MT. 100

Figure 6-4. The Feature Interaction Network (FIN) captured the total spike interaction between the areas in the SNN models representing 62 EEG channels as input neurons during the STDP learning for: (a) non-depressed (ND); (b) responsive-depressed (D^+); and (c) unresponsive depressed (D^-). FIN nodes represent the input neuronal areas of the SNN model and lines represent the amount of spike transmission between these areas (clusters) of neurons that correspond to the input neurons (EEG channels. 101

Figure 6-5 Spatiotemporal connectivity generated in the SNN models for responsive-depressed (D+) participants. The SNN models are visualised in both 3D (x, y, z) and 2-D (x, y) projections for the Delta frequency sub-band at T1 and delta at T2. 102

Figure 6-6. Spatiotemporal connectivity generated in the SNN models for responsive-depressed (D+) participants. The SNN models are visualised in both 3D (x, y, z) and 2-D (x, y) projections for the Theta frequency sub-band at T1 and theta at T2.....103

Figure 6-7. Spatiotemporal connectivity generated in the SNN models for responsive-depressed (D+) participants. The SNN models are visualised in both 3D (x, y, z) and 2-D (x, y) projections for the Alpha frequency sub-band at T1 and alpha at T2. 104

Figure 6-8. Spatiotemporal connectivity generated in the SNN models for responsive-depressed (D+) participants. The SNN models are visualised in both 3D (x, y, z) and 2-D (x, y) projections for the Beta frequency sub-band at T1 and beta at T2.....106

Figure 6-9. Histogram of the number of connections and the connection weights in the SNN models for the D^+ group trained on data corresponding to four EEG frequency sub-bands before (T1) and after (T2) mindfulness training. (a) Delta, (b) Theta, (c) Alpha, and (d) Beta.....106

Figure 6-10. Clustering of EEG channels into five sites for both hemisphere (left and right) with respect to their topological information including: Left Frontal (Fp1, AF3, F5,F3 and F1); Right Frontal (Fp2, AF4, F6, F4 and F2); Left Frontocentral (FC5, FC3, FC1, C5, C3 and C1); Right Frontocentral (FC6, FC4, FC2, C6, C4 and C2); Left Temporal (F7, FT7, T7 and TP7); Right Temporal (F8, FT8, T8, TP8); Left Centroparietal (CP5, CP3, CP1, P7, P5, P3, P1); Right Centroparietal (CP6, CP4, CP2, P8, P6, P4 and P2); Left Occipitoparietal (PO7, PO5, PO3,O1 and CB1); and Right Occipitoparietal (PO8, PO6, PO4, O2 and CB2). 111

Figure 6-11. The SNN connection weights prior to MT (T1) and after following 6 weeks of training (T2) in (a) ND group, (b) D^+ group and (c) D^- group at Frontal, Temporal, Frontocentral, Centroparietal and Occipitoparietal clusters. Blue line represents the connectivity values in the SNN model of T1 (before mindfulness training) and green line represents T2 (after the mindfulness training). 112

List of Tables

Table 5-1. The mean amplitude of early ERP components (P100, P200 and N100) for familiar and unfamiliar logos across 19 EEG electrodes, averaged for all participants. It shows higher mean amplitude across EEG channels located in posterior brain regions (P3, P4, O1 and O2) towards familiar stimuli than unfamiliar one. 71

Table 5-2. Repeated-measures ANOVA for the early ERP components P100, N100 and P200 at ($P<0.05$). 72

Table 5-3. The total number of spikes emitted by neurons at each time point for EEG epochs of 50ms, 100ms, 150ms, and 200ms. 78

Table 5-4. The activated brain areas are reported according to the numbers of activated neurons in the SNN models during learning, over time steps: 50, 100, 150 and 200ms. The level of activation is denoted as low, medium and strong. 82

Table 5-5. The classification accuracy of 120 EEG samples of familiar logos (class 1) and unfamiliar logos (class 2) are obtained using leave-one-out cross validation in a SNN model. In the confusion table, the rows are the real values and the columns are the predicted values. 82

Table 5-6. The classification accuracy of EEG data using Multilayer Perceptron (MLP), Multiple Linear Regression (MLR) and Support Vector Machine (SVM) through leave-one-out cross validation (computed using NeuCom at www.theneucom.com). The MLP configuration is: Number of Hidden Units: 9; Number of Training Cycles: 1800; Output Value Precision: 0.0001; Output Function Precision: 0.0001; Output Activation Function: linear. The SVM configuration is: SVM kernel: Polynomial, Degree Gamma: 1. 82

Table 6-1. The average of the connection weights for each SNN model as an activation metric for three groups of participants: non-depressed (ND); responsive-depressed (D^+); and unresponsive depressed (D^-) over two time points: before training (T1) and after training (T2). 107

Table 6-2. The average of the connection weights for each SNN model of sub-bands frequency for the responsive-depressed (D^+) group before training (T1) and after training (T2). 107

Table 6-3. Classification accuracy of 120 EEG samples (10 samples per participant) from six D^+ participants at T1 (class 1) and T2 (class 2), performed using four EEG frequency sub-bands (modelled separately). The diagonals on the confusion tables represent the correctly classified samples. Highest classification accuracy is seen for alpha (91%) and beta (85%). 107

Table 6-4. Classification accuracy of 110 EEG samples from T1 (10 samples per participant) into two classes D^+ and D- . There were six D^+ participants as class 1 and five D^- participants as class 2. This is to predict which participant is likely to response to the mindfulness at time T2 (after training) when the SNN model was only trained by the EEG data from T1. The diagonal on the confusion table represents the correctly predicted

samples. Classification accuracy is also obtained via traditional machine learning methods. The parameters of the MLP model are: number of hidden neurons 3; number of training cycles 300; output value precision 0.0001; output function precision 0.0001; output activation function - linear. The SVM model uses polynomial kernel. 108

Table 6-5. Repeated-measures ANOVA 110

List of Abbreviations

AI	Artificial Intelligence
ANN	Artificial Neural Network
ANOVA	Analysis Of Variance
AFNI	Analysis of Functional Neuro-Images
BCI	Brain computer Interface
BLAI	Brain-Like Artificial Intelligence
BOLD	Blood-Oxygen-Level Dependent
CNV	Contingent Negative Variation
EEG	Electroencephalogram
ERP	Event-Related Potential
ERN	Error-Related Negativity
ECoG	Electrocorticographic
fMRI	Functional Magnetic Resonance Imaging
ICA	Independent Component Analysis
KNN	K Nearest Neighbour
LIF	Leaky Integrate-and-Fire
MRI	Magnetic Resonance Imaging
ML	Machine Learning
MLP	Multilayer Perceptron
MLR	Multiple Linear Regression
MT	Mindfulness Training

MBI	Mindfulness-Based Intervention
MBSR	Mindfulness Based Stress Reduction
NN	Neural Network
PSP	Post-Synaptic Potential
QEEG	Quantitative electroencephalography
RO	Rank-Order
SPSS	Statistical Package for Social Sciences
SPM	Statistical Parametric Mapping
SVM	Support Vector Machine
SWC	Small World Connectivity
SW	Small World
TBR	Threshold Based Representation

Attestation of Authorship

I hereby declare that the work presented in this dissertation is my own and is, to the best of my knowledge and belief, original except as acknowledged in the text. This dissertation has not previously been submitted either in whole or in part for a degree at this or any other university.

Acknowledgements

I am deeply indebted to my primary supervisor, *Professor Nikola Kasabov* for his fundamental role in my doctoral work. I would like to thank him for encouraging my research and for allowing me to grow as a research scientist at KEDRI. His advice and support on both research as well as on my career have been invaluable.

I would also like to thank my supervisory team, *Dr. Grace Wang* and *Associate Professor Alexander Sumich* for the continuous support of my Ph.D. study and related research, for their patience, motivation, and immense knowledge. Their guidance helped me in all the time of research and writing of this thesis. I could not have imagined having a better supervisory team for my PhD study.

I would like to express my sincere gratitude to *Joyce D'Mello* who is the manager of KEDRI, for supporting me spiritually throughout writing this thesis and my life in general. Without her precious support, it would not be possible to conduct this research.

My time at KEDRI was made enjoyable in large part due to the many friends and groups that became a part of my life. I am grateful for the time spent with professional colleagues, *Dr. Elisa Capecci*, *Mrs Helena Bahrami and Associate Professor Enmei Tu* for their insightful comments and encouragement to widen my research from various perspectives.

I am also profoundly grateful to *Barry Dowdeswell* for his diligent proofreading of this thesis. He has generously reviewed, edited and enriched the study with his attentive reading.

Last but not least, I would like to thank my family for all their love and encouragement. For my parents who raised me with a love of science and supported me in all my pursuits. For my loving, supportive, encouraging, sister, brother and brother-in-law, *Mahsa*, *Milad* and *Dr Reza Enayatollahi* whose faithful support in my life and also during the final stages of this Ph.D.

This last word of acknowledgment I have saved for my lovely sister *Maryam* who has always been here for me all these years and has made them the best years of my life. For all of the advice and wise words you have provided me over the last several years and all of the incredible strength, you have forced me to see in myself. Thank you for all the sacrifice you have made, I can never bless you enough and I am forever grateful for that.

“Anything you can imagine you can create”.

Oprah Winfrey

Chapter 1 Introduction

1.1 Rational and Significance of the Study

Since the 19th century, scientists have sought to understand the formidable complexities of the highly-interconnected system that underpins our thought and behaviour (Abdullah, Khan, Basuhail, & Hussain, 2015; Bullmore & Sporns, 2009). The human brain comprises billions of interconnected cells known as neurons. These fundamental processing elements exchange information biochemically and via electrical pulses that create a spatiotemporal trajectory of sequential activities (Telesford, Simpson, Burdette, Hayasaka, & Laurienti, 2011) that culminates in our behavioural response.

Over the last few decades, a marked increase in interest in understanding neuropsychological mechanisms of human behaviour has spurred an eruption of innovative methods to measure and interpret brain activities across different fields and sectors. This includes Spatiotemporal Brain Data (STBD), such as Electroencephalogram (EEG), Event-Related Potential (ERP), Functional Magnetic Resonance Imaging (fMRI), and Magnetic Resonance Imaging (MRI) as well as sophisticated analytical methods involving statistical and experimental psychology based-techniques to make sense of data emerging from these methods.

Some examples of the commonly used neuroimaging analytical tools are Statistical Parametric Mapping (SPM) (Ashburner, 2012; Friston, Jezzard, & Turner, 1994), Analysis of Functional NeuroImages (AFNI) (Cox, 1996), , EEGLAB (Delorme, 2004), and Neuroguide (Thatcher, 2008) which contain a set of tools to perform calculate statists and graphical mapping.

Multivariate STBD is intrinsically complex as it contains both time and space dimensions that represent the patterns of cognitive processes in the brain. Analysing dynamic patterns of STBD is a challenging task, as temporal features may manifest complex interactions that may also change dynamically over time. When dealing with such complex data, statistical analysis tools often require heavy pre-processing of data such as averaging the temporal information which comes at the cost of time and information lost.

In addition, the majority of extant statistical techniques create models by separately processing the *spatial* and *temporal* information. Scrutinising the spatiotemporal interactions between variables in STBD data demands incorporating the spatial and temporal aspects into one unifying computational model.

The other crucial factor that needs to be considered is the lack of "biological plausibility" of statistical methods (Holzinger, 2016; Rätsch, Sonnenburg, & Schäfer, 2006) which refers to computational models that are inspired by the mechanisms in neurological systems. The biologically-inspired systems can contribute to a better understanding and interpretation of the STBD and the cognitive processes that generated it.

Another issue with the current analytical tools for STBD analysis is the lack of a model's interpretability. This refers to understanding the relationships between the built model and the predicted outputs. The model's interpretability allows us to comprehend why certain outcomes have resulted from the model. However, the existing analytical methods are seen as black-box information processing systems that solve a problem without discovering the causal interactions that have resulted in the output.

In the last decade, Artificial Intelligence (AI) has emerged as a fast-growing field of study for modelling the human data in several applications such as Brain-Computer Interface (BCI) (Lotte, 2007). AI technologies have shown an eminent aptitude as they can learn from sets of data to extract meaningful patterns for the purpose of regression, prediction and classification tasks (Costantini, 2009). Nevertheless, there is still a need for the development of sufficient methods that can explain the dynamic patterns from spatiotemporal data in relation to brain activities. To overcome the above-mentioned limitations, the current thesis seeks to develop and apply brain-inspired[1] analytics to STBD to overcome the above-mentioned limitations related to traditional STBD analysis, and to improve the modelling and understanding of the brain information underpinning human behaviour. This multidisciplinary research combines experiments across disciplines from cognitive psychology, neuroscience, and computer sciences.

The computational models of the brain data proposed in this thesis are based on one of the most promising trends of Artificial Neural Networks (ANN), called Spiking Neural Networks (SNN). SNN models have been developed as neurobiologically-plausible computational architecture that incorporates both *spatial* and *temporal* characteristics of data into the computation. They are considered a suitable tool for the analysis of the STBD, where both space and time components are crucial to be learnt (Izhikevich, 2006; N. Kasabov, Dhoble, Nuntalid, & Indiveri, 2013).

In view of this, the present thesis focuses on designing and applying SNN architecture for both *pattern recognition*[2] and *pattern prediction*[3] in two different types of

[1] Brain-inspired refers to the mathematical implementation of a method which gets inspiration from neuroscience research on brain activity.

[2] Pattern recognition in artificial intelligence is the process of recognising patterns by using a machine learning algorithm. Pattern recognition can be defined as the classification of data based on knowledge already gained or on statistical information extracted from patterns and/or their representation.

[3] Identifying patterns in data and using them to automatically make predictions or decisions. It is a machine learning algorithm mostly used for classification problems.

neuroimaging data: EEG and ERP. To validate the feasibility analysis of the SNN models, two real-life empirical scenarios from neuroinformatic were designed as follows:

1) SNN models of ERP in neuromarketing: Computational modelling of consumers[1] brain responses towards marketing-related products.

2) SNN models of EEG in mindfulness: Computational modelling of brain responses followed by mindfulness training.

The pattern recognition phase includes the design of an SNN-based methodology for mapping, modelling, visualising and classifying of human brain activity patterns, measured by EEG and ERP. The pattern prediction phase involves investigation of the dynamic trajectories in the SNN models of the EEG and ERP for early prediction of the brain responses at different mental states.

1.2 Aims of the Study and Research Questions

This thesis focuses on the main objectives:

- Design of SNN-based methodology for both dynamic *pattern recognition* and *pattern prediction* from EEG and ERP STBD.
- Application of the developed methods in Psychology, and more specifically in Neuromarketing and Mindfulness.

In order to perform pattern recognition and prediction in EEG and ERP dataset using SNN architectures in a real-life scenario, this thesis addresses the following specific objectives:

- In the context of neuromarketing study:

1 A consumer is the one who pays something to consume goods and services produced in a marketing environment.

- To design SNN models of brain activity patterns, measured by ERP, while consumers perceive different marketing stimuli.
- To design SNN models of ERP for prediction of early brain responses to marketing stimuli, when consumers are not consciously attending.

- In the context of mindfulness training study:
  - To elucidate discriminative patterns in SNN models of EEG at two stages: “before” and “after” mindfulness training across individuals with a different mental health condition.
  - To design SNN models of EEG data for prediction of response to mindfulness training.

Through the development of this thesis, the following research questions (RQ) will be addressed:

- **General Questions:**

Research question 1. How a SNN model can be optimally designed for dynamic pattern recognition related to different mental states?

Research question 2. How can a designed SNN discriminate neural patterns at individual-levels?

Research question 3. Can SNN models lead to knowledge discovery by creating predictive systems of brain mental states according to the dynamic/discriminate patterns?

- **Specific Questions:**

In the context of Neuromarketing study:

Research question: How can brain-inspired SNN architecture be used to investigate the spatiotemporal information flow in ERP data related to viewing familiar vs unfamiliar marketing logos? Are familiar and unfamiliar logos distinguished at a peri-perceptual[1] stage of processing? (This is addressed in Chapter 5).

- **Specific Questions:**

In the context of mindfulness training study:

Research question 1. How SNN architecture can be applied to identify discriminative patterns in EEG data related to before and after mindfulness training across individuals with different mental states? (This is addressed in Chapter 6).

Research question 2. How can SNN be used for modelling the trajectories of dynamic functional connectivity, measured by EEG, for predicting brain response to mindfulness training? (This is addressed in Chapter 6).

1.3 Thesis Structure

Figure 1-1 depicts a self-explanatory bird's eye view of the relationships between the different components of interest in this thesis. This thesis is presented in seven chapters as follows:

Chapter 1 Signifies the research motivations, aims, research questions and outlines the empirical studies to address these questions.

Chapter 2 Reviews the research on information processing in biological neurons. It also explains two relevant neuroimaging techniques for measuring STBD including EEG

[1] Peri-perceptual is the subconscious accumulation of information from the environment. All available information is pre-attentively processed. Information that has the highest salience (a stimulus that stands out the most) or relevance to what a person is thinking about is selected for further and more complete analysis by conscious (attentive) processing.

and ERP. This section is then followed by a review of both conventional[1] and AI analytical methods for STBD analysis.

Chapter 3 Introduces a brain-inspired SNN architecture as an appropriate framework for modelling both *space* and *time* components of STBD in a unifying model. This framework is employed in the current thesis for modelling and analysing of EEG and ERP data.

Chapter 4 Introduces a step-wise design of the SNN-based methodology for dynamic pattern recognition and pattern prediction using EEG and ERP data.

Chapter 5 Presents the designed in this study SNN architecture for ERP data analysis to model the complexity of the brain subconscious processes during a neuromarketing experiment while familiar and unfamiliar marketing logos were presented. This investigates how early brain processes are involved in the perception of marketing stimuli at a subconscious level and elucidates the dynamics of information processes underpinning perception.

Chapter 6 Introduces the designed in this study SNN architecture for modelling of brain activities measured by EEG (resting-state) before and after mindfulness training across participants with different mental health conditions (healthy and depression). The SNN models are used to reveal how mindfulness rewires the brain and who is more likely to benefit from this training.

Chapter 7 Summarises the thesis achievements, contributions, and key findings, as well as the future direction of this research.

[1] Conventional methods refer to methods that have been proposed for data analysis, besides neural network techniques.

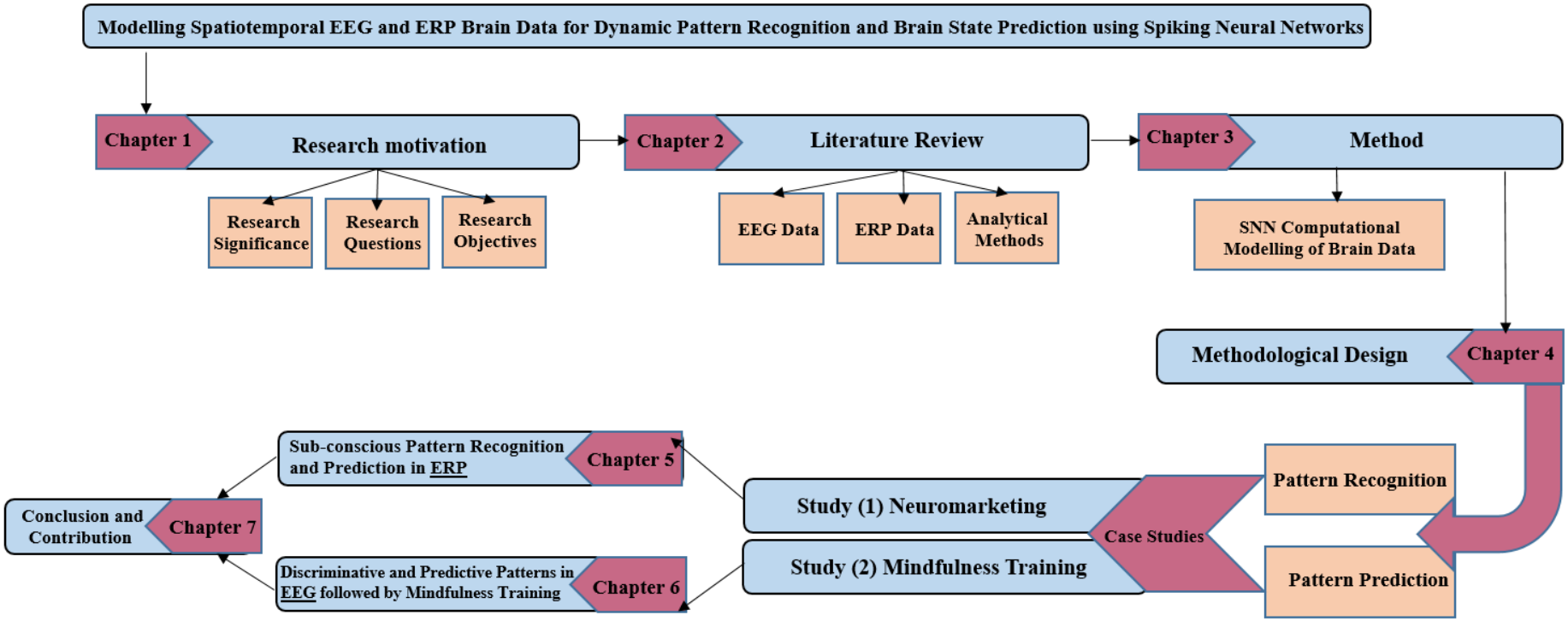

Figure 1-1. A bird's eye view of the relationships between the different components of interest of this thesis

1.4 Scientific contribution

The scientific contributions of the current thesis are as follows:

- A designed SNN-based methodology, as a generic framework for a precise analysis of different types of STBD (EEG and ERP).
- A designed SNN architecture, as a model of consumers' behaviour for detection and prediction of preference.
- A designed SNN architecture, as a mental wellbeing application for detection and prediction of mindfulness effects on STBD.

During the progression of the thesis, my contribution to science also includes peer-reviewed publications in international journals and conferences as follows:

Type	Publication	Year	My personal contribution
Journal	**Doborjeh, Z. G**., Doborjeh, M., Taylor, T., Kasabov, N., Wang, G., Sigert, R.., & Sumich, A. (2019). Spiking Neural Network Modelling Approach Reveals How Mindfulness Training Rewires the Brain. Nature Scientific reports, 9(1), 6367.	2019	EEG data collection, designing and performing the experiments, analysing and interpreting the data and writing the majority of the manuscript.
Journal	**Doborjeh, Z. G**., Kasabov, N., Doborjeh, M. G., & Sumich, A. (2018). Modelling peri-perceptual brain processes in a deep learning spiking neural network architecture. Nature Scientific reports, 8(1), 8912.	2018	EEG data collection, designing the cognitive task, performing the experiments, analysing and interpreting the data and writing of the majority of the manuscript.
Journal	**Doborjeh, Z. G**., Doborjeh, M. G., & Kasabov, N. (2018). Attentional bias pattern recognition in spiking neural networks from spatio-temporal EEG data. Cognitive Computation, 10(1), 35-48.	2018	The EEG data collection, designing the cognitive task, performing the experiments, analysing and interpreting the data and writing of the majority of the manuscript.
Journal	Doborjeh, M. G., Kasabov, N., & **Doborjeh, Z. G**. (2018). Evolving, dynamic clustering of spatio/Spectro-temporal data in 3D spiking neural network models and a case study on EEG data. Evolving systems, 9(3), 195-211.	2018	EEG data analysis, interpretation and writing part of the manuscript.
Journal	Doborjeh, M. G., **Doborjeh, Z. G**., Gollahalli, A. R., Kumarasinghe, K., Breen, V., Sengupta, N., ... & Othman, M. (2018). From von Neumann Architecture and Atanasoff's ABC to Neuromorphic Computation and Kasabov's NeuCube. Part II: Applications. In Practical Issues of Intelligent Innovations (pp. 17-36). Springer, Cham.	2018	Writing the section related to the brain data and its applications, contributed by me.
Journal	Sengupta, N., Ramos, J.I.E., Tu, E., Marks, S., Scott, N., Weclawski, J., Gollahalli, A.R., Doborjeh, M.G., **Doborjeh, Z.G**., Kumarasinghe, K. and Breen, V., 2018. From von Neumann Architecture and Atanasoffs ABC to Neuro-Morphic Computation and Kasabov's NeuCube: Principles and Implementations. In Learning Systems: From Theory to Practice (pp. 1-28). Springer, Cham.	2018	Writing the section related to the brain data and its applications, contributed by me.

Journal	Kasabov, N., Zhou, L., Doborjeh, M. G., **Doborjeh, Z. G.,** & Yang, J. (2017). New algorithms for encoding, learning and classification of fMRI data in a spiking neural network architecture: A case on modeling and understanding of dynamic cognitive processes. IEEE Transactions on Cognitive and Developmental Systems, 9(4), 293-303.	2017	Participation in brain data analysis, interpretation of results and writing part of the manuscript.
Journal	Kasabov, N. K., Doborjeh, M. G., & **Doborjeh, Z**. G. (2017). Mapping, learning, visualization, classification, and understanding of fMRI data in the NeuCube evolving spatiotemporal data machine of spiking neural networks. IEEE transactions on neural networks and learning systems, 28(4), 887-899.	2017	Participation in brain data analysis, interpretation of results and writing part of the manuscript.
Conference	**Doborjeh, Z. G**., Doborjeh, M., & Kasabov, N. (2018, July). EEG Pattern Recognition using Brain-Inspired Spiking Neural Networks for Modelling Human Decision Processes. In 2018 International Joint Conference on Neural Networks (IJCNN) (pp. 1-7). IEEE.	2018	Designing and the experiments, analysing and interpreting the data and writing part of the manuscript.
Conference	Omori, Y., Kawano, H., Seo, A., **Doborjeh, Z. G**., Kasabov, N., & Doborjeh, M. G. (2017, November). EEG Comparison Between Normal and Developmental Disorder in Perception and Imitation of Facial Expressions with the NeuCube. In International Conference on Neural Information Processing (pp. 596-601). Springer, Cham.	2017	Brain data analysis, interpretation of results and writing part of the manuscript.
Conference	Capecci, E., **Doborjeh, Z**. G., Mammone, N., La Foresta, F., Morabito, F. C., & Kasabov, N. (2016, July). Longitudinal study of alzheimer's disease degeneration through EEG data analysis with a NeuCube spiking neural network model. In 2016 International Joint Conference on Neural Networks (IJCNN) (pp. 1360-1366). IEEE.	2016	Brain data analysis, interpretation and writing the manuscript, contributed by me.
Conference	**Doborjeh, Z. G**., Doborjeh, M. G., & Kasabov, N. (2016). Efficient recognition of attentional bias using EEG data and the NeuCube evolving spatio-temporal data machine. In International Conference on Neural Information Processing (pp. 645-653). Springer, Cham.	2016	EEG data collection, designing the cognitive task, performing the experiments, analysing and interpreting the data and writing of the manuscript, contributed by me.
Conference	Kawano, H., Seo, A., **Doborjeh, Z. G**., Kasabov, N., & Doborjeh, M. G. (2016, October). Analysis of similarity and differences in brain activities between perception and production of facial expressions using EEG data and the NeuCube spiking neural network architecture. In International conference on neural information processing (pp. 221-227). Springer, Cham.	2016	Data analysis, interpretation and writing the manuscript, contributed by me.

1.5 Chapter Summary

This introductory chapter outlined the following:

- The problem and motivations of the research.
- Research aims and research questions.
- Thesis structure.
- My scientific contribution through this study

“The human brain keeps us primed to respond to the world around us. It is at the hub of a vast and complex communications network that constantly seeks and collects information from the rest of the body and the outside world. As the brain interprets this information, it generates experiences, sights, and sound, emotions and thoughts. But its primary function is to produce changes in the body. These include life-sustaining basics such as the regular contractions of the heart through to the complex actions that constitute behaviour”.

Rita Carter

Chapter 2 Review on EEG and ERP, and Analytical Methods

2.1 Introduction

The brain is one of the largest and most complex organs in the human body, comprising more than 100 billion nerves, with trillions of interconnections called synapses (von Bartheld, Bahney, & Herculano-Houzel, 2016). This chapter presents an overview of the basic components of neurons and functional brain cells (Section 2.2) that underpin complex information processing of the brain. Sections 2.3 and 2.4 will then review the two techniques, used to measure neural information processing from the scalp: EEG and ERP. These methods are used as case studies for the resolution of problems posed by STBD. Section 2.5 reviews some of the major data analysis techniques and refers to their limitations when dealing with STBD. Section. 2.6 summaries the chapter and discusses the SNN approach as one of the main techniques of this thesis for a better understanding of STBD.

2.2 The Human Brain and the Information Processing System

The human brain with a three-pound mass of grey and white matter sits at the centre of all human activity. The brain regulates the body's basic functions, enabling humans to interpret and respond to everything they experience, and shaping thoughts, emotions, and behaviour (Carter, 2014). The brain is made up of many parts that are responsible for coordinating and performing specific functions (Ackerman, 1992). The brain as a communications centre consisting of billions of neurons also called nerve cells. Neurons are the fundamental information processing units of the brain, interconnected to construct

a complex neural network (Ackerman, 1992). They use biochemical reactions to receive, process, store and transmit input information (Ackerman, 1992; Sporns, Tononi, & Kötter, 2005). A typical neuron as shown in Figure 2-1 consists of three major parts: the cell body, the dendrites, and the axon.

Neurons can be categorised structurally according to the location of the cell body in relation to the axon and dendrites, and also the number of dendrites and axon branches (Carter, 2014). In the cortex, one neuron may receive signals from many thousands of other neurons via its multitudinous branching dendrites. Signals are conducted to the soma, around this, and then away along the axon always by the cell membrane (Carter, 2014).

The cell membrane of the axon and soma contain voltage-gated ion channels that allow the neuron to generate and propagate an electrical signal. These signals are generated and propagated by charge-carrying ions including sodium (Na^+), potassium (K^+), chloride ($C1^-$), and calcium ($Ca2+$) (Ackerman, 1992). Neurons communicate by chemical and electrical synapses in a process known as neurotransmission, also called synaptic transmission. The fundamental process that triggers the release of neurotransmitters is the action potential, a propagating electrical signal that is generated by exploiting the electrically excitable membrane of the neuron. This is also known as a wave of depolarisation (Platkiewicz & Brette, 2010; von Bartheld et al., 2016). Figure 2-2 shows a slice of the soma membrane embedded with several channels for ion transportation.

As shown in Figure 2-2, when neuron stimulated by an electrical pulse, neurotransmitters of various types are released, and they cross the cell membrane into the synaptic gap between neurons. The presynaptic membrane stores neurotransmitter chemicals at the end of the axon terminals (Lodish et al., 2000), which are used to communicate with the dendrites of the neighbouring neurons and allow the transmission

of information from one sending neuron (pre-synaptic neuron) to other receiving neurons (post-synaptic neurons) (Lodish et al., 2000; Platkiewicz & Brette, 2010). The speed of the action potential is accelerated by saccadic[1] propagation from node to node separated by myelin sheaths, which offer insolation and prevent the dissipation of the depolarisation wave caused by an electrical spike triggered in the soma (Ackerman, 1992; Platkiewicz & Brette, 2010). The whole process takes less than one five-hundredth of a second. In this way, a message within the brain is converted, as it moves from one neuron to another, from an electrical signal to a chemical signal and back again, in an ongoing chain of events which is the basis of all brain activity (Carter, 2014; Kelly, 1993; Lauder, 1993; Perry, Li, & Kennedy, 2009).

A variety of techniques has been devised for recording and scanning brain dynamics, such as EEG, ERP, MRI, and fMRI. Different recording modalities have different resolutions. While some approaches have a very high temporal (time-based) resolution but a low spatial (space-based) resolution, other modalities have an opposite relation. For example, fMRI has a very good spatial specificity compared to EEG. Thus, fMRI is used to localise brain functions. In contrast, EEG has excellent temporal resolution and relatively poor spatial precision (Jeannerod, 1997). EEG provides a direct measure of electrocortical activity with millisecond precision and is sensitive to changes in arousal, perception and cognitive function (Bell, 2012). More specifically, EEG measures changes in extracellular potentials from large arrays of neurons, predominantly pyramidal cells. The time-locked EEG response to the presentation of a stimulus or behavioural response can be measured as an ERP (Luck, 2014). The principle of the EEG and ERP data will be explained in the following Section 2.3 and Section 2.4.

[1] A saccade is a quick, simultaneous movement of both eyes between two or more phases of fixation in the same direction. In terms of speed, saccades are one of the fastest movements produced by the human body (blinks may reach even higher peak velocities).

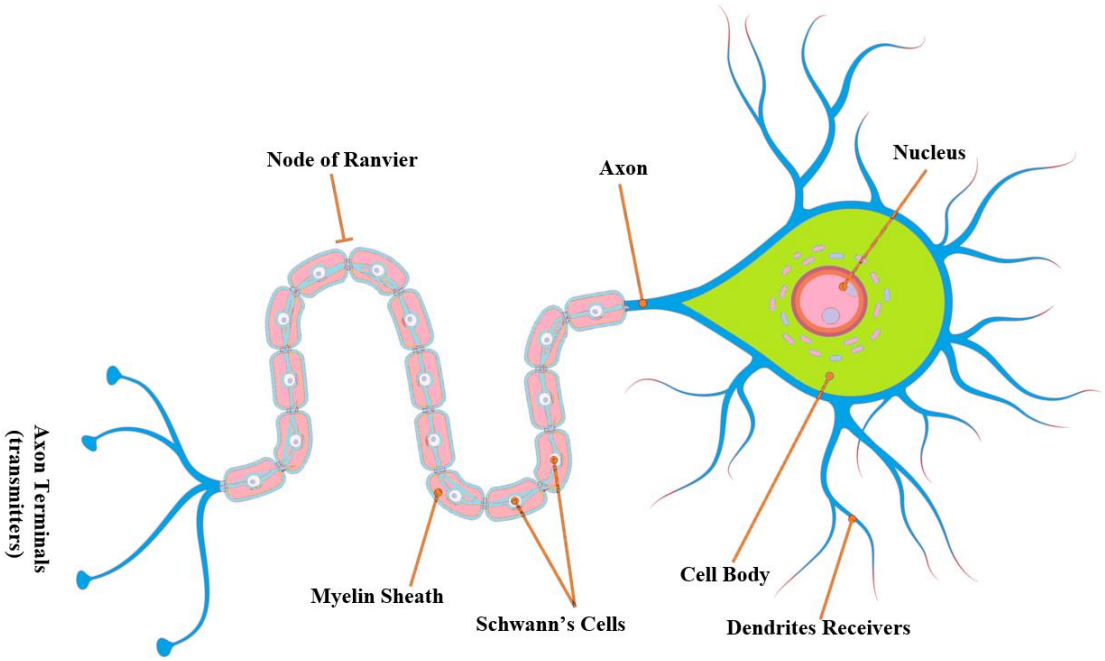

Figure 2-1. The neuron's structure.

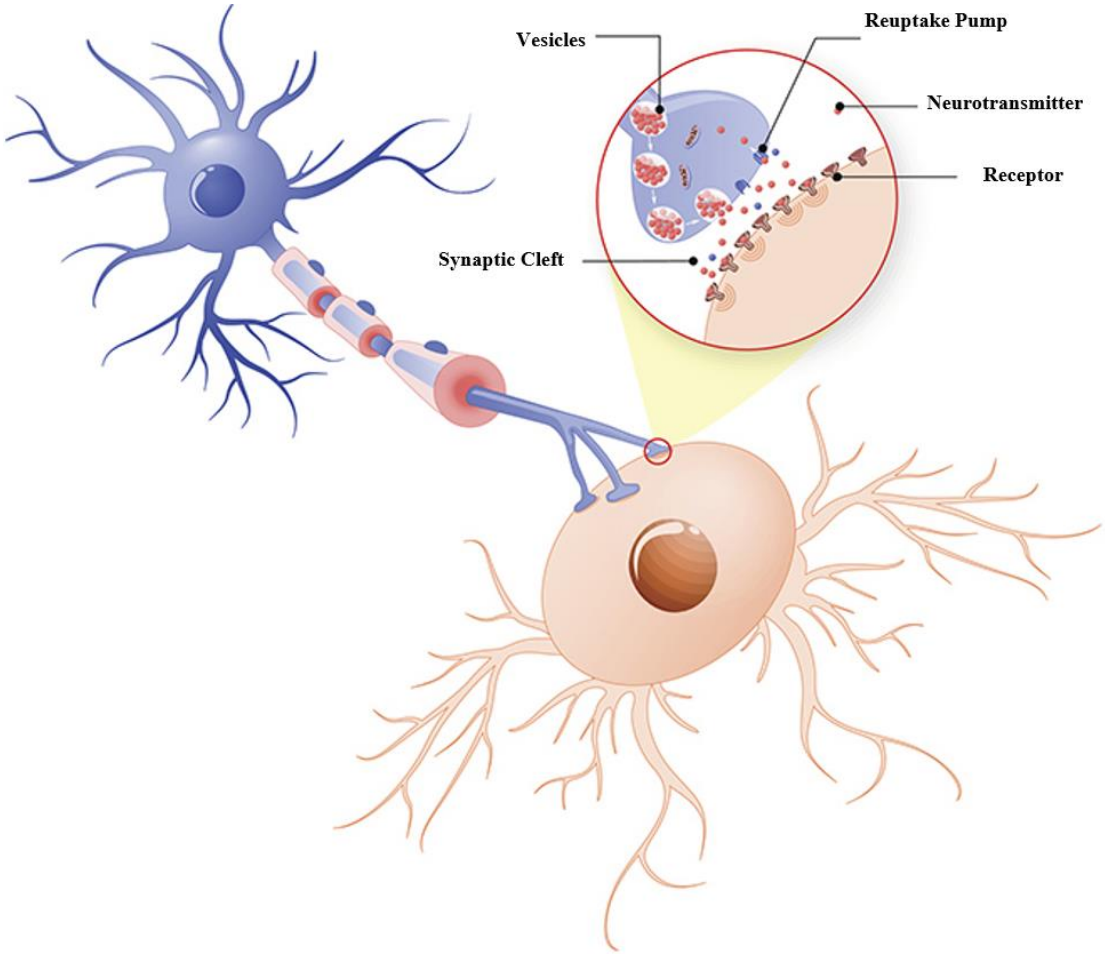

Figure 2-2. The flow of an action potential across the axon of a neuron, including the action of Na+ and K+ gated ion channels. The figure is originally from Human Brain Book (Carter, 2014) and has been slightly modified here.

2.3 Review of EEG Data Used for the Study of Cognitive Activity

The EEG measures the extra-cellular post-synaptic electrical potential from predominantly surface pyramidal cells. The gross activity from many neurons diffuses through biological tissue (e.g., skull, skin) and is reflected in alternating positive and negative potentials signals across different scalp sites using electrodes. Electrodes are distributed at specific locations, typically using so-called 10-20 system (Jasper, 1958), where 10-20 electrodes are separated 10-20% the total distance around the circumstance of the head (Niedermeyer & da Silva, 2005; W. Tatum IV, Hausain, Banbadis, & Kaplan).

Figure 2-3 shows the 10-20 electrode distribution (***left side***) and a monopolar recording of a normal subject with eyes open (***right side***). EEG can be used to measure a potential difference between an active electrode and a reference electrode. The ground electrode is used to reduce artefacts (electrical circuit, movement). The reference is the activity of a pair of linked electrodes placed at the earlobes (A_1 and A_2). As shown in Figure 2-3, the capital letters denote the different electrode locations, F for frontal, C for central, P for parietal, T for temporal, and O for occipital. Odd numbers correspond to the left side and even numbers to the right side, with z denoting centre.

EEG signal patterns vary in different cognitive states according to the voltage fluctuations resulting from ion flow between neurons. The frequency of the voltage fluctuations is measured using EEG spectra (Freeman & Quiroga, 2012).

2.3.1 EEG spectra

The EEG signal oscillation is rhythmic; thus, it is typically described in terms of bands of different frequencies as follows (Duffy, Burchfiel, & Lombroso, 1979; Gevins & Rémond, 1987; Nuwer et al., 1999; Quiroga & Schürmann, 1999):

- Alpha rhythms (7.5-12.5 Hz): they appear spontaneously in normal adults during wakefulness, under relaxation and mental inactivity conditions. They are best seen with eyes closed, most pronounced in the occipital locations.
- Beta rhythms (12.5-30 Hz): they are the best defined in central and frontal locations, with less amplitude than alpha waves. They are enhanced upon mental calculations, expectancy or tension over the entire surface of the scalp.
- Theta rhythms (3.5-7.5 Hz): they are typical during deep sleep. They play an important role in infancy and childhood. In the awake adult, high theta activity is considered abnormal and related to brain disorders, such as epilepsy.
- Delta rhythms (0.5-3.5 Hz): they are also characteristic of deep sleep stages. Depending on their morphology, localisation, and rhythmicity, delta oscillations can be normal as in slow wave sleep or pathological as in brain tumours.
- Low Gamma rhythms (30-60 Hz in human EEG): of minor interest until the 1990's, gamma oscillations became very popular after they have been proposed to play a major role in linking stimulus features into a single perception. Several follow up works have shown correlations of gamma activity with different sensory and cognitive processes, notably during visual, auditory, somatic and olfactory perception as well as with attention.
- High Gamma rhythms (variously defined between 80 and 120 or above) also called epsilon rhythms have been found in both human and animal Electrocorticographic (ECoG) in association with chattering action potentials.

Figure 2-4 shows the frequency and amplitude of an example of an EEG channel. The signal amplitudes in five different frequencies (2 Hz, 6 Hz, 10 Hz, 22 Hz, and 35 Hz) are shown in the waveform's patterns.

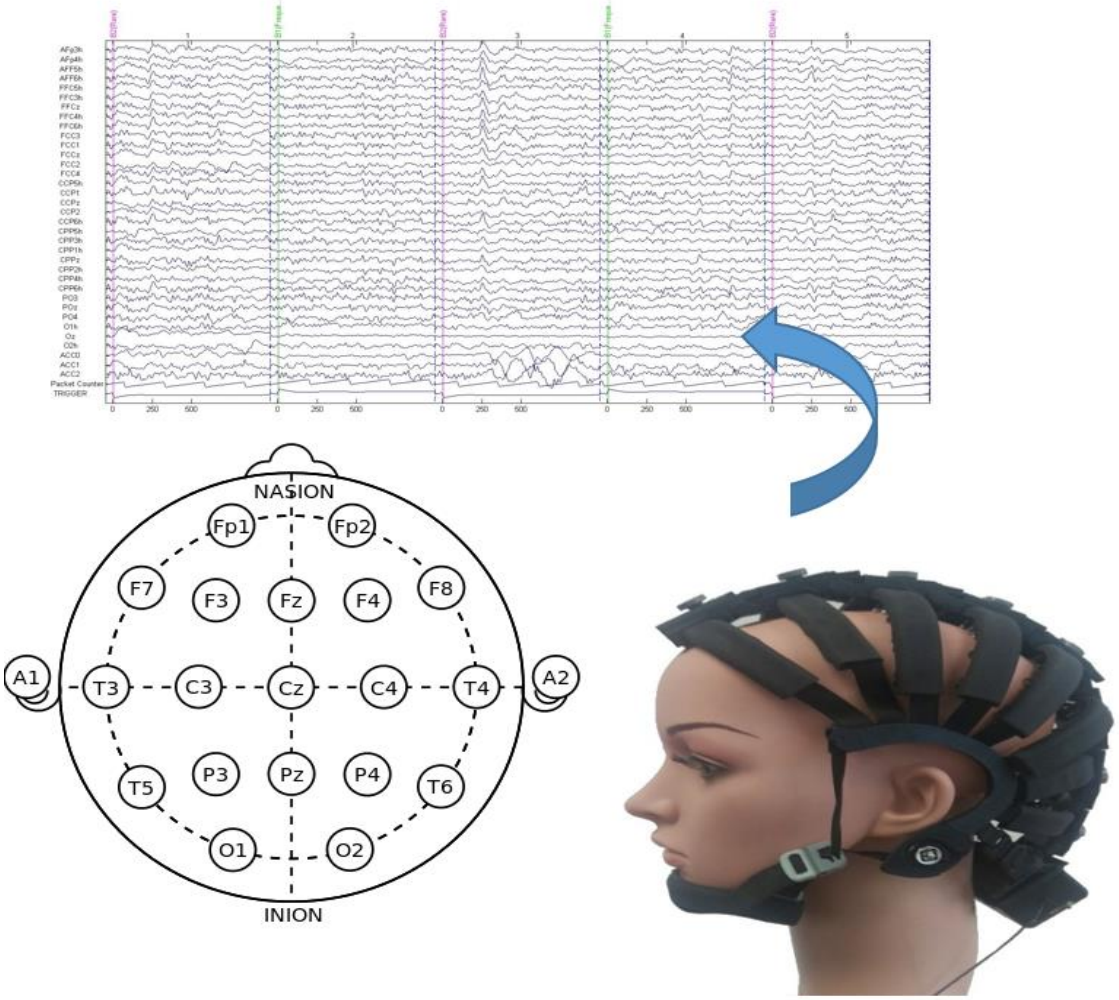

Figure 2-3. EEG recordings that show electrical charges resulted from the activity of brain cells.

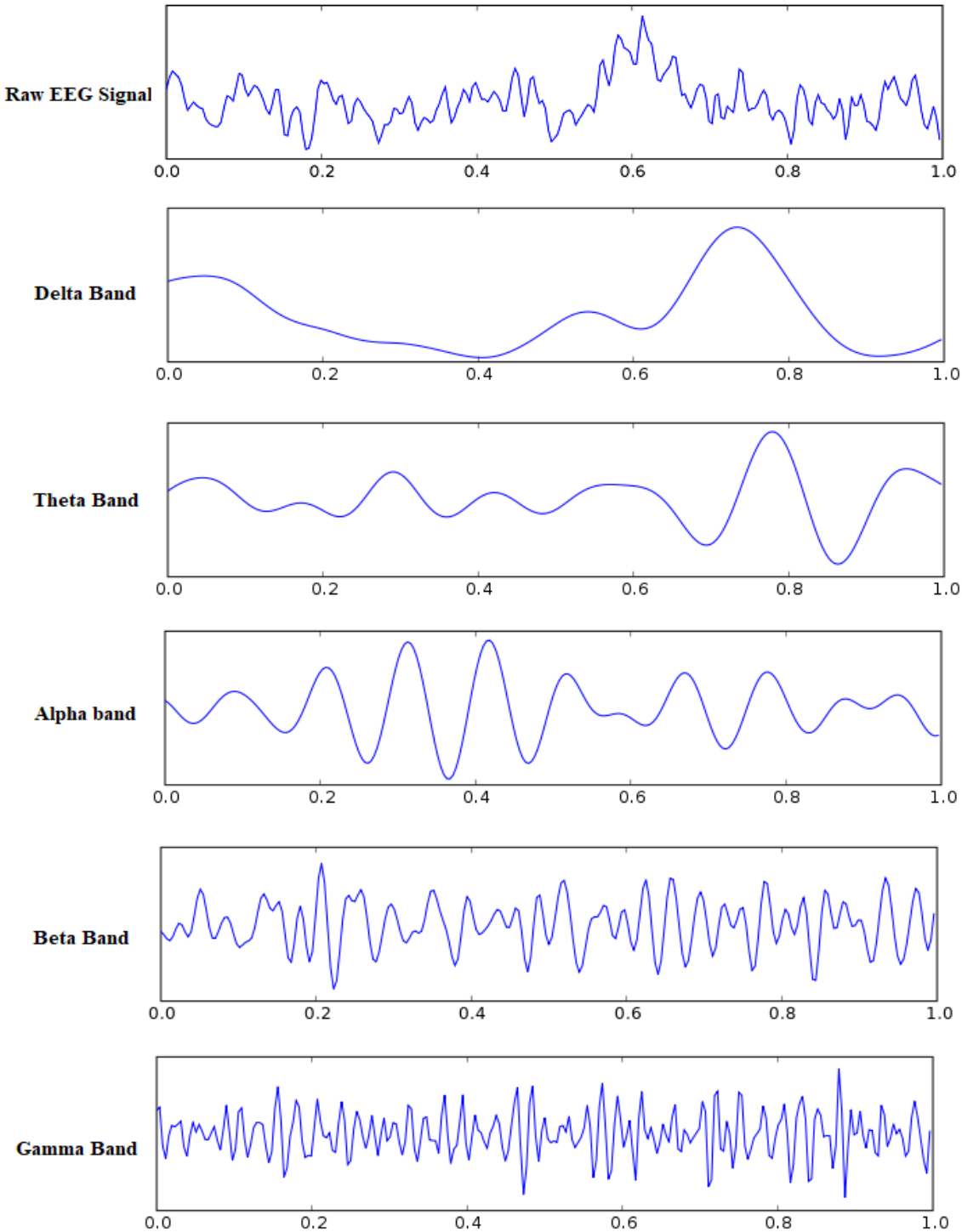

Figure 2-4. EEG band frequency corresponding to signals recorded from an electrode and filtered signals into five bands including: delta, theta, alpha, beta and gamma.

Quantitative electroencephalography (QEEG) is primarily concerned with the spectral analysis of the EEG frequency bands. In addition to absolute power within specified bands, several parameters offer additional information about brain mechanisms, such as the relative power between bands (being the most used the alpha/theta ratio), reactivity (ratio between eyes closed/eyes open alpha activity), asymmetry index (the difference between the left and right power). The information from the different electrodes can be arranged in topographic maps (Duffy et al., 1979) as shown in Figure 2-5. With these plots, it is easy to visualise asymmetries and to localise the activity of the different frequency bands in different mental states (Nuwer et al., 1999). However, the current thesis extends this work offering a novel approach to visualising the propagation of dynamic EEG patterns in both space and time.

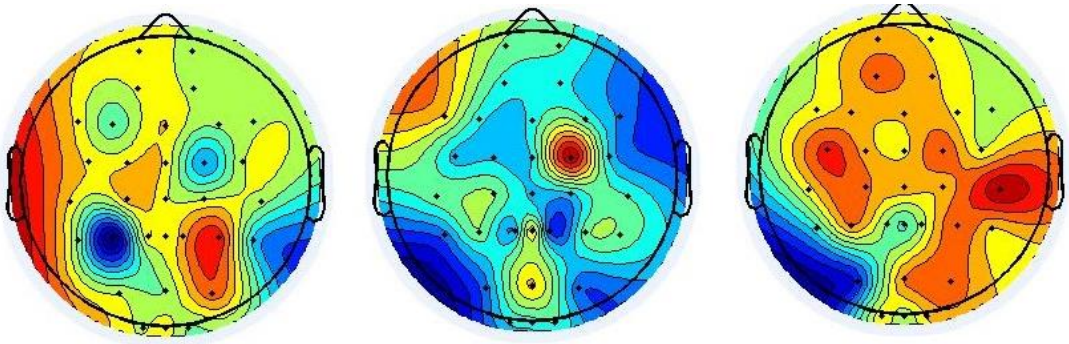

Figure 2-5. An example of topographic mapping of brain activity under different mental activities obtained using Neuroguide software (Thatcher, 2008). (a) when subjects dealing with target stimuli; (b) when subjects dealing with non-target stimuli; and (c) when subjects dealing with neutral stimuli.

2.4 Review of ERP Data for the Study of Cognitive Activity

Typically, the term evoked potentials refer to EEG responses that are time-locked to sensory stimulation. Sequences of stimuli can be organised in paradigms and participants can be asked to perform different tasks. ERPs constitute a broader category of responses that are elicited by "events" such as the recognition of a "target" stimulus or the lack of a stimulus in a sequence (Luck, 2014; Luck & Kappenman, 2011).

ERP waveforms consist of a series of positive and negative voltage deflections, which are related to a set of underlying components (Luck & Kappenman, 2011). Though some ERP components are referred to with acronyms (e.g., contingent negative variation-CNV, error-related negativity – ERN), most components are referred to by a letter (N/P) indicating polarity (negative/positive), followed by a number indicating either the latency in milliseconds or the component's ordinal position in the waveform. For instance, a negative-going peak that is the first substantial peak in the waveform and often occurs about 100 milliseconds after a stimulus is presented is labelled as N100 (indicating its latency is 100ms after the stimulus and that it is negative). It is often followed by a positive peak, usually called the P200 or P2. The stated latencies for ERP components are often quite variable, particularly so for the later components that are related to the cognitive processing of the stimulus (Luck & Kappenman, 2011). For example, the P300 component may exhibit a peak anywhere between 250ms – 350ms (Polich, 2007), ERP waveforms and substantial peaks are shown as

Figure 2-7. ERPs comprise multiple variables that can be analysed as the following:

- **Absolute latency,** which is the time interval between stimulus presentation and the point of maximal value (peak) of a defined component. It is expressed in milliseconds and represents the time taken by the stimulus information to generate the component.
- **Relative latency (inter-peak latency),** which is the time interval between two components and measures the conduction of the impulse between two generators.
- **Amplitude,** which is vertical distance measured from the trough to the maximal peak (negative or positive). It expresses information about the size of the neuron population and its activation synchrony during the component generation.

- **Duration**, which is the time interval from the beginning of the voltage change to its return to the baseline. It is also a measurement of the synchronous activation of neurons involved in the component generation. Longer durations indicate less synchronous neuronal activation.

To record the ERPs, two networked personal computers are used in the data measuring: one for the EEG recording and the other for sequentially displaying the designed cognitive task as shown in Figure 2-6. An example of a common ERP task is the oddball paradigm (García-Larrea, Lukaszewicz, & Mauguiére, 1992; Jongsma et al., 2013). In this task, two different stimuli are distributed pseudo-randomly in a sequence: one of them appearing frequently (standard stimulus) and the other one being a target stimulus appearing less often and unexpectedly. Standard and target stimuli can be tones of different frequencies, figures of different colours or different shapes. Participants are usually asked to respond (e.g., by counting or pressing a button) to the occurrence of target stimuli. Both target and non-target stimuli elicit earlier sensory-perceptual components (e.g., P50, N100, and P200), also known as exogenous given that they are more determined by the physical properties of a stimulus than any task demands. Later components (e.g., N200 and P300) are endogenous and rely more on the cognitive demands of any task.

ERPs provide an excellent temporal resolution as the speed of ERP recording is only constrained by the sampling rate that the recording equipment can feasibly support, whereas hemodynamic monitoring[1] (such as fMRI) are inherently limited by the slow speed of the Blood-Oxygen-Level-Dependent (BOLD) response (Kim, Richter, & Uğurbil, 1997). The spatial resolution of an ERP, however, is much poorer than that of hemodynamic methods, in fact, the location of ERP sources is an inverse problem that

[1] Hemodynamic monitoring measures brain activity by detecting changes associated with blood flow. This technique relies on the fact that cerebral blood flow and neuronal activation are coupled. When an area of the brain is in use, blood flow to that region also increases.

cannot be exactly solved, only estimated. Thus, ERPs are well suited to research questions about the speed of neural activity and are less well suited to research questions about the location of such activity.

Figure 2-6 Experimental protocol of ERP data collection.

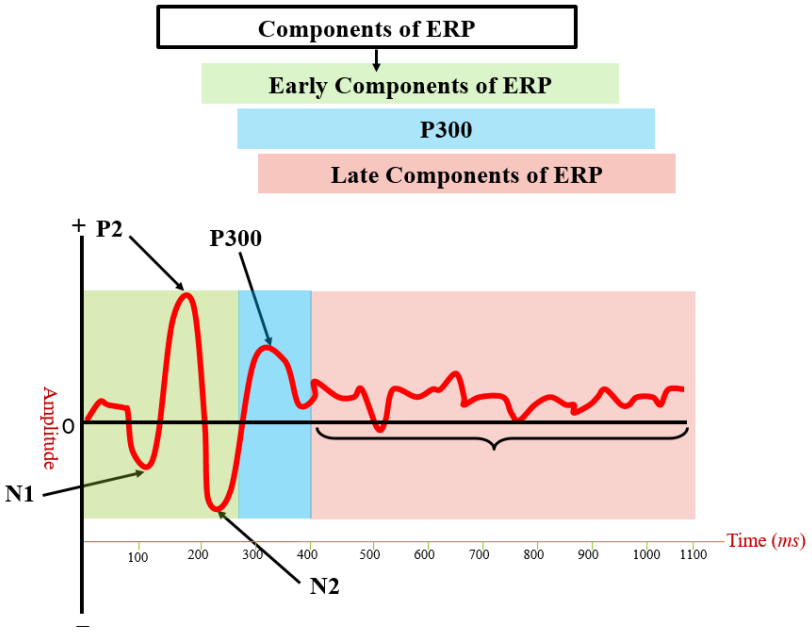

Figure 2-7. Event Related Potential (ERP) waveforms across 1100 millisecond epoch after stimuli presentation. ERP waveforms consist of a series of positive and negative voltage deflections with a peak amplitudes that is corresponding to a set of main underlying components as shown in different colours: Green colour: Early ERP component (including N100, P100, P200 and N200); Blue: P300 (the most common component across studies); and Pink: Late ERP Component (related to the cognitive processing of the stimulus).

Section 2.5 describes the most widely used signal processing environments for processing of EEG data, with particular regard to AI and computational modelling techniques.

2.5 Analytical Methods for EEG and ERP STBD

This section overviews some of the current common methods and how these methods are interrelated. It refers to both statistical and AI methods for data mining procedure. A summary of these methods is presented in Figure 2-8.

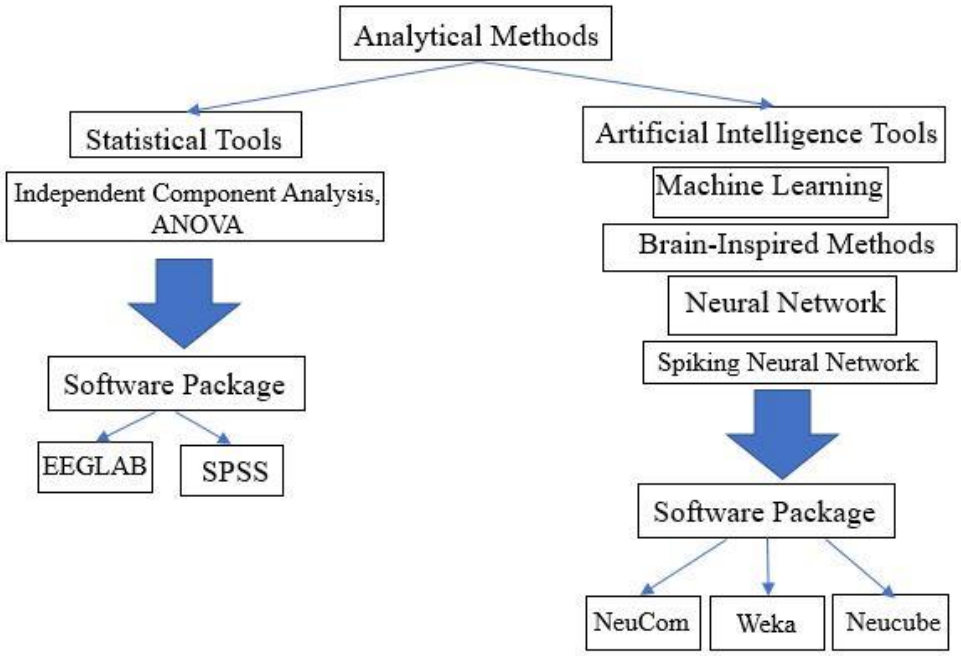

Figure 2-8. Analytical methods for STBD, summarised in two aspects: statistical and AI-based methods.

2.5.1 Statistical tools

- **Classical statistics:** Classical statistics provide powerful tools, both basic and advanced, for any type of analysis. Simple descriptive statistics such as mean and standard deviation have been used almost in all kind of brain data investigations. Hypothesis testing, p-values, and confidence intervals are

powerful instruments of statistical inference. Analysis of variance (ANOVA), statistical independence tests like chi-squared test and correlations give an opportunity to find relations in the data (Field, 2013). For example, ANOVA is used to compare the means of more than two sets of data, to identify if they are statistically different from each other. Through the ANOVA analysis, the resulting F-value and significance level elucidate that at least one group is different from at least one other. However, it does not show exactly the number of groups, or which groups, differ statistically. This can be done through follow-up comparisons in lower ANOVA analysis such as Post-hoc test.

- **Independent Component Analysis (ICA):** The EEG signal mixtures at each sensor can be separated into several independent components. Some of these will correspond to artefacts such as eye blinks, heartbeats and in some cases, the experimental apparatus (Isomura & Toyoizumi, 2016). ICA is a mathematical technique for extracting components, where the extracted components describe temporally independent activities from spatially fixed overlapping sources (Stone, 2004). What distinguishes ICA from other methods is that it looks for components that are statistically independent (Hyvärinen, Karhunen, & Oja, 2001; Isomura & Toyoizumi, 2016; Stone, 2004). ICA method is used for EEG data to remove sources corresponding to artefacts from the signal mixtures to facilitate further analysis of the data. In this case, the important information can be obtained considering only the relevant signals, obtained after applying the ICA method. The fundamental principle of ICA is estimating the un-mixing matrix to estimate the independent components from the mixtures. Thus, the estimated independent components are the linear combination of the recorded data. If the number of sources is more than the number of recordings, the estimated independent components must contain some original sources. If some of the original sources

are predominant, the estimated independent components will be quite similar to the original sources. Thus, when the number of recordings is less than the total number of signal sources (including artefact sources), ICA is able to separate only those components with relatively high magnitude (Djuwari, Kumar, & Palaniswami, 2006).

2.5.2 Artificial Intelligence (AI) Tools

AI involves machines that can perform tasks that are characteristic of human intelligence. While this is rather general, it includes things like planning, understanding language, recognising objects and sounds, learning, and problem-solving. AI has a set of tools through which it enables a machine to mimic human intelligence. One of the tools of AI is Machine Learning (ML) techniques that give the machines to learn without being told explicitly what to do. Machine learning again has various tools, one of them being Neural Networks (NN).

- **Machine Learning (ML):** Over the past few decades the use of machine learning methods has increased dramatically. ML is a field of study that applies the principles of computer science and statistics to create statistical models, which are used for future predictions (based on past data or big data) and identifying patterns in data (Mannila, 1996). ML is itself a type of AI that allows software applications to become more accurate in predicting outcomes without being explicitly programmed (Alpaydin, 2009; Russell & Norvig, 2016). While machine learning emphasises making predictions about the future, AI typically concentrates on programming computers to make decisions (Alpaydin, 2009). Methods of ML can be divided into two main groups: supervised and unsupervised (Caruana & Niculescu-Mizil, 2006). Supervised methods involve creating a predictive statistical model based on mapping an input to an output. In

unsupervised learning there is no model at all; all data is unlabelled and the algorithms learn to an inherent structure from the only input data. (Caruana & Niculescu-Mizil, 2006). ML algorithms solve several tasks: clustering, classification, prediction. Clustering is the first task in exploratory data analysis (Alpaydin, 2009). Classification can be used for categorical data and prediction for nominal datasets. The classification of STBD data has often been done using traditional ML methods such as the Support Vector Machine (SVM) (Giovanni Costantini et al., 2009; Rätsch et al., 2006), Multilayer Perceptron (MLP) (Gardner & Dorling, 1998; Murtagh, 1991), and Multiple Linear Regression (MLR) (Yao et al., 2004). For example, SVM is a supervised learning model with associated learning algorithms that analyse data used for classification and regression analysis. Given a set of training examples, each marked as belonging to one or the other of two categories, an SVM training algorithm builds a model that assigns new examples to one category or the other, making it a non-probabilistic binary linear classifier. (Alpaydin, 2009; Caruana & Niculescu-Mizil, 2006). Both SVM and MLR have been widely used for classification of EEG data (Giovanni Costantini et al., 2009; Subasi & Gursoy, 2010). However, when dealing with complex STBD streams, samples cannot be linearly discriminable. This problem is called non-linear classification which cannot be handled by drawing straight discriminative lines in the data space.

- **Artificial neural networks (ANNs):** ANNs are statistical models directly inspired by, and partially modelled on biological neural networks. They are capable of modelling and processing nonlinear relationships between inputs and outputs in parallel. The related algorithms are part of the broader field of ML, and can be used in many applications such as speech recognition, Brain Computer Interface (van Gerven & Bohte, 2018). ANNs are characterised by containing

adaptive weights along paths between neurons that can be tuned by a learning algorithm that learns from observed data in order to improve the model. In addition to the learning algorithm itself, one must choose an appropriate cost function. The cost function is what is used to learn the optimal solution to the problem being solved (Agatonovic-Kustrin & Beresford, 2000). The loss function or error of the model minimises the squared differences between the estimated and existing target values. As shown in equation below, y_i is the target value, $h(x_i)$ is predicted value and x_i denotes the feature set of a single sample.

$$loss_{function} = \sum_{i=1}^{N} \left(y_i - h(x_i)\right)^2 \qquad (2-1)$$

This involves determining the best values for all of the tuneable model parameters, with neuron path adaptive weights being the primary target, along with algorithm tuning parameters such as the learning rate. It is usually done through optimisation techniques such as gradient descent[1] or stochastic gradient descent[2]. These optimisation techniques basically try to make the ANN solution be as close as possible to the optimal solution, which when successful means that the ANN is able to solve the intended problem with high performance (Zurada, 1992). Architecturally, an ANN is modelled using layers of artificial neurons, or computational units able to receive input and apply an activation function along with a threshold to determine if messages are passed along. In a simple model of ANN as shown in Figure 2-9, the first layer is the input layer, followed by one hidden layer, and lastly by an output layer. Each layer can contain one or more neurons. Models can become increasingly complex, and with increased

[1] Gradient descent is a first-order iterative optimisation algorithm for finding the minimum of a function.
[2] Stochastic gradient descent is an iterative method for optimising a differentiable objective function.

abstraction and problem-solving capabilities by increasing the number of hidden layers, the number of neurons in any given layer, and/or the number of paths between neurons (van Gerven & Bohte, 2018; Zurada, 1992). According to their computational units, they were categorised into three generations. Rosenblatt proposed the first generation of ANNs (Rosenblatt, 1957), called perceptron which was based on McCulloch-Pitts neurons and was inspired by the concept of thresholding in biological neurons. A perceptron neuron is a computational unit with several inputs, each is associated with a weight that resembles synaptic efficiency. A perceptron integrates the inputs and fires if the synaptic weighted sum of inputs reaches a threshold. This is computed using a step function to perform binary outputs (−1 or 1). This function is time-independent, meaning that the time in which the threshold is exceeded is not considered. The second generation of ANNs is related to improving the computational units by including an activation function. In contrast to a fixed threshold value to determine the output, here an activation function (such as non-linear sigmoid) produces outputs which are proportional to the inputs; thus, performing non-linear classifications. Although these ANNs are inspired by some properties observed in brain research (Hodgkin, Huxley, & Katz, 1952; Hall, 2015), the neuron's state depends only on the current time of inputs, employing an activation function. To enhance this, the third generation of ANNs, SNNs emerged in which accumulated inputs over time control an action potential function; thus, it encodes the neuron's firing-time information.

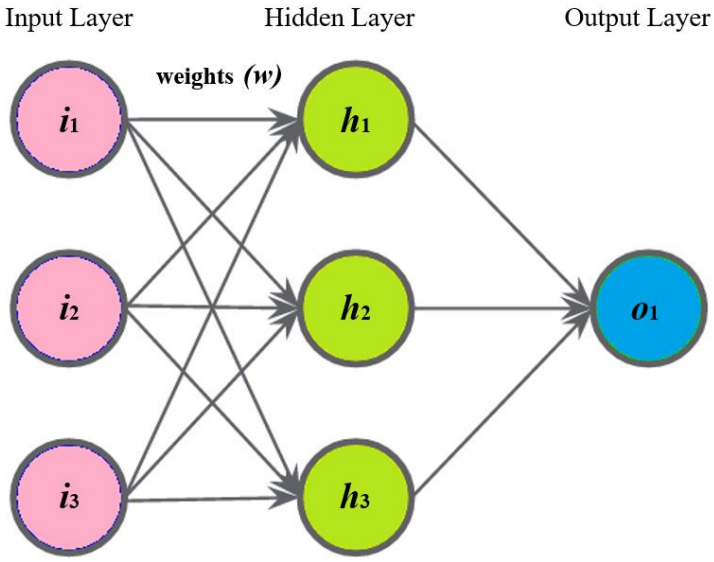

Figure 2-9. A diagram of a simple ANN with three input neurons, three hidden layers, and one output neuron.

- **Spiking Neural Network (SNN):** SNNs are artificial neural network models that more closely mimic natural neural networks. In addition to neuronal and synaptic state, SNNs also incorporate the concept of time into their operating model (Izhikevich, 2006). SNN aims to bridge the gap between neuroscience and ML, using biologically-realistic models of neurons to carry out the computation (Izhikevich, 2006). SNNs operate using spikes, which are discrete events that take place at points in time, rather than continuous values (N. K. Kasabov, 2014). The occurrence of a spike is determined by differential equations that represent various biological processes, the most important of which is the membrane potential of the neuron. Essentially, once a neuron reaches a certain potential, it spikes, and the potential of that neuron is reset (Masquelier, Guyonneau, & Thorpe, 2009).

2.5.3 Software Packages Based on Statistical and AI Methods

- **EEGLAB/ERPLAB:** EEGlab and ERPlab have been extensively used for brain studies. EEGlab is the most widely used signal processing environment for processing of raw EEG data. It has elaborated structure, powerful methods for

time-series and independent component analysis (Delorme & Makeig, 2004). The ERPlab toolbox is also used for analysing and processing of ERP components, grand-averaging, visualising the waveforms in the MATLAB environment (Delorme & Makeig, 2004).

- **SPSS:** Statistical Package for the Social Sciences (SPSS) is a comprehensive and flexible statistical analysis and data management tool. It is one of the most popular statistical packages which can perform highly complex data manipulation and analysis with ease. It is designed for both interactive and non-interactive users (Field, 2013).
- **Weka:** Weka is a stack of over 100 ML algorithms for data mining. It is a free open-source Java application developed at the University of Waikato, New Zealand. It can solve typical for ML task: clustering, classification, regression, attribute selection, finding association rules (Holmes, Donkin, & Witten, 1994).
- **NeuCom:** NeuCom is a generic knowledge engineering environment for data analysis, modelling and knowledge discovery, developed by the Knowledge Engineering and Discovery Research Institute (KEDRI), Auckland University of Technology. It includes various techniques for: Feature selection; Signal-to-Noise Ratio (SNR); Correlation; Classification and Prediction model creation, model testing and model optimisation.
- **NeuCube:** A computational architecture for the creation of Brain-Like Artificial Intelligence (BLAI) that includes applications across domain areas. It is based on SNN (N. K. Kasabov, 2014). A NeuCube architecture for STBD modelling is presented in the next chapter.

STBD have often been analysed using statistical and conventional ML methods such as the SVM, MLP, MLR, and neural network architectures. Now the question is: what is missing in the current technologies for STBD analysis?

The brain is a highly interactive and deep learning network, but nearly all multivariate models employed in cognitive neuroscience are linear and do not model interactions. Understanding the dynamic patterns of spatiotemporal brain data through the traditional methods is limited because temporal features manifest complex interactions that change dynamically over time. Therefore, it is crucial to develop new computational models that are capable of learning spatiotemporal interactions between multivariate data streams. SNNs are the third generation of NN and comparing to conventional neuronal networks which deal with static vector-based data (temporal information needs to be converted into vectors of static features), SNNs incorporate spatial and temporal components of data into one operating. Therefore, SNN is a way of using spike-time dynamics to extract interactive structures from the brain data, without over-fitting to a particular classification problem, and which constrains the immense space of possible interactions in a biologically plausible way. A properly designed SNN model can be used to model brain data and to detect deep spatiotemporal patterns for a better understanding of data.

2.6 Chapter Summary

This chapter presented two main techniques for recording STBD which have been widely studied in cognitive science and neuroscience research. Also, some introduction, limitations of analytic methods for modelling complex STBD were briefly stated.

In summary, EEG and ERP have been extensively used for brain study by applying different statistical and topographical mapping methods. Various techniques have been developed to analyse the brain's activation, functional connectivity or effective connectivity in STBD, however, these methods cannot capture precisely the spatiotemporal patterns 'hidden deep' in the data that represent the dynamics of the cognitive processes. SNNs framework is suggested to be suitable for learning spatiotemporal brain data analysis, as spatial and temporal components of data are both essential to be preserved. Chapter 3 will discuss the SNN principle, models and applications.

“The Science of Today is the Technology of Tomorrow”.

Edward Teller

Chapter 3 Spiking Neural Networks

3.1 Introduction

This chapter discusses SNN architectures and principles. Section 3.2 introduces SNN as a computational framework that visualises the brain data in a 3D space of artificial neurons and elucidates the connectivity and interaction between data variables. Then, sections 3.1.1 to 3.1.4 depict the main functional modules of the SNN framework, which are: (1) input data encoding and mapping; (2) unsupervised learning in a 3D SNN model; (3) supervised learning and classification; and (4) knowledge extraction. Finally, section 3.3 summarises the chapter.

3.2 Brain-inspired Spiking Neural Networks

SNNs are computational models that are inspired by the brain's neural structure. According to (Indiveri, Corradi, & Qiao, 2015; Maass, 1997), the SNN follows a biologically plausible structure, in that:

- A brain template (atlas) is used to construct a 3-dimensional SNN model that maps the location of brain structures.
- Spatial mapping of input features (data variables) in the SNN model preserves spatial information in the brain data.
- Input data (brain signals) are encoded to a 'spike train' (series of binary events when the brain signal reaches a threshold value) at a millisecond time scale.
- The initialisation of the SNN model uses the brain-inspired small-world connectivity rule.

- Biologically plausible learning rules are applied to evolve the SNN functional connectivity in a deep learning mode, resulting in long chains of connections.

In a SNN, an artificial spiking neuron is an information-processing unit that learns from input temporal data over time to approach putative learning processes of the brain. That is, spiking neurons are interconnected through their synapses, which memorise the learning patterns. They incorporate the concept of time into their operating models and thus are considered to be superior in biological plausibility in neural networks compared to previous models that do not account for temporal dynamics (Agatonovic-Kustrin & Beresford, 2000; Schmidhuber, 2015). Thus, SNNs are considered suitable models for processing STBD (N. K. Kasabov, 2014). A SNN model can be implemented using several models, such as leaky Integrate-and-Fire (LIF) models (as shown in Figure 3-1). In this model(Knight, 1972), the membrane potential $v(t)$ increases with every input spike at a time *t*, multiplied by the synaptic efficacy (strength), until it reaches a certain threshold θ. After that, an output spike is emitted and the membrane potential is reset to an initial state. Like a biological neuron performs, when the simulated neuron emits a spike, it does not produce a new spike within a refractory period and its membrane potential $v(t)$ leaks. The membrane potential can have certain leakage between spikes, which is defined by a parameter

$$\tau_m \frac{dv}{dt} = v_{rest} - v(t) + RI(t) \qquad (3-1)$$

where τ_m is the membrane time constant, v_{rest} is the resting potential, I and R are the input current and the resistance respectively. As shown in Figure 3-1, as soon as the PSP reaches a threshold θ, the neuron generates an output spike and sends it to its connected

neighbours. The PSP can leak by a certain value (temporal parameter τ) when no spike arrives within a given time period (N. K. Kasabov, 2014).

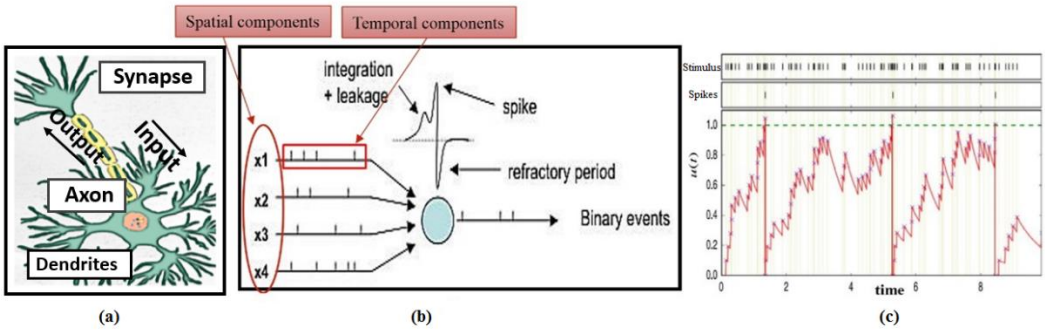

Figure 3-1 a) Structure of a biological neuron which receives input information across axon terminals and processes it; (b) Picture of a simulated artificial spiking neuron with the model of Leaky-Integrate-Fire (LIF); (c) Functionality of LIF model using an input spike sequence (upper spike train), the output emitted spikes (middle spike train) and the changes of post-synaptic potential.

The SNN-based methodology is based on the framework of evolving spiking neural networks, designed to learn from both temporal and spatial information called NeuCube (N. K. Kasabov, 2014). The SNN architecture includes several functional modules (as shown in Figure 3-2): an input-encoding module; a 3D SNN module for unsupervised training; an output classification/regression module for supervised training; an optimisation module; and a knowledge extraction and visualisation module (Bullmore & Sporns, 2009; N. K. Kasabov, 2014) . These modules are described in the following sections.

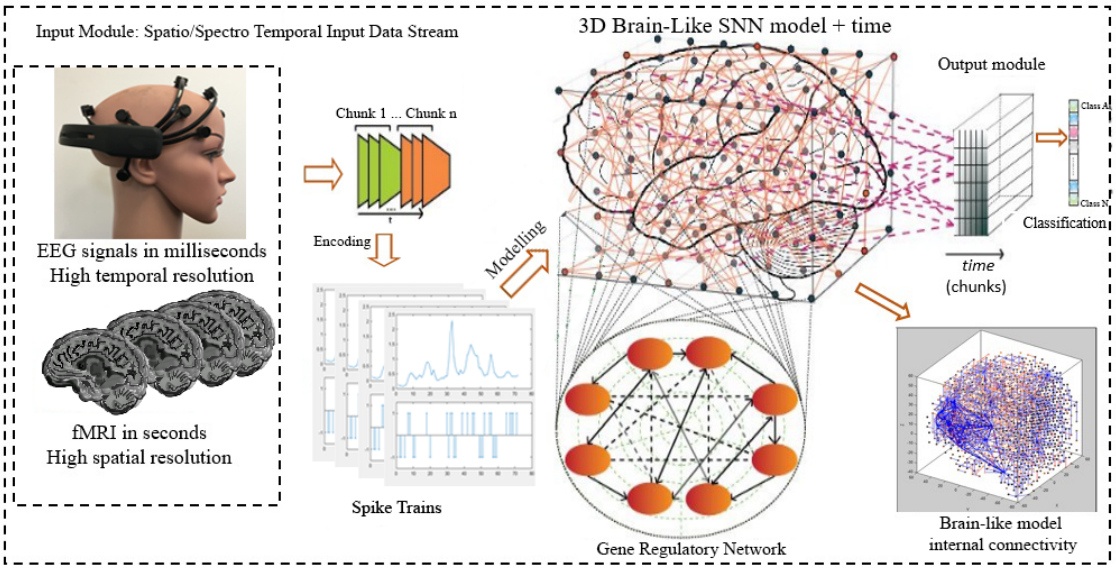

Figure 3-2. The NeuCube SNN architecture, which contains several modules: input spike-time data encoding; a 3D SNN reservoir for unsupervised learning; a SNN classification/regression module using RO and STDP for supervised learning; gene regulatory network (GRN) as a system parameter optimisation model (optional and not used in the current thesis).

3.1.1 Input Data Encoding and Mapping

The EEG signal from each electrode is translated into a spike train (as demonstrated in Figure 3-3), and spikes from a given electrode will enter to the SNN model at a particular location. Each electrode corresponds to a single unit (input neuron) in the SNN.

For a temporal signal $S(t)$ over time $t = 1, 2, \ldots, n$, the signal amplitude variation over time is denoted by $V(t)$, where at baseline, $V(1) = S(1)$. At the next time point t, if the upcoming signal amplitude $S(t)$ is greater than $V(t-1) + \theta$ (sum with a threshold θ), then a positive spike is generated, whereas for a decreased signal, a negative spike is generated. The encoding of positive and negative spikes is defined as follows:

$$spike(t) = \begin{cases} 1 \; then \; V(t) \leftarrow V(t-1) + \theta; & if \; S(t) \geq V(t-1) + \theta \\ -1 \; then \; V(t) \leftarrow V(t-1) - \theta; & if \; S(t) \leq V(t-1) + \theta \\ 0 & otherwise \end{cases} \quad (3\text{-}2)$$

As shown in Relation 3-2, the encoded spike sequences are in the form of binary events, in which -1 refers to a negative spike (the site of downward changes in signal

values) and 1 is a positive spike (the site of upward changes). This method has been successfully used in dynamic vision sensors (DVS) (Song, Miller, & Abbott, 2000). Figure 3-3 shows an example of encoding EEG data recorded from the Cz channel into a sequence of positive and negative spikes using a threshold-based representation (TBR) algorithm. In this method, if the signal's change increases above a spike threshold at consecutive time moments, a positive spike is generated. On the other hand, if the signal decreases below a threshold, then a negative spike is generated; otherwise, there is no spike generated. The generated spike trains represent changes in the STBD that exceeded a threshold TBR_{thr}. Figure 3-3 shows that out of a total of 115 spikes generated, 58 is positive (indicated as +1) and 57 negatives (indicated as -1). The spike trains are used for training the SNN model.

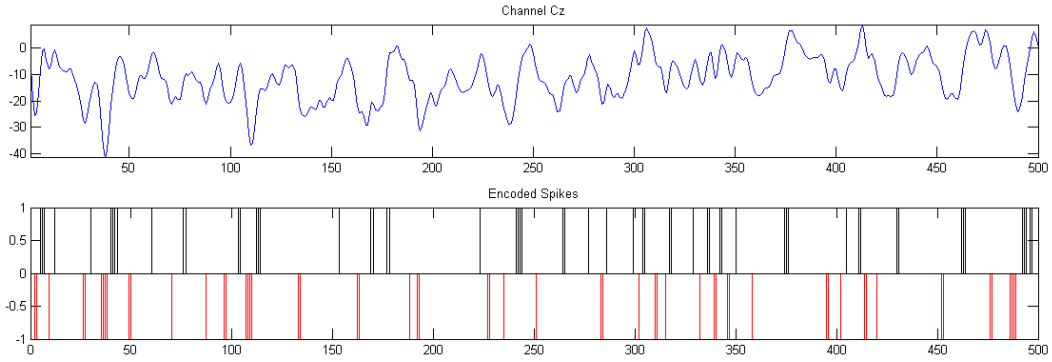

Figure 3-3. An example of encoding EEG data into sequence of positive (black) and negative spikes (red) using the TBR algorithm that is the format of the input data into the SNN architecture. The image shows 500 EEG data time points of electrode CZ from one subject.

In the SNN model, after defining a biologically plausible 3D SNN, data will be initialised with Small-World Connectivity rule (SWC) (Liao, Vasilakos, & He, 2017). Small-World (SW) structure is an organising principle in many natural systems, including networks of brain *neurons*, as both anatomical connections (Braitenberg & Schüz, 2013; Sporns, Chialvo, Kaiser, & Hilgetag, 2004) and synchronisation networks of cortical *neurons* (Yu, Huang, Singer, & Nikolić, 2008) exhibit small-world topology (Liao et al.,

2017). The neurons in the SNN reside at coordinates defined within the Talairach[1] brain atlas (Giacometti, Perdue, & Diamond, 2014; Talairach & Tournoux, 1988), and neurons are connected probabilistically, such that neurons that are anatomically adjacent are very likely to be connected and those that are anatomically distant from one another are very unlikely to be connected. This constrains the space of potential interactions in a biologically plausible way. For instance, SW networks are observed in several large-scale networks of brain *neurons*, such as the visual system (Latora & Marchiori, 2001). The brain information processing is performed in both segregated and dispersed functional areas, as presented in (Humphries, Gurney, & Prescott, 2006; Liao et al., 2017; Sporns et al., 2004; Yu et al., 2008). Similarly, the SW rule can include both short-distance connectivity (local clusters) within nearby *neurons* (similar to segregated information processing) and long-distance connectivity by linking the local clusters (similar to spread information processing).

Using SW rules in computational modelling has several advantages, as it supports high local and global efficiency in parallel processing, dynamic operation and rapid adaptation in network reconfiguration (Simard, Nadeau, & Kröger, 2005). It also results in higher rates of information processing and learning than other techniques, such as random graphs (Simard et al., 2005). These theoretical and empirical reasons led to use of SW rules for the initialisation in the SNN model. The SNN models in this thesis are initialised using the SW connectivity rule (Braitenberg & Schüz, 2013; Bullmore & Sporns, 2009) in which a probability of a neuron *i* to be connected to another neuron j depends on the distance between the two neurons, the larger the distance – the smaller the probability. In some cases, a radius is defined which represents the maximum distance of connections of one neuron to another in the 3D space of the SNN. The initial connections are assigned

[1] Talairach coordinates, is a 3-dimensional coordinate system (known as an 'atlas') of the human brain, which is commonly used in functional brain imaging to map the location of brain structures independent from individual differences in the size and overall shape of the brain.

as small random weights so that, for example, 80% of them are weighted by positive values while 20% of them are weighted by negative values. All the above parameters can be selected based on the task in hand. These initial connection weights are then adjusted by biologically plausible unsupervised learning rules which rely on the temporal dynamics and spiking activity triggered by input neurons as explained in the next section.

3.1.2 Unsupervised Learning in a 3D SNN Model

The known unsupervised Spike-Time-Dependent Plasticity (STDP) learning rule is used for learning in the SNN models applied in this thesis. Through STDP learning, a connection $W_{i,j}$ between *neurons* i and j are adapted according to the timing of their output spikes. If *neuron* i emits a spike earlier than j, then W_{ij} will increase; otherwise, that would imply that neuron *j* is driving neuron *i* so W_{ij} will decrease. STDP is described as follows:

$$F(\Delta t) = \begin{cases} A_+ \exp(\Delta t/\tau_+) & if\ \Delta t < 0 \\ -A_- \exp(-\Delta t/\tau_-) & if\ \Delta t \geq 0 \end{cases} \qquad (3\text{-}3)$$

$F(\Delta t)$ describes the adjustment of synaptic plasticity with respect to the pre-synaptic and post-synaptic spiking time in the interval of $\Delta t = t_{pre} - t_{post}$. The parameters A+ and A- are the maximum amounts for synaptic adjustment, which apply if Δt is close to zero. The parameters τ_+ and τ_- control the interval of pre- to post-synaptic spikes during which the weakening and the strengthening of the synaptic connection occur. During this learning procedure, the input neuron will accumulate spikes to the SNN model and, if neurons cross an activation threshold, they will also emit output spikes. That spike is sent out to all the units it is connected with, and what reaches each distal neuron is the spike scaled by the connection weight. That neuron will likewise accumulate activity as a function of receiving spikes and, after crossing some threshold, fire (Chan, Liu, & van

Schaik, 2007). In such a way, spikes are transferred between neurons and propagated to the SNN model. Therefore, the STDP rule captures 'hidden' spatiotemporal relations in the STBD stream, in the form of neuronal connections between spatially located *neurons* in the SNN model

3.1.3 Supervised Learning and Classification using a SNN Classifier

At this step, a dynamic evolving SNN (deSNN) (N. Kasabov et al., 2013; N. K. Kasabov, 2014; Tu, Kasabov, & Yang, 2017), fully connected to all *neurons* in the 3D SNN, is used for classification/regression of the activated spiking patterns in the 3D SNN when input data are propagated through it. Other classifiers can also be employed (Thorpe & Gautrais, 1998). The deSNN applies supervised learning in an output classifier layer using the class labels of the training samples. For each sample in the training set, one *neuron* is evolved in the output layer and linked to all the *neurons* in the already trained 3D SNN. The connection W_{ij} between *neuron* i from the 3D SNN and *neuron* j from the output layer is initialised by using a Rank-Order (RO) rule. The RO rule emphasises a higher priority for earlier spikes to an output *neuron*. Data with class labels are propagated through the trained 3D SNN and a supervised learning process is applied to train an output classifier. The potential $PSP(j,t)$ of output *neuron* j at time t is defined using the following relation:

$$PSP(j,t) = \sum mod^{order(i)} W_{ij} \qquad (3\text{-}4)$$

where order (i) represents the order of the first spike transmitted through W_{ij} and mod is a modulation factor (a parameter between 0 and 1). Therefore, the first spike that reached to the output *neuron* j from the 3D SNN model causes the highest increase in the corresponding connection weight. After the first spike has arrived, for the next spikes

coming at time t from *neuron* i, the connection weight W_{ij} will rise by parameter *Drift*; if there is no spike at the time moment t, W_{ij} will decrease by a drift value as shown in the following formula:

$$W_{ij}(t) = \begin{cases} W_{ij}(t-1) + drift & if\ spike_j(t) = 1 \\ W_{ij}(t-1) - drift & if\ spike_j(t) = 0 \end{cases} \quad (3\text{-}5)$$

In the deSNN a new output neuron is created for any new spatio-temporal input. If the distance between the newly created output neuron weight vector and that of anyone of the already trained output neurons is smaller than a similarity parameter, they are considered to be close and they are merged. Closeness is decided based on the similarity between the weight vectors (Wij) of every output neuron i to the weight vector produced by the newly input sample. This distance-based strategy is based on the closest k-Nearest Neighbours (kNN), one of the most utilised algorithms in machine learning due to its simplicity and effectiveness.

During the recall phase, when the output of a new sample is not known in advance, the majority of the output neurons among these k – nearest that belong to a given output class define the class of the new input data.

3.1.4 Parameter Optimisation

For model parameter optimisation, an exhaustive grid search method has been utilised to minimise the cross-validation classification error. Each parameter will be searched within a range, specified by the minimum and maximum, through a number of iterations related to the number of steps for moving from minimum to maximum. For every model created out of *N* models, three main parameters (STDP learning rate, neuron firing threshold, and classifier parameter *mod*) will be chosen to be optimised. The parameters will be selected by assigning 10 steps between the minimum and maximum values of each

parameter. Therefore, for every model creation, 1000 iterations of training (using N samples) and testing (using the single holdout sample) will be performed using a different combination of these three parameters. Then the parameters that resulted in the best accuracy in most of the iterations, will be reported as the optimal parameters. When the optimisation procedure was completed, the most selected values for the parameters across all the N models will be selected as STDP learning rate= 0.01; neuron firing threshold= 0.5; deSNN classifier parameter *mod*= 0.4.

3.3 Chapter Summary

This chapter exposes an overview of computational models of SNNs and introduced the NeuCube SNN-based architecture for modelling STBD. An SNN model supports a meaningful mapping of spatial variables, modelling, learning, and model visualising. In the SNN architecture, the connections in the network are simulated by meaningful brain-inspired connections and the learning procedure is based on STDP which captures the spatiotemporal interactions. These features make an SNN model meaningful in terms of its interpretation for a better understanding of spatiotemporal characteristics of data.

The next chapter demonstrates a step-wise design of the SNN-based methodology for dynamic pattern recognition and pattern prediction in two real-life case studies of cognitive data in this thesis: EEG and ERP.

“Design is not just what it looks like and feels like, design is how it works”.

Steve Jobs

Chapter 4 Methodological Design

4.1 Introduction

The SNN architecture is developed here to map different types of STBD into a 3D space of spiking neurons, where the topological information of the brain regions is spatially preserved. As explained in the previous chapter, every spiking neuron is a computational unit that resembles the brain information processing mechanism with the use of the STDP learning algorithm. Therefore, the SNN models are capable of learning from the temporal information of the STBD over time and capture the spatiotemporal relationships in the data. In this thesis, the SNN connectivity captures the relationships between the EEG and ERP variables in a computational model, not the precise organisation of the brain's physical neural connectivity. This chapter presents the design of the SNN-based methodology for dynamic pattern recognition and pattern prediction tasks in EEG and ERP data modelling. Sections 4.2 and 4.3 depict the step-wise design of the SNN method for addressing the three main research questions of this thesis:

- "*Research question 1. How a SNN model can be optimally designed for dynamic pattern recognition related to different mental states?*
- *Research question 2. How can the designed SNN discriminate the neural patterns at an individual-levels?*
- *Research question 3. Can SNN models lead to knowledge discovery by creating a predictive system of brain mental states according to the dynamic/discriminate patterns?"*

Section 4.4 explains how SNN models can be evaluated. Finally, section 4.5 refers to employing SNN in two case studies: neuromarketing and mindfulness.

In this thesis, the SNN architecture is designed in accordance with the following main approaches:

1- Knowledge representation through dynamic pattern recognition (this is addressed for research questions one and two).

2- Predictive modelling of streaming data (this is addressed for research question three).

4.2 A Method for Dynamic Pattern Recognition and Knowledge Representation from EEG and ERP Data based on brain-inspired SNN

The following is a procedure that represents the design of the study for dynamic pattern recognition in the SNN framework.

4.2.1 Initialisation and Encoding of the EEG and ERP Data in the SNN Model

A model is pre-structured to map the structural and functional of the modelled process presented by spatiotemporal data. The SNN structure consists of spatially allocated spiking neurons, where the location of neurons maps a spatial template of the problem space (brain template). In this case, STBD data samples are mapped spatially into 3D artificial neural space where the spatial information of brain areas is topologically preserved according to the Talairach atlas. Employing an appropriate encoding method, the input data are then encoded into spike sequences that reflect the temporal changes in the data.

4.2.2 Unsupervised learning of EEG and ERP data in the SNN Model, Visualisation and Interpretation of Dynamic Patterns

Unsupervised time-dependent learning is applied in the SNN model to learn the spatiotemporal relationships in the input spikes. The learning process modifies the

connection weights between neurons based on the timing of their spiking activity. During the learning process in SNN models, consecutive snapshots of the firing state of the neurons are captured to represent a trajectory of dynamic, deep-learned patterns of neurons' spiking activity with respect to the temporal order in which clusters of neurons emitted spikes. This allows capturing the sequential spiking activity patterns in the SNN models for different mental states. Figure 4-1 represents an example of sequentially activated areas as a trajectory of deep-learned patterns in the SNN models. It shows how early the information was transferred to different parts of the brain at different times. Figure 4-1b shows the neuronal connections created during the learning in the SNN models are visualised over time. This reflects the dynamic patterns of EEG/ERP data corresponding to different epoch lengths.

4.2.3 Knowledge Representation in the SNN Model

A deep functional pattern in Figure 4-1 is revealed as a sequence of spiking activity of clusters of neurons in the SNN model that represents the active functional areas of the modelled process. The connections of the trained SNN models in Figure 4-1b can be interpreted as deep knowledge showing sequential events (activated neurons) at different SNN areas over four time-intervals. A trajectory of SNN activities over time can be displayed as an aggregated event, presented in Figure 4-2.

4.2.4 Supervised Learning and Patterns Discrimination of Different Brain Mental states

Experimental results in the SNN are illustrated mainly to represent the visual exploration of the models, but numerical information (such as connection weights and spiking intensity) is also facilitated and can be exported from the models. Different SNN models can be compared in terms of the "spike intensity" and "connection weights" in their activated neural areas.

In order to compare two different trained SNN models (denoted by S_1 and S_2) where each of them has n number of neurons in the cube SNN, the connection weight vectors (**W**) of S1 and S2, as two different trained SNN models, are subtracted as shown in the below formula. An example of the subtracted connectivity from two different SNN models is depicted in Figure 4-3.

$$\boldsymbol{W}^{(\mathrm{D})} = \boldsymbol{W}^{(\mathrm{S1})} - \boldsymbol{W}^{(\mathrm{S2} \tag{4-1}$$

where $\boldsymbol{W}^{(\mathrm{S1})}$ is the connection weight vector of the cube of the SNN model S1 and $\boldsymbol{W}^{(\mathrm{S2})}$ is the connection weight vector of the cube of the SNN model S2.

4.3 A Method for Predictive Modelling of EEG and ERP Data to Predict Future Brain States

The trained SNN models represent discriminative patterns between different mental states. Now, the question is, *could the dynamic patterns be discriminated at an earlier stage to perform prediction of events in streaming data?* An SNN model is incrementally learning the data patterns while sequences of spikes are streaming to the model. During an unsupervised learning process, internal spatiotemporal connections are evolving over time that forms discriminative patterns which differentiate the mental states. These evolving patterns are stored over time for retrospective analysis. When the training process is completed, if an input pattern of a specified length is entered, with a known output, a specified pattern will be activated (as a trajectory of spikes in the model). This pattern can be learnt in a supervised mode in an output module for classification. However, as the SNN model generates longitudinal spatiotemporal connections over time; thus, retrospective pattern classification can suggest a prediction of output at an earlier time point.

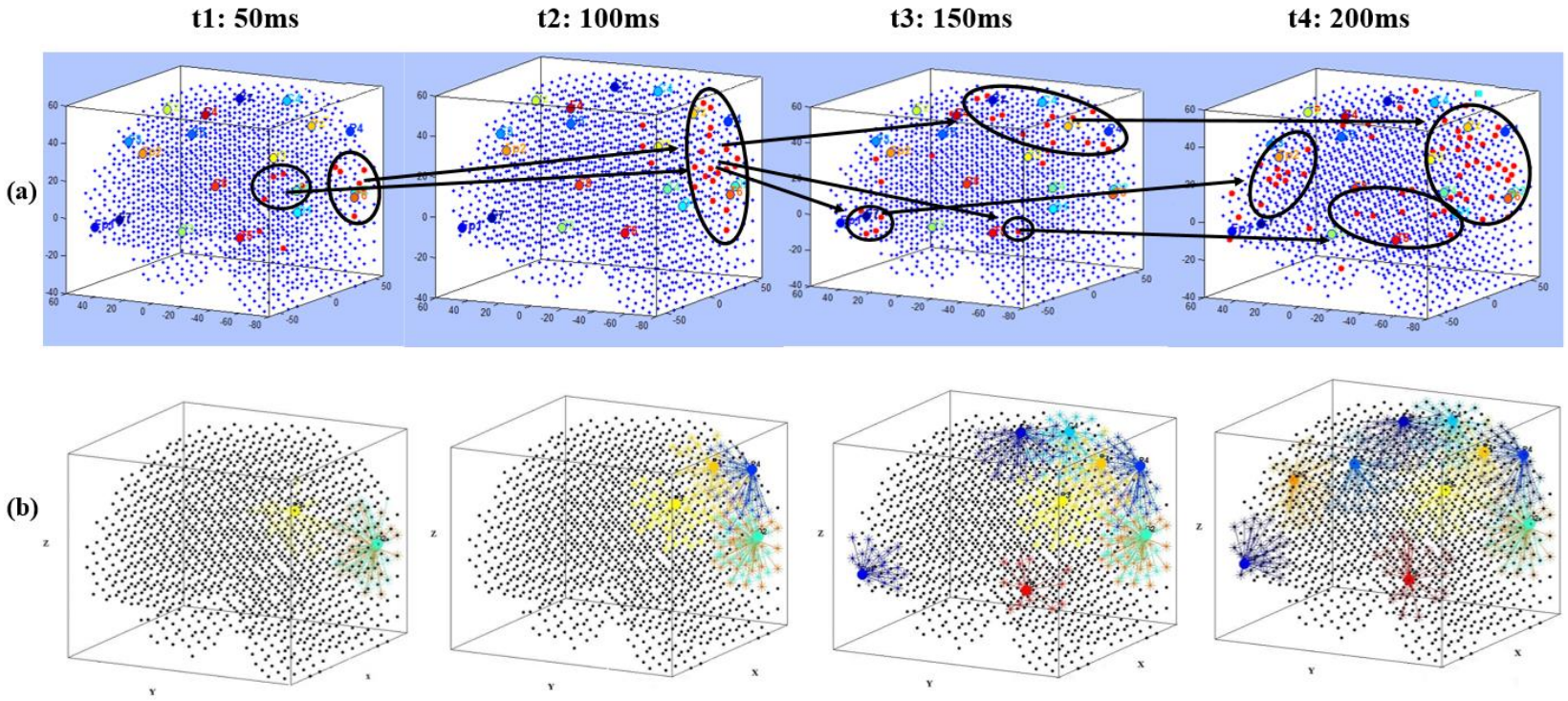

Figure 4-1. (a) An example of sequentially activated areas in a clusters of neurons (circles) as a trajectory of deep-learned patterns in the SNN models showing changes of spiking activity every 50 millisecond; (b) The connections of the trained SNN models.

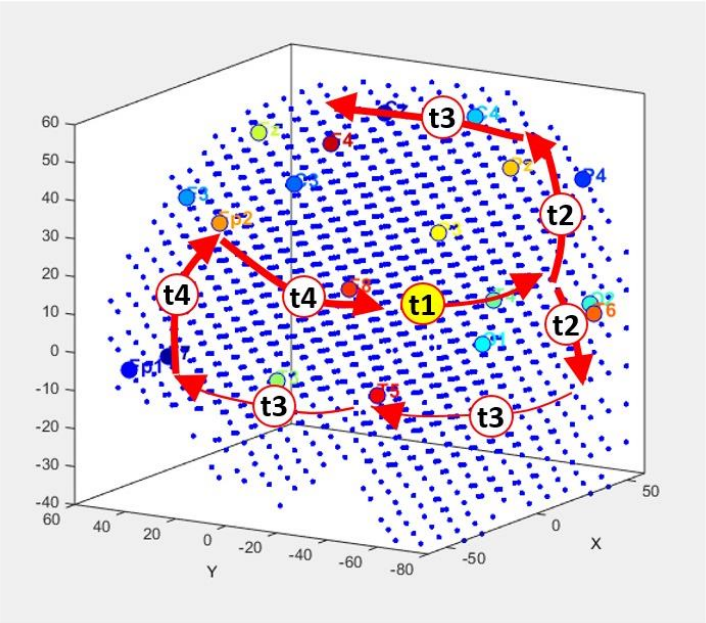

Figure 4-2. The trajectory of functional pathway as deep knowledge, representing a sequence of four events at times t1 …,t4 that are executed as 4 large cortical locations in a sequence of 4 aggregated time segments.

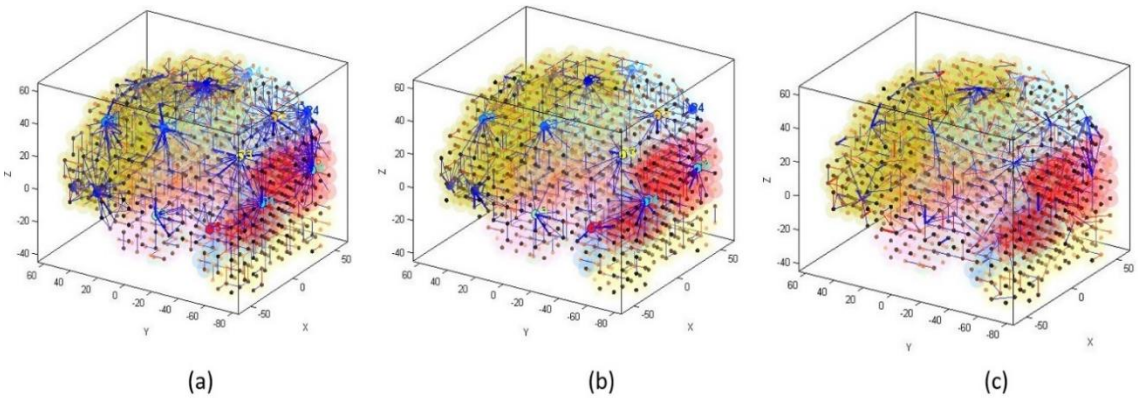

Figure 4-3. The connectivity of SNN models trained on two conditions (a and b) measured by EEG data. (c) the differences in connectivity between the SNN models (a) and (b) reflecting the spatiotemporal differences between mental state condition.

4.4 SNN Model Evaluation through Leave One Cross Validation

In order to evaluate the level of significance in the trained SNN models, each experiment is performed with respect to the following criteria: For a mental activity (called class) of each individual data, one SNN model is created. Each class of data contains *n* samples that are used to train the SNN model through an iterative procedure of leave-one-out as follows (shown in Figure 4-4):

1. The SNN model is initialised.
2. The initialised SNN model is trained with $(n-1)$ samples (one sample is excluded, left out, from the training).
3. The average of the quantitative information (spatiotemporal connectivity) in the trained SNN model is calculated.
4. The model is recalled and tested on the left-out sample for correct classification or prediction.

The hold-out sample is replaced by another sample, then it returns to step 1 until all the samples are excluded from the training set, one by one. This means that a set of SNN models are initialised and trained with different folds of samples. The quantitative information of the trained SNN models can be statistically analysed to evaluate the models' significance. To this end, for every trained SNN model, an activation level was measured through computing the average value of its connection weights. The ANOVA statistical analysis was applied to the activation levels of several trained SNN models to evaluate the significance of the models.

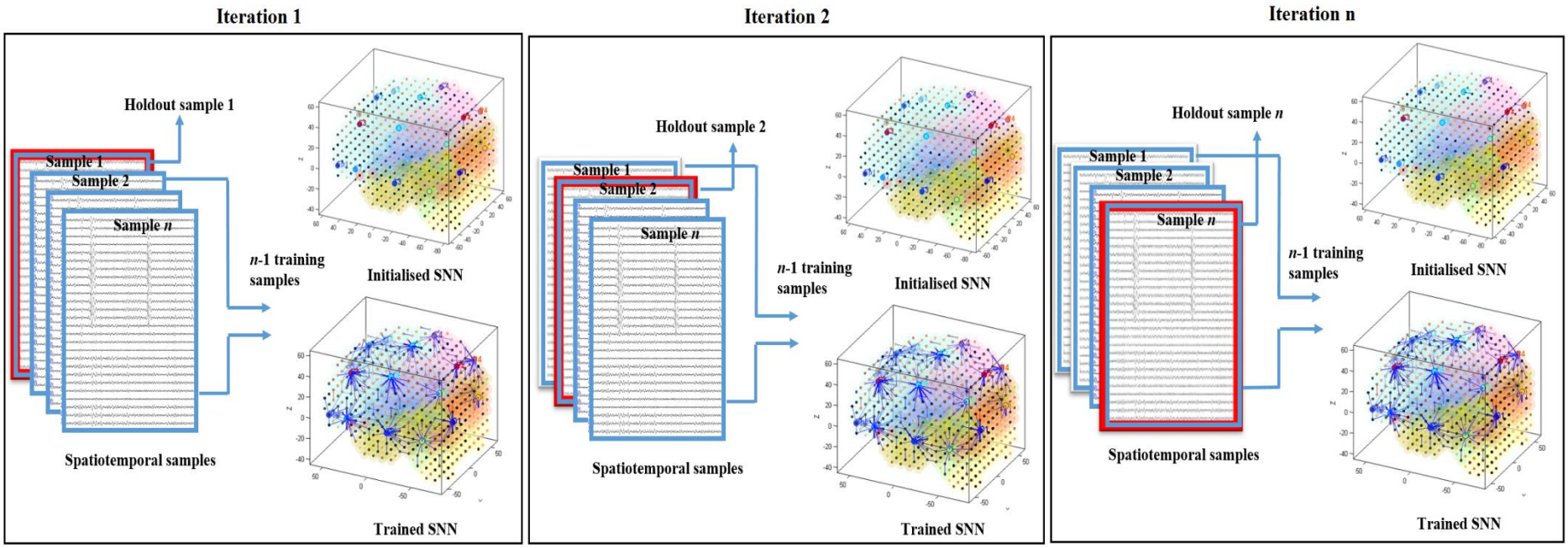

Figure 4-4. Iterative SNN modelling through the leave-one-out method. For n samples, the SNN model is initialised n times, and trained by a fold of different (n-1) samples. Then the trained model is cross-validated by the hold-out sample.

4.5 Applying the Designed SNN Methods for Real-Life Scenarios in Psychology

Employing a designed SNN method, this thesis contributes to an improved modelling, better understanding, interpretation, and analysis in the following real-life case studies (A) neuromarketing and (B) neurobiological effects of mindfulness training.

-**Case study A** — this study is conducted to model the brain activity patterns, measured by ERP, while participants are performing a marketing-related task. The objective here is to build an appropriate model of ERP that can capture the interactive spatiotemporal patterns that are involved in the processing of different marketing stimuli. In this study, the SNN models are also designed to distinguish different features of marketing products based on the activation of different brain networks, reflected in the dynamic patterns of ERP data. To this end, the following empirical studies are designed:

1. **Dynamic pattern recognition**:
   - ✓ Building of SNN models to investigate the differences between ERP patterns of perceiving familiar vs unfamiliar marketing logos at sub-conscious level (this is presented in chapter 5).
2. **Pattern prediction:**
   - ✓ Building of SNN models to study whether the familiar and unfamiliar logos are distinguishable at an earlier stage of information processing. This comes to the fore when developing a predictive system of human choice behaviour (this is presented in chapter 5).

-**Case study B —** this study is performed to investigate how the brain activity patterns, measured by EEG, are modified by mindfulness training. The objective here

is to model the EEG data that are measured at both “before” and “after” the mindfulness training to investigate the brain neural changes.

To this end, the following empirical studies are designed:

1. **Dynamic pattern recognition**:
   - ✓ Building of SNN models to investigate the effects of mindfulness on the EEG of participants with a different level of depression (this is presented in chapter 6).
2. **Pattern prediction:**
   - ✓ Building of SNN models to study whether the effects of mindfulness training can be predicted at an earlier stage and for whom it might be the most beneficial (this is presented in chapters 6).

4.6 Chapter Summary

This chapter represents the designed in this study methods for the creation of SNN models in the framework of a brain-like SNN architecture. In the method for dynamic pattern recognition, the trained SNN models are used for determining the patterns in EEG and ERP samples that belong to different mental activities. This is performed through an empirical study that involves mapping, learning, and classifying of EEG/ERP samples. Also, the SNN models of different mental activities are visualised in a 3D space and then statistically analysed to evaluate the level of significance.

In the method for pattern prediction, the SNN models are trained to detect the predictive patterns of mental activities in an earlier stage when the models are learning from streaming EEG/ERP samples over time. This leads to classifying the EEG and ERP samples into pre-defined mental activities.

The next chapter represents the application of the above two method for the creation of a SNN model for pattern recognition/prediction of ERP data to investigate the complexity of the brain subconscious processes during a neuromarketing experiment while familiar and unfamiliar marketing logos are presented.

4.7 Contribution

In this chapter, I have made the following contributions:

---

1. A designed SNN-based methodology for a better understanding, precise analysis of different types of STBD (EEG and ERP). This generic methodology includes several steps: cognitive task preparation, data collection, defining samples, data mapping, learning, visualising, classifying, and validating the results that can be efficiently applied to different real-life scenarios.
2. An optimally designed framework for empirical studies based on SNN architecture for both dynamic pattern recognition and prediction tasks of different types of STBD (EEG and ERP).

“Listen to what people say and what people don’t say. Unspoken words are usually the most important as they are the hidden secrets or truths”.

Sigmund Freud

Chapter 5 Study 1 in Psychology - Neuromarketing

5.1 Introduction

Understanding how human decision-making and preferences manifest before conscious thought has long challenged researchers focused on cognitive and information science. Now, the field of neuromarketing – a discipline that looks at the neurocognitive underpinnings of consumer behaviour – is starting to uncover, in amazing detail, exactly how the brain goes about recognising a brand. This chapter presents an SNN method that tracks brain responses to logos on the *millisecond* timescale even before conscious thoughts are formed. Section 5.2 of this chapter overviews the neuromarketing and the role of brain sub-conscious process in a consumer's preference. Section 5.3 represents the design of the experiment for pattern recognition and prediction in real-life ERP data that measured the brain activity patterns of a number of consumers while perceiving familiar and unfamiliar marketing stimuli. Section 5.4 explained the cognitive task and ERP data recording. Finally, Section 5.5 reports the analytical results that include both statistical analysis and the SNN modelling of ERP.

5.2 Neuromarketing and the role of sub-conscious marketing stimuli processing in Consumers' Preferences

Neuromarketing is a novel area that has been developed to understand the neurobiological mechanisms underpinning preferences towards marketing stimuli, with the view to predicting differences in consumer thought processes that might not necessarily be observable in overt behaviour (Brammer, 2004; Charron, Fuchs, & Oullier,

2008; N. Lee, Broderick, & Chamberlain, 2007; Touhami et al., 2011; Zurawicki, 2010). "Branding" can be considered a major factor in consumer purchasing behaviour; thus, "brand familiarity" is typically a proxy for consumer's preferences towards products (McClure et al., 2004; Shang, Pei, Dai, & Wang, 2017; Wang, Chang, & Chuang, 2016). Recent theories of response to branding distinguish sub-processes such as brand attachment and attitude towards a brand (Whan Park, MacInnis, Priester, Eisingerich, & Iacobucci, 2010) and proposes that a preference towards familiar stimuli may occur at an early stage in information processing. Understanding how these early stages of processing are affected by familiarity, e.g. by logos, has important theoretical implications in the models of memory in general and applications to neuromarketing in terms of objective evaluation of product presentation and development. Consumers continuously operate with some degree of automaticity. Familiarity provokes automaticity, whilst perception and integration of features in unfamiliar stimuli require greater cognitive effort (Bargh, 2002; Bargh, Chen, & Burrows, 1996; Dijksterhuis & Nordgren, 2006; Martin & Morich, 2011). Most research on familiarity has been conducted in relation to faces, for which distinct neural mechanisms have been proposed for various types of familiarity (e.g. famous or personally familiar faces (Natu & O'Toole, 2011). Automaticity-related studies suggest consumers are unaware of the interior mechanisms that drive their decisions (Bargh, 2002) such claims might be strengthened by expanding the currently limited empirical evidence from neurocognitive measures.

Although the last three decades have witnessed development in the mechanistic understanding of conscious behaviour in consumers (Dijksterhuis, 2004; Dijksterhuis & Nordgren, 2006; N. Martin & Morich, 2011), models of unconscious decisions making and choices in the context of neuromarketing have not been fully delineated.

The recent years have been characterised by an increasing interest in the very early visual ERP components, happening before 300ms after stimulus onset. These early processes, and in particular, the early components (N100 and P200), were thought to be only modulated by the physical characteristics of the triggering stimulus, but immune to endogenous modulations, and more specifically attention (Martínez et al. 1999; Noesselt et al. 2002; Di Russo et al. 2003; Hillyard et al. 1998).

According to the large studies on the amplitude of the visual N1 component, the N1 has provided a wealth of evidence about attentional processes (Luck, 2014; Luck & Kappenman, 2012). When attention is focused on areas of the visual field in which relevant information is presented, the largest amplitude of the N1 can be observed that indicates a benefit of correctly allocating attentional resources and facilitates further perceptual processing of stimuli (Olofsson, Nordin, Sequeira, & Polich, 2008). Also, the N1 component is studied in conditions that require differentiation between classes of stimuli (Falkenstein, Hoormann, & Hohnsbein, 1999).

On the other hand, the P2 component has also been identified in many different cognitive tasks including selective attention (Johnson, 1989; Hackley, et al. 1990; Hillyard, et al., 1973), stimulus change (Naatanen, 1990), feature detection processes (Luck & Hillyard, 1994), and short-term memory (Golob & Starr, 2000; Starr & Barrett, 1987). The earlier visual P2 component is strongly sensitive to the emotional valence of a stimulus, regardless of whether evaluations are implicit or explicit.

While these results are extremely promising, as they suggest that the brain processes and modulates visual information more quickly than is generally thought, difficulties of replication (e.g., Santesso et al., 2008; Fu et al., 2010b) make it hard to draw conclusions on what underpinning mechanisms are at play. One possible reason for such inconsistencies is that experimental paradigms and methods vary widely.

In neuromarketing, few studies have investigated how a consumers brain initially react to stimuli in the very early stages (<300 ms) or modelling the related dynamic spatiotemporal brain activity (Campus, Sandini, Morrone, & Gori, 2017; Wu, Zhou, Qian, Gan, & Zhang, 2015). Prior studies have mostly focused on consumer buying behaviour in terms of directly attending to various marketing materials in their environment. However, a fundamental question is: *How do marketing materials influence consumers even when they are not consciously attending to them?*

Observing and understanding the specific details of how these processes occur dynamically over time (especially at a subconscious level) are not investigated in depth in current neuroscience research, and little work in computational neuroscience has been performed on this topic (Poldrack, 2017). The current chapter applies SNN architecture for modelling and analysing of early ERP components data that reveals the complexity of peri-perceptual processes of familiarity (Z. G. Doborjeh, Kasabov, Doborjeh, & Sumich, 2018). This case study includes the following objectives through two approaches:

a) Pattern recognition: To study and visualise the ERP patterns generated by familiar versus unfamiliar logos with respect to the spatiotemporal relationships between the continuous ERP data streams.

b) Prediction: To investigate the early brain responses and activities of consumers in the face of the marketing logos.

5.3 Experimental Design

The SNN-based methodology (that fully explained in Chapter 4), for mapping, modelling, learning, classifying and understanding of ERP data for this case study is depicted graphically in Figure 5-1. It is constituted of the following steps:

1. **Mapping**: Spatially map the ERP data into a 3D SNN model that represents a brain template.
2. **Learning**: Train the SNN model with the ERP epochs extracted within 50-200 milliseconds post-stimulus time window.
3. **Pattern visualisation**: Visualise the learnt patterns of interactions between the EEG channels over time as evolved chains of connectivity in the SNN model.
4. **Classification**: Classify the learned patterns of spiking activity when familiar and unfamiliar logos are presented.

The above experimental steps are elucidated using ERP data collected for the case study as the following procedure:

Firstly, a cognitive task was designed according to the standard paradigm (explained in Chapter 2 section 2.4) and the ERP data was recorded when participants were performing the cognitive task. Secondly, the WinEEG[1] (Mitsar system) was used to derive grand-averaged ERP waveforms across 19 channels.

To create the computational modelling, the ERP data was encoded into spike sequences using a TBR method (TBR was explained in Chapter 3, section 3.1.1). If the change of the intensity value exceeds a TBR threshold, a spike occurs. To investigate the consumer performance towards familiar-related logos versus unfamiliar-related logos, ERP time series of different time intervals (50, 100, 150 and 200ms after stimuli presentation) related to the peri-perpetual processes of the brain were used. The ERP data were spatially mapped into 3D SNN models using a standard mapping as follows:

[1] http://www.mitsar-medical.com/eeg-software/qeeg-software/download.html.

- Mapping of the ERP data coordinates to standard brain template coordinates (Talairach) and then mapping the template coordinates into an SNN model. For every input from ERP data, the nearest Talairach-based coordinate in the relevant Brodmann area are found in Appendix Table A-1.
- The mapped SNN models are initialised using the SW connectivity rule (the SWC was explained in Chapter 3, section 3.1.1) and then the model connectivity is modified and adapted through STBD of temporal data. The SNN model connectivity and spiking activity are visualised to reveal a better understanding and interpretation of the interaction between multivariate ERP data.
- The average weight of all neural connections in each SNN model is also extracted as a metric for comparison.

Subsequently, consecutive snapshots of the firing state of the neurons were captured to represent a trajectory of dynamic, deep-learned patterns of neurons' spiking activity with respect to the temporal order in which clusters of neurons emitted spikes.

Finally, the deSNN classifier (deSNN was explained in Chapter 3, Sec 3.1.3) is trained using the training data and then is tested using new unknown data samples. An SNN supervised learning algorithm was applied to train a classifier to identify whether SNN model activity was generated in response to the familiar or unfamiliar logo. The classification accuracy is optimised and the best accuracy along with the best parameters are reported.

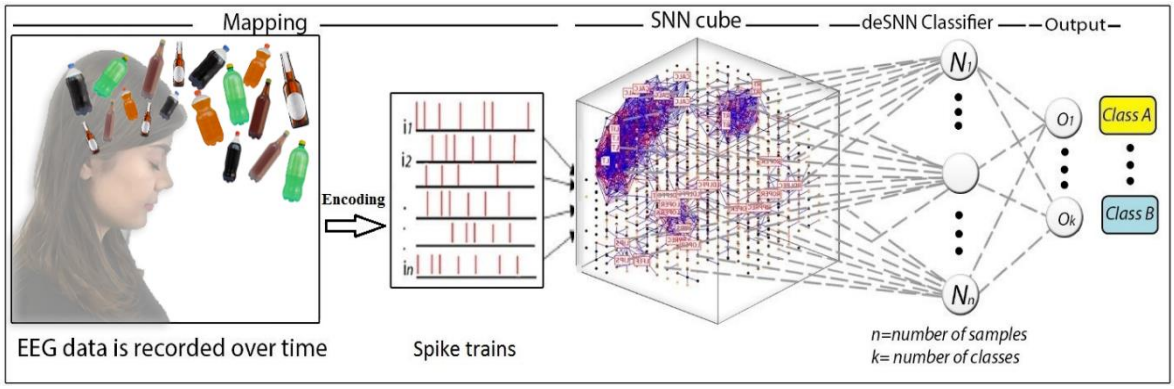

Figure 5-1. The SNN architecture performs as follows: encoding EEG data as spike sequences; mapping of these sequences into a 3D SNN model created with the use of a brain template; unsupervised learning of the spike sequences in the SNN model; supervised learning and classification of the learned patterns in a SNN classifier.

5.3.1 ERP Data Acquisition and Cognitive Task Description

Twenty right-handed volunteers, who had no neurological abnormalities, participated in the data acquisition procedure (10 males with Mean age of 24.40 and Standard Deviation= 1.33; 10 females with Mean age of 22.60 and Standard Deviation = 2.87). The recording procedure was performed in the "Hamrah Clinic" of Tabriz, Iran. Prior to commencing this research, ethical approval was granted by the Ethics Committee of the Hamrah Clinic, Tabriz, Iran, and informed consent were provided by all participants. Identifying information of participants, including names and initials, is not reported in the written descriptions.

Prior to completing the task, participants listened to a short story about choosing a drink brand, in order to equalise the participants' context and engage their attention to the paradigm. Participants completed a visual oddball paradigm (García-Larrea et al., 1992; Jongsma et al., 2013) (Oddball Task was explained in Chapter 2, Sec 2.4) that consisted of three blocks. Every block started with the target logo presentation (a logo for water) that was presented 28 times in each block randomly (pre-set order) dispersed among 8 non-target logos (4 locally widely familiar logos and 4 non-familiar logos), each presented 14 times. Thus, 140 stimuli (duration = 200ms; interstimulus interval = 1300-1500ms) were presented in each block. Participants were instructed to respond to the

target logo as soon as they observed it on the screen (counterbalanced across participants to press either the left or right mouse button with left or right hand). In this task, the same target stimulus was used for all the participants. Prior to designing the cognitive task, brand familiarity was measured using a survey that was done in various local supermarkets in the city where the EEG data were recorded[1].

EEG was measured through nineteen channels: C3, CZ, C4, F7, F3, FZ, F4, F8, P3, PZ, P4, T3, T4, T5, T6, FP1, FP2, O1, and O2 positioned in an adaptable cap with the standard 10–20 configuration. The EEG data sampling rate was 256 Hz. The channel Fpz was used as a ground electrode, and all the channels' impedances were under 5 kΩ. Off-line artefact rejection was used to eliminate the effects of eye/muscle movements. To run the cognitive task on a PC monitor, Psytask software[2] was used as a stimulus presentation system. During the task presentation, ERPs were also measured along with EEG data.

- **Dataset and sample files preparation:**

The dataset used in this study corresponds to a task of dealing with marketing stimuli (familiar and unfamiliar stimuli). This task was performed on twenty participants and ERP data was samples from 19 channels at a sampling rate of 258 Hz. Forty samples were created (20 for familiar and 20 for unfamiliar), each sample file (sam1.csv, sam2.csv, sam3.csv…..sam20.csv) contains data of one participant. Each sample corresponds to a data matrix arranged in comma separated format. The rows correspond to ordered times points, and the columns are the EEG channels.

[11] Before designing the cognitive task and selecting the brands, brand familiarity was measured using a survey which has been done in different local supermarkets in the city, where the EEG data was recorded. Therefore, a comprehensive information was collected in terms of:

- Well known/unknown local brands.
- The brands that were frequently requested by consumers in the supermarkets, etc.

Through this survey, the most local familiar and unfamiliar brands as the stimuli set was selected.

[2] PSYTASK is a software for visual/auditory stimuli presentation and psychophysiology investigations.
PSYTASK works together with WinEEG software and provides a synchronous stimuli presentation with EEG recording. The recoded data is used for event related potentials (ERP) and/or event related desynchronization (ERD) calculation and analysis.

5.4 Results

The experimental results are categorised as follows:

- Statistical ERP components analysis.
- Pattern recognition and prediction in ERP using SNN models.

5.4.1 Statistical ERP components analysis

As an initial analysis, WinEEG (Mitsar system) was used to derive grand-averaged ERP waveforms across 19 channels. Analysis of ERPs was confined to occipital and parietal electrodes – O1, O2, P3 and P4 – where the peak amplitudes for early ERP components (P100, N100, and P200) were maximal compared to other sites as shown in Figure 5-2 and Figure 5-3. In order to study how different areas of the brain responded towards marketing stimuli, EEG channels were clustered into five sites with respect to their topological information as depicted in Figure 5-4. The five sites are: frontal, parietal, central, temporal, and occipital.

The mean amplitude for early ERP components (P100, 70-180; N100, 100-180ms; and P200, 180-240ms) across all 19 electrodes are reported in Table 5-1 and descriptive statistic of mean values for five sites of the brain (frontal, parietal, central, temporal and occipital), both hemisphere (left and right), both types of stimuli (familiar and unfamiliar) and for early ERP components are reported in Appendix Tables B- 1, B- 2 and B- 3.

As reported in Table 5-1, the mean amplitudes of P100 in parietal and occipital lobes; N100 in occipital lobe were higher in the right hemisphere for familiar logos than unfamiliar ones. The mean amplitudes of P200 were also higher in parietal and occipital lobes compared with other sites of the brain.

To determine if the variables of the study are statistically significant, Analysis of variance (ANOVA) was used to test for difference between variables (ANOVA) (Field, 2013) and is reported in Table 5-2.

Repeated-measures ANOVA was performed separately for each time window (P1, P2, and N1), with respect to three within subjects' variables, including, *Hemispheres* (left and right), *Sites* (frontal, parietal, central, temporal and occipital), *Conditions* (familiar and unfamiliar), and *Components* (P1, P2 and N1). Figure 5-5 shows the line graphs of mean amplitude values as a function of *Sites, Conditions,* and *components*.

As shown in Table 5-2, for the P1 ERP component, there was a significant main effect of *Hemisphere* [F (1, 19)=9.15, p=0.007, η^2 = 0.32 (LH<RH); *Sites* effect [(2.44, 46.46)=19.76, p=0.001, η^2 = 0.51] (Parietal>Occipital>Temporal>Frontal=Central) ; and *conditions* effect [(142.07,1.41)=100.51, p=0.001, η^2 = 0.84] (Familiar>Unfamiliar). Through the lower ANOVA analysis, for the "parietal" P100 amplitude, there was a significant main effect of the factor *Sites* [F (1, 19) =4.54, p =0.04 and a significant *Hemisphere and conditions* interaction [F (1, 19) = 4.61, p =0.01]. For the P100, higher amplitude values towards familiar stimuli at all sites of the brain can be observed.

For the N1 amplitude, there was a significant main effect of *Hemisphere* [F (1, 19)=8.98, p=0.007, η^2 = 0.32; *Conditions* effect [(1,19)=138.48, p=0.001, η^2 = 0.88] ; *Hemisphere and Sites interaction* [(2.25, 42.83)=72.77, p=0.001, η^2 = 0.79]; and *Site and Conditions interaction* [(1.55, 29.46)=105.46, p=0.001, η^2 = 0.85]. Through the lower ANOVA analysis, for the "occipital" N100 amplitude, there were significant main effects of *Hemisphere* [F (1, 19) = 11.45, p = 0.01)] and *Conditions* [F (1, 19) = 3.51, p = 0.01]. A significant interaction between *Sites and Conditions* was also observed [F (1, 19) = 4.66, p = 0.04)]. For the N100, significant changes between familiar and unfamiliar

stimuli can be only seen at Occipital site, no changes between stimuli is observed at other sites.

For the P2 amplitude, there was a significant main effect of *Sites* [F (4, 39.66)=229.49, p=0.001, η^2 = 0.92; *Conditions* effect [(1,19)=31.14, p=0.001, η^2 = 0.62] ; *Hemisphere and Sites interaction* [(2.96, 56.17)=16.40, p=0.001, η^2 = 0.46]; and *Hemisphere and Conditions interaction* [(1, 19)=19.04, p=0.001, η^2 = 0.50]. Through the lower ANOVA analysis, for the parietal P200 amplitude, there was a significant main effect of the factor *conditions* [F (1, 18) =4.54, p =0.04 and a significant *Hemisphere and Conditions interaction* [F (1, 18) = 4.61, p =0.01]. For the P200, higher amplitude values towards both familiar and unfamiliar stimuli at Occipital and Parietal sites than other sites (Temporal, Central and Frontal) were observed. Details are reported in Table 5-2.

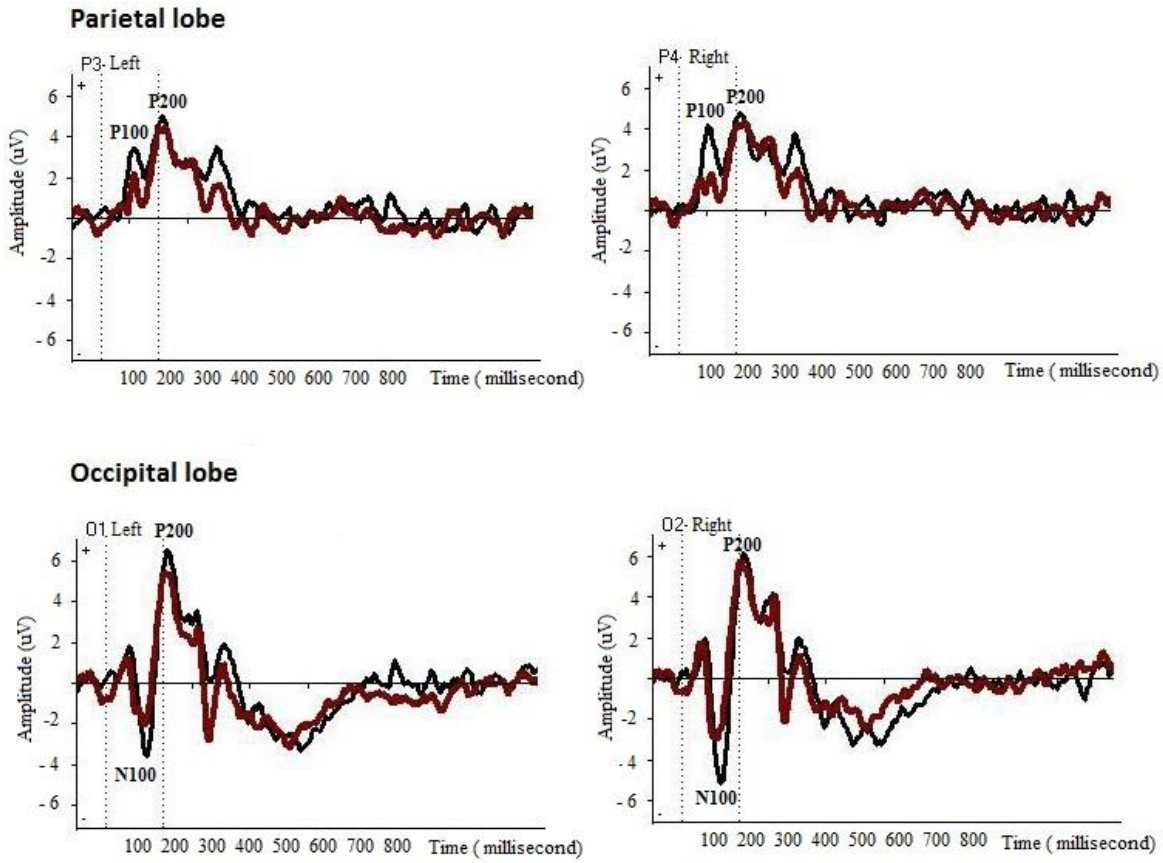

Figure 5-2. Grand average ERP waveforms of all participants across 800-milliseconds epoch after familiar versus unfamiliar marketing stimuli presentation. Peak amplitudes correspond to the P100, N100 and P200 components of ERPs across the EEG channels located at posterior areas of the brain (O1, O2, P3 and P4 channels). Black line = familiar logos; red line = unfamiliar logos.

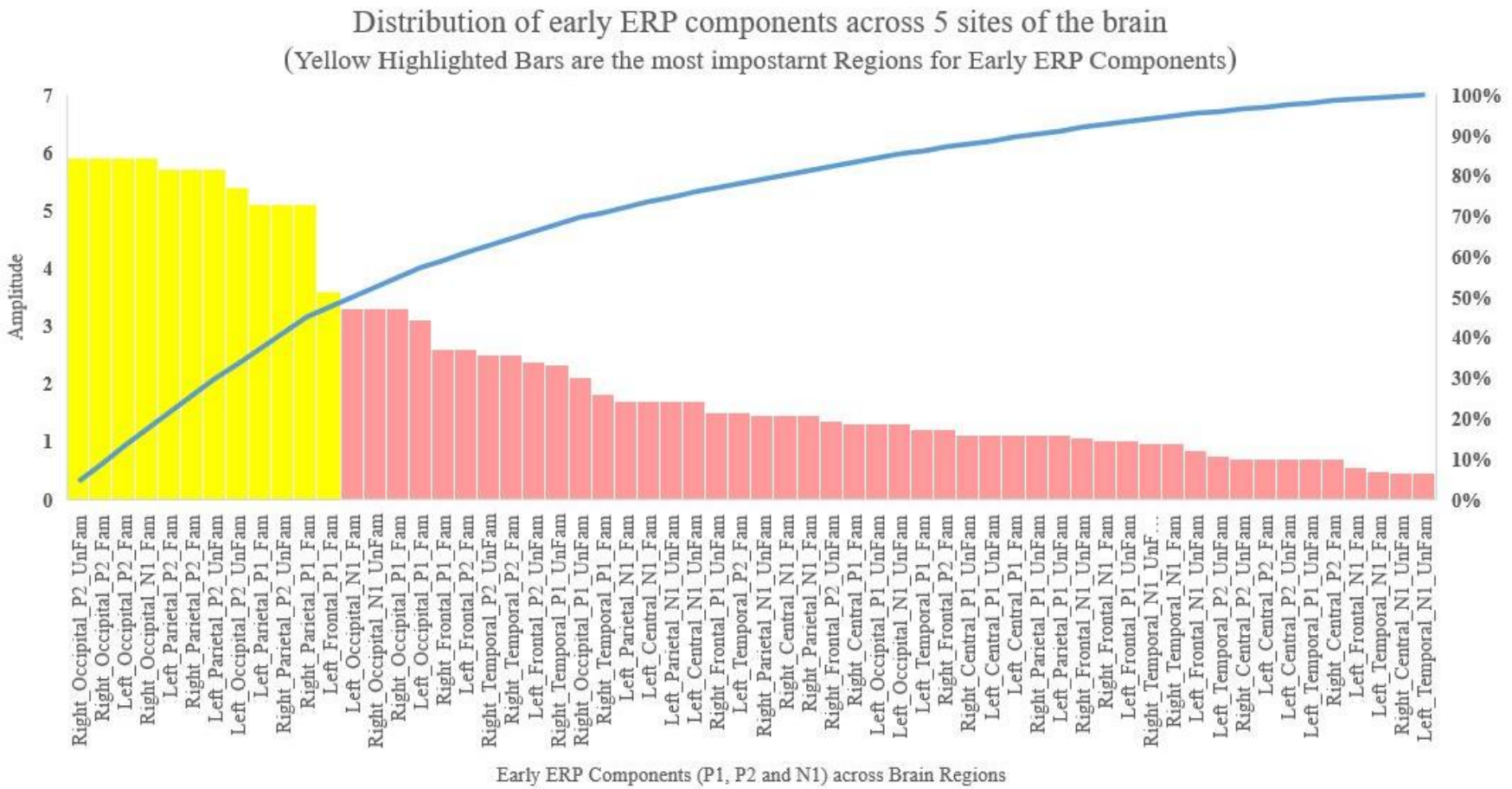

Figure 5-3. A pareto chart showing distribution of early ERP (P1, P2 and N1) components across five sites of the brain (Frontal, Temporal, Central, Parietal and Occipital) for both familiar and unfamiliar stimuli that represented in descending order by bars. The left vertical axis is the mean amplitude values. The right vertical axis is the cumulative percentage of the total values of the variables. It shows early ERP components are mostly distributed with higher amplitudes across the posterior regions of the brain (Occipital and Parietal-highlighted in yellow color) in compared with other sites of the brain (highlighted in pink color).

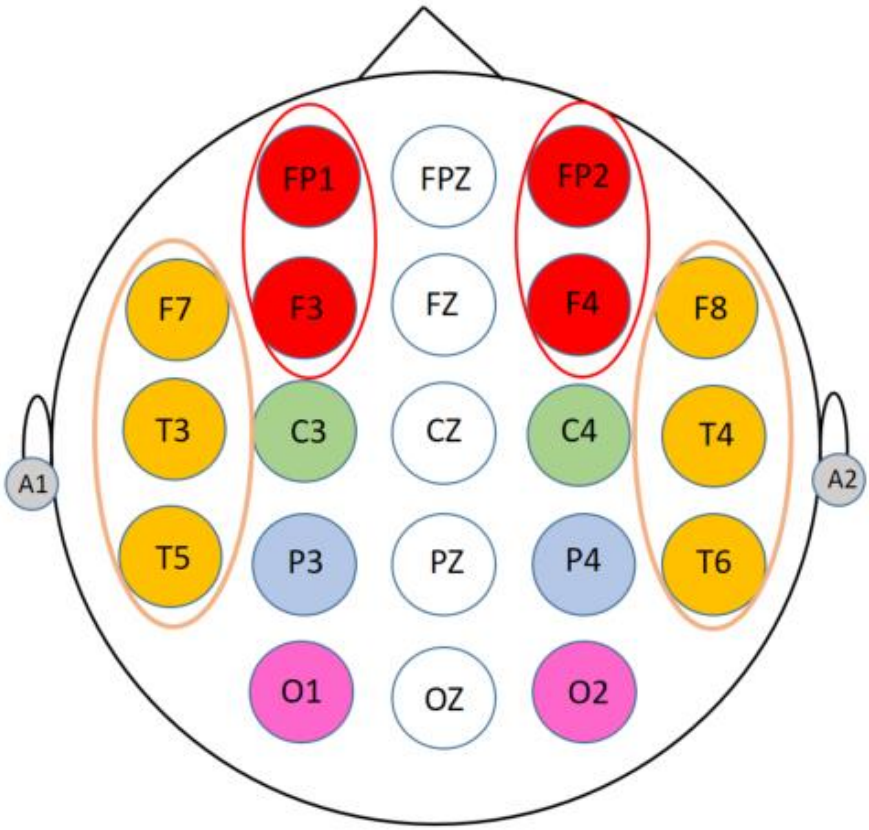

Figure 5-4. Clustering of EEG channels into five sites for both hemisphere (left and right) with respect to their topological information including: Left Frontal (Fp1 and F3); Right Frontal (Fp2 and F2); Left Central (C3); Right Central (C4); Left Temporal (F7, T3 and T5); Right Temporal (F8, T4 and T6); Left Parietal (P3); Right Parietal (P4); Left Occipital (O1); and Right Occipital (O2).

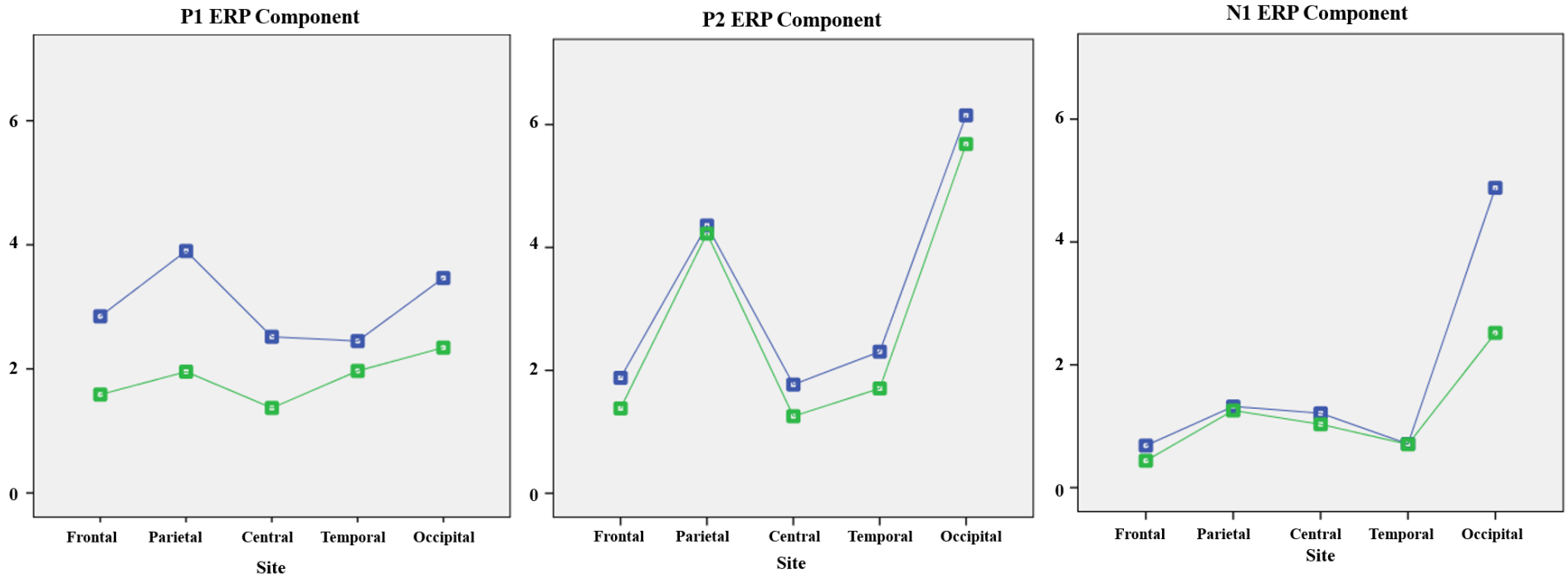

Figure 5-5. The mean amplitude values of early ERP components (P1, P2 and N1) towards familiar and unfamiliar stimuli at Frontal, Parietal, Central, Temporal and Occipital. Green line corresponding to the unfamiliar stimuli and blue line representing the familiar stimuli.

Table 5-1. The mean amplitude of early ERP components (P100, P200 and N100) for familiar and unfamiliar logos across 19 EEG electrodes, averaged for all participants. It shows higher mean amplitude across EEG channels located in posterior brain regions (P3, P4, O1 and O2) towards familiar stimuli than unfamiliar one.

Electrodes	**Mean amplitude of ERP components (P100)**		**Mean amplitude of ERP components (P200)**		**Mean amplitude of ERP components (N100)**	
	Familiar stimuli	**Unfamiliar Stimuli**	**Familiar stimuli**	**Unfamiliar Stimuli**	**Familiar stimuli**	**Unfamiliar Stimuli**
Fp1	3.11	1.6	2.1	1.4	-1.2	-0.3
Fp2	2.7	1.3	1.6	1.3	-0.7	-0.4
F7	1.7	0.4	1.2	0.3	-0.2	-0.3
F3	3.14	1.34	2.3	1.6	-0.5	-0.6
Fz	3.12	1.4	2.3	1.2	-0/3	-0.4
F4	2.45	2.11	1.47	1.23	-0.34	-0.43
F8	2.13	1.2	1.3	0.6	-0.3	-0.33
T3	1.61	0.58	1.2	0.3	-0.3	-0.23
C3	2.38	1.22	1.88	1.25	-0.76	-0.65
Cz	2.9	1.6	1.99	1.2	-0.54	-0.45
C4	2.66	1.52	1.65	1.3	-0.54	-0.42
T4	2.37	1/8	1/9	1/53	-0/32	-0.25
T5	2.70	2.48	3.11	2.32	-0.46	-0.53
P3	**3.77**	**2.02**	**4.33**	**4.25**	**-1.88**	**-1.65**
Pz	3.62	2.11	2.13	1.88	-0.87	-0.88
P4	**4.02**	**1.89**	**4.38**	**4.20**	**-0.76**	**-0.87**
T6	3.11	2.98	2.98	2.66	-1.76	-1.80
O1	**3.27**	**2.70**	**6.21**	**5.41**	**-3.96**	**-2.48**
O2	**3.66**	**1.99**	**6.09**	**5.96**	**-5.80**	**-2.56**

Table 5-2. Repeated-measures ANOVA for the early ERP components P100, N100 and P200 at (P<0.05).

	F	Df	p*	eta	Post Hoc Test
For P1 window					
Hem*	9.15	1,19	.007	.32	RH>LH
Sites	19.76	2.44, 46.46	<.001	.51	Familiar stimuli: Parietal>Occipital>Frontal>Temporal=Central Unfamiliar stimuli: Occipital>Temporal>Parietal>Frontal>Central
Conditions	100.51	142.07,1.41	<.001	.84	Familiar>Unfamiliar
Hem*Sites	7.94	4, 52.04	<.001	.29	Effect of Hem (RH>LH)
For N1 Window					
Hem	8.98	1,19	.007	32	RH>LH
Conditions	138.48	1,19	<.001	.88	Familiar>Unfamiliar
Hem*Sites	72.77	2.25,4 2.83	<.001	.79	Left Hem: Occipital>Parietal=Central>Frontal>Temporal Right Hem: Occipital>Temporal>Parietal>Central=Frontal
Sites*Conditions	105.46	1.55, 29.46	<.001	.85	Familiar>unfamiliar Occipital>Parietal>Central>Frontal=Temporal
For P2 Window					
Sites	229.49	4, 39.66	<.001	.92	
Conditions	31.14	1, 19	<.001	.62	
Hem*Sites	16.40	2.96, 56.17	<.001	.46	Left=Right at Occipital and Parietal Right>Left at Frontal, Central and Temporal
Hem*Conditions	19.04	1, 19	<.001	.50	Familiar>Unfamiliar Occipital>Parietal>Central=Frontal>Temporal

***H: Hemisphere**
***P<0.05**

5.4.2 ERP Pattern Recognition and Prediction using SNN-based Methodology

To investigate the consumer brain responses towards familiar-related logos versus unfamiliar-related logos, ERP time series of different time intervals (50, 100, 150 and 200ms after stimuli presentation) related to the peri-perpetual processes of the brain were used. Figure 5-6 and Figure 5-7 show a spatial mapping of EEG electrodes into the same 3D space of spiking neurons, positioned according to the Talairach template (Giacometti et al., 2014; Talairach & Tournoux, 1988). The generated spike trains from EEG channels are then entered into the specially mapped SNN models via input neurons and the spatiotemporal patterns of EEG data were captured in the form of neuronal connectivity.

Figure 5-6 and Figure 5-7 visualise the neuronal connections created during the STDP learning in the SNN models, reflecting the dynamic patterns of EEG data corresponding to different epoch lengths: 100ms, 150ms, and 200ms after the presentation of familiar and unfamiliar marketing logos. The average weight of all neuronal connections in each

SNN model is also reported in Figure 5-6 and Figure 5-7 as a metric for comparison. In Appendix Table B-4, the average weight of the neuronal connections that were formed around each EEG channel (between input neurons and its connected neurons) were reported. Appendix Figures B- 6, B- 7 and B- 8 also plot the connection strengths of all EEG inputs in the SNN models of familiar and unfamiliar marketing stimuli at three times (100, 150 and 200ms). The connections, generated during learning for an input neuron, reflect on the changes of the data in the corresponding EEG channel. As many input neurons spike at different times, reflecting on the dynamics of brain activity, clusters of neurons get connected in a chain, reflecting on the temporal dynamics in the multivariable brain data. The SNN creates a functional connectivity model, where many-to-many neurons become connected to capture functional dynamical patterns from the data, even though the learning rule is applied to neuron-to-neuron connections.

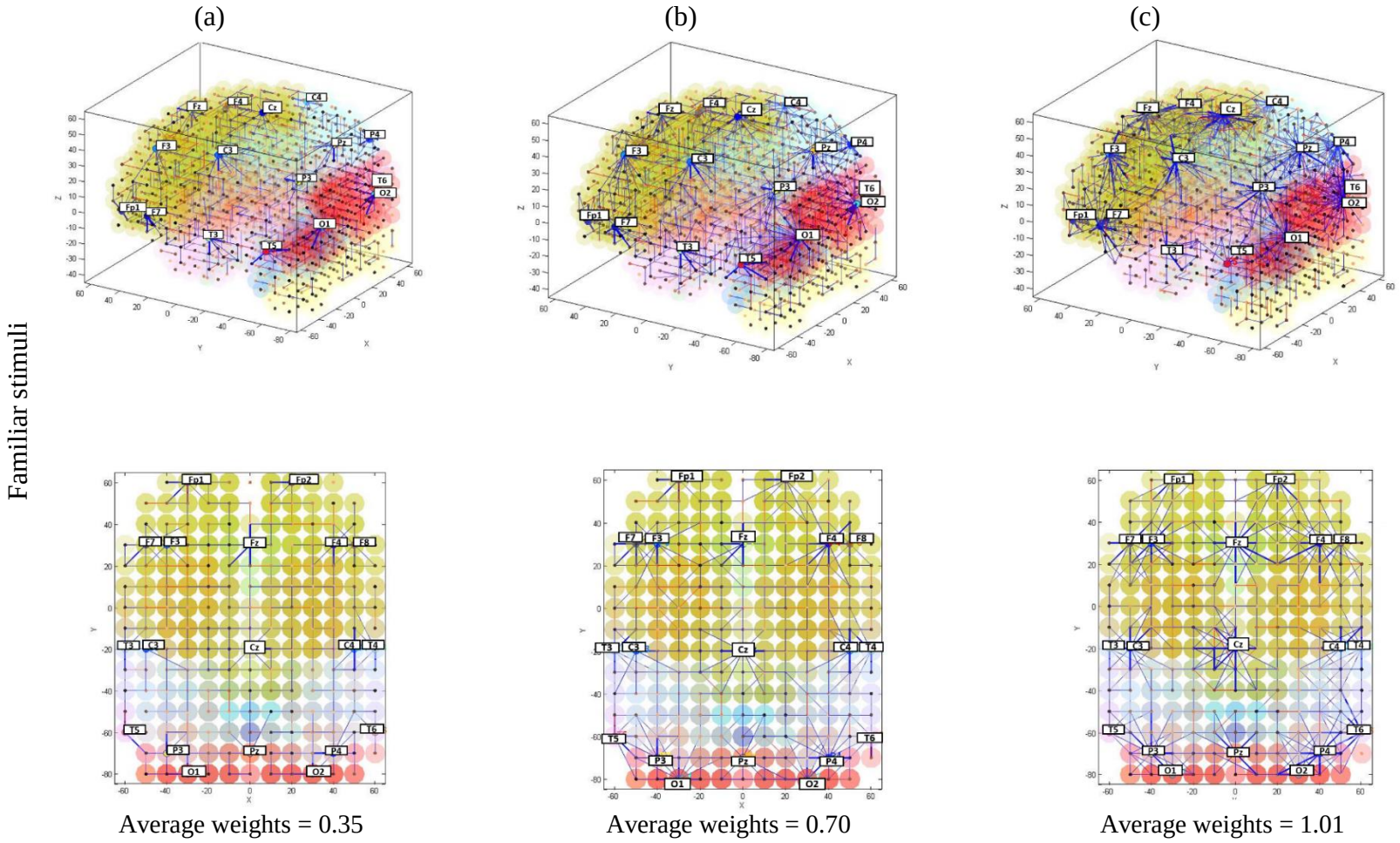

Figure 5-6. Neuronal connections created during learning in the SNN models, reflecting the dynamic patterns of EEG data corresponding to different epoch lengths: (a) 100ms, (b) 150ms and (c) 200ms after presentation of familiar marketing logos. Excitatory connections are represented by blue lines, while inhibitory ones are in red. The thicker the line, the greater the enhancement of the connection captured after the learning process. Neurons in the SNN models are labelled by eight brain areas from the Talairach template: Temporal (pink), Parietal (light-blue), Frontal (yellow-green), Sub-lobar (orange), Cerebellar (light yellow), Limbic (green), Pituitary (blue) and Occipital (red). The connection weights are averaged and reported for each SNN model. For a clear visualisation, we only visualised the connection weight greater than 0.08. The pictures show that familiar stimuli result in a higher connectivity and higher connection weights at average.

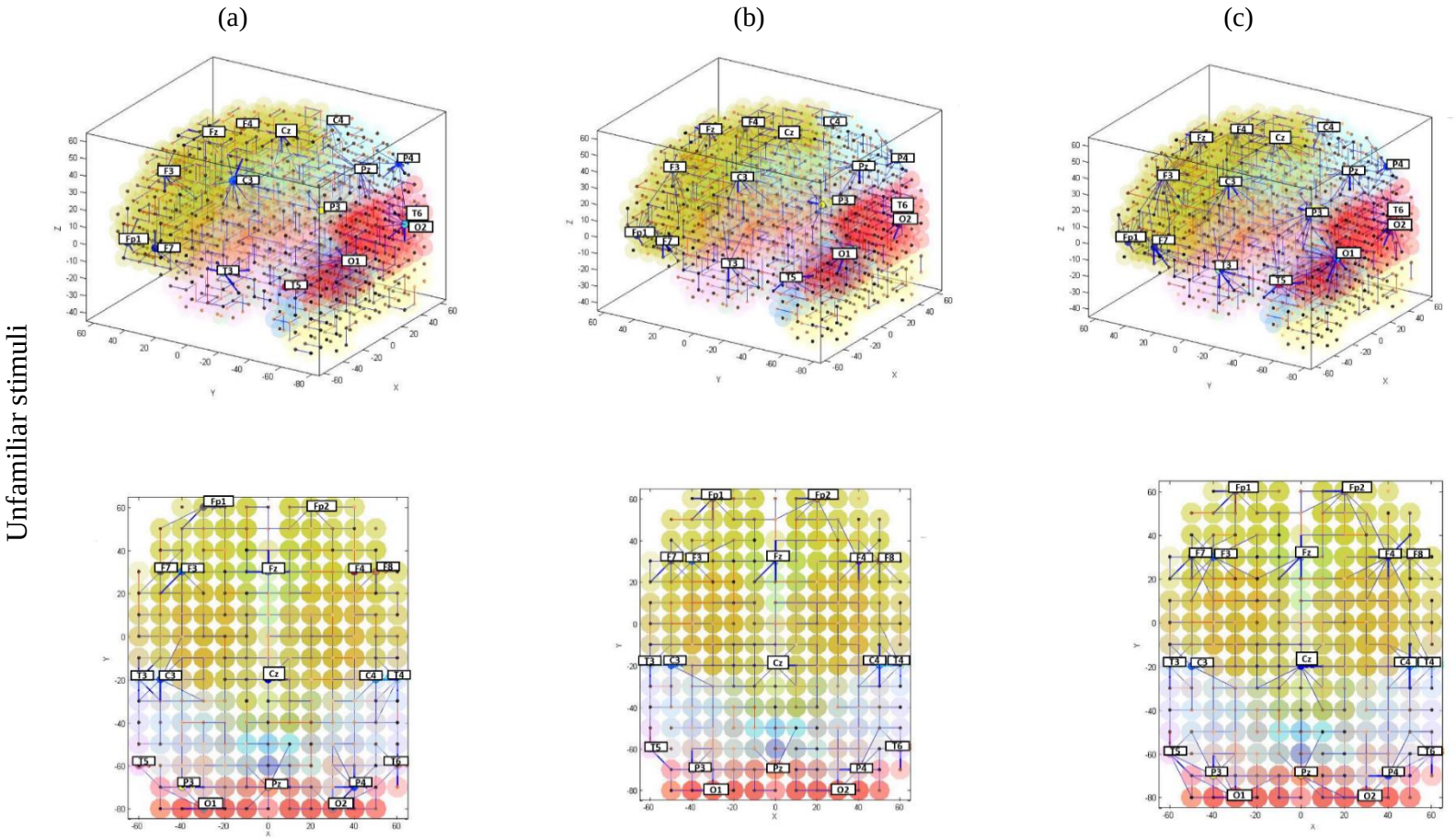

Figure 5-7. Neuronal connections created during learning in the SNN models, reflecting the dynamic patterns of EEG data corresponding to different epoch lengths: (a) 100ms, (b) 150ms and (c) 200ms after presentation of unfamiliar marketing logos. Excitatory connections are represented by blue lines, while inhibitory ones are in red. The thicker the line, the greater the enhancement of the connection captured after the learning process. Neurons in the SNN models are labelled by eight brain areas from the Talairach template: Temporal (pink), Parietal (light-blue), Frontal (yellow-green), Sub-lobar (orange), Cerebellar (light yellow), Limbic (green), Pituitary (blue) and Occipital (red). The connection weights are averaged and reported for each SNN model. For a clear visualisation, we only visualised the connection weight greater than 0.08. The pictures show that familiar stimuli result in a higher connectivity and higher connection weights at average.

During the STDP learning process in SNN models, consecutive snapshots of the firing state of the neurons were captured to represent a trajectory of dynamic, deep-learned patterns of neurons' spiking activity with respect to the temporal order in which clusters of neurons emitted spikes. Figure 5-8a and b illustrate the sequential spiking activity patterns in the SNN models for familiar and unfamiliar logos. The earlier a cluster of neurons (surrounding an EEG channel) fires in time (shown as red neurons, which their post-synaptic potential crosses the firing threshold and emits an output spike), the earlier spiking activity is observed in a chain of functional activity. It illustrates how early different areas of neurons in the SNN models fired (sent their spikes out) at different time points (every 50ms) towards familiar and unfamiliar logos. Although there was a similar pathway of spiking activity in both models, the size of the activated clusters of neurons was significantly different between the familiar logos and the unfamiliar ones. Numerical information about the number of spikes in time and space is also reported in Figure 5-8. A comparison between the activated neurons in SNN models, shown in Figure 5-8, is presented in Table 5-3. Appendix, Figures B- 9, B- 10, B- 11 and B- 12 plot the activated areas every 50ms towards familiar and unfamiliar stimuli in the SNN models.

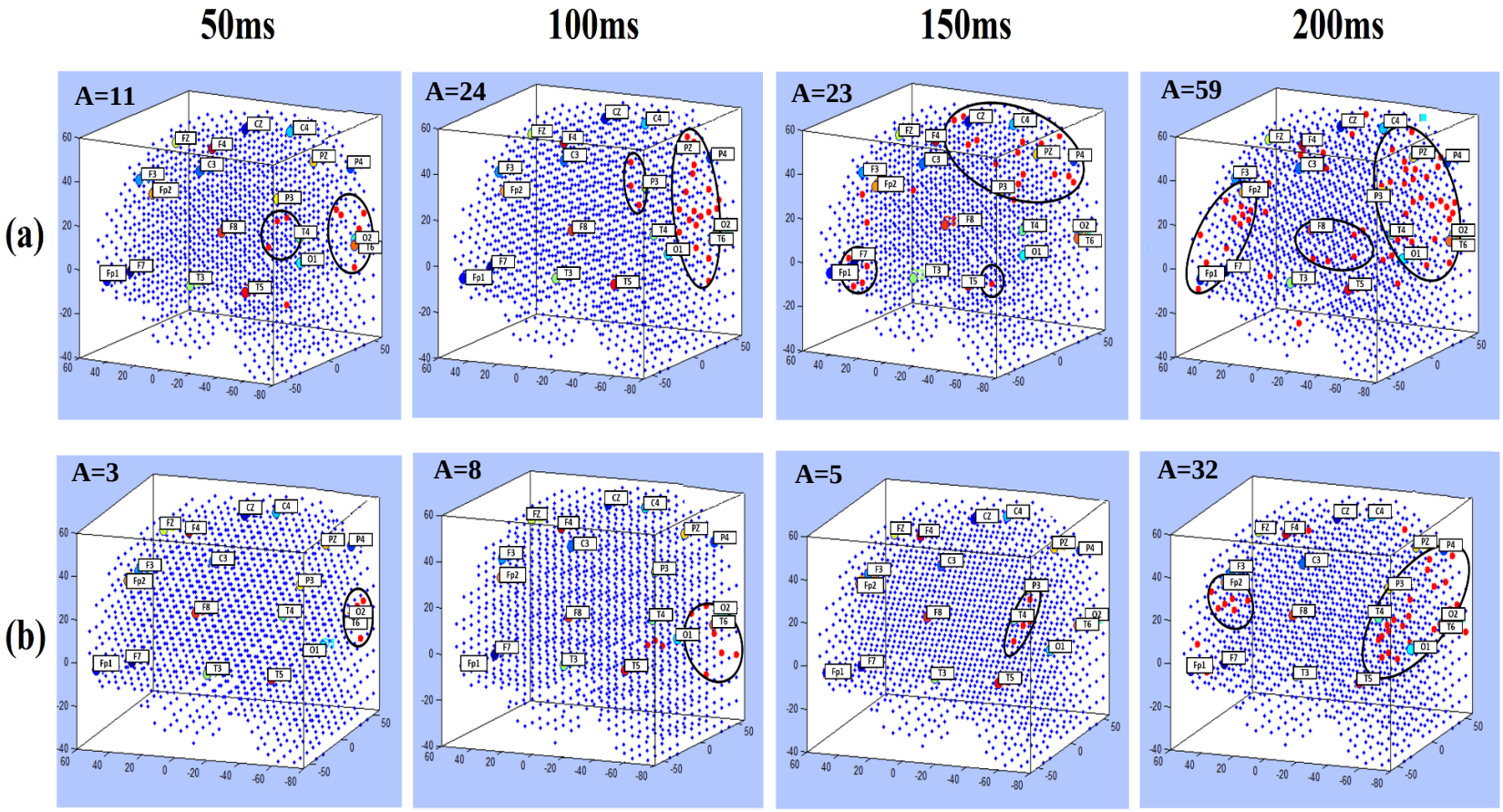

Figure 5-8 Clusters of active neurons (spiking) in the 3D SNN models are illustrated for every 50ms while learning from the input EEG data streams of (a) familiar logos and (b) unfamiliar ones. The value A refers to the number of active neurons at each time frame.

Table 5-3. The total number of spikes emitted by neurons at each time point for EEG epochs of 50ms, 100ms, 150ms, and 200ms.

	50	**100**	**150**	**200**
Familiar	11	24	24	59
Unfamiliar	3	8	5	32
Fam/UnFam	3.7	3.00	4.6	1.84

Considering the temporal order in which clusters of neurons around the EEG channels emitted spikes (red neurons) during 200ms (one frame every 50ms), a chain of sequentially activated areas as a trajectory of deep-learned patterns in the SNN models was captured. As illustrated in Figure 5-9, the trained SNN model forms a deep architecture as whole spiking input sequences which are learned as chains of spiking activities. Unlike hand-crafted layers used in second-generation neural networks (Amari, 2003; Bengio, 2009; Hinton, 2007; Hinton & Salakhutdinov, 2006; Schmidhuber, 2015), or randomly connected neurons in the computing reservoir of a liquid state machines (Izhikevich, 2006), the chains of directional connections established in this designed SNN model represent the spatiotemporal relationships (adapted over time) between the sources of the spike sequences (the input variables). Due to the scalable size of an SNN model, the chains of connected neurons are not restricted in length during learning, which can be considered as unrestricted deep learning, in contrast to existing deep learning methods that use a fixed number of layers.

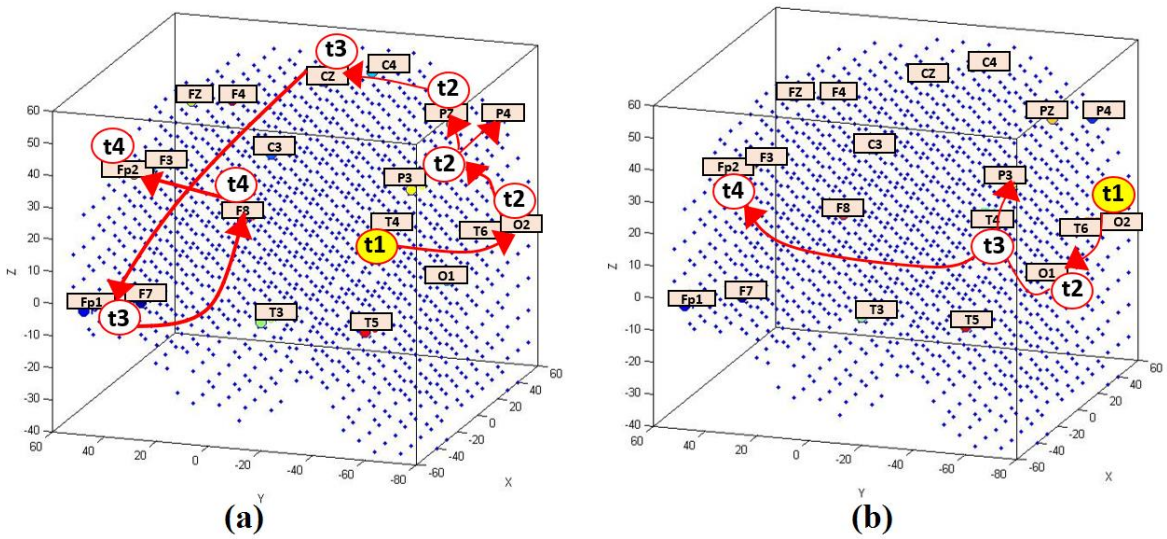

Figure 5-9. Spatiotemporal patterns of activities in the trained SNN models shown as trajectories of 4 aggregated stages (t1=50, t2=100, t3=150 and t4=200ms) during learning in the SNN models for (a) familiar logos versus (b) unfamiliar logos. In fact, the time for a deep-learning step in the SNN model is a millisecond, and the actual activation trajectories (chains) in the SNN are 200 neuronal clusters long, but here the activity of only 4 steps of learning are visualised.

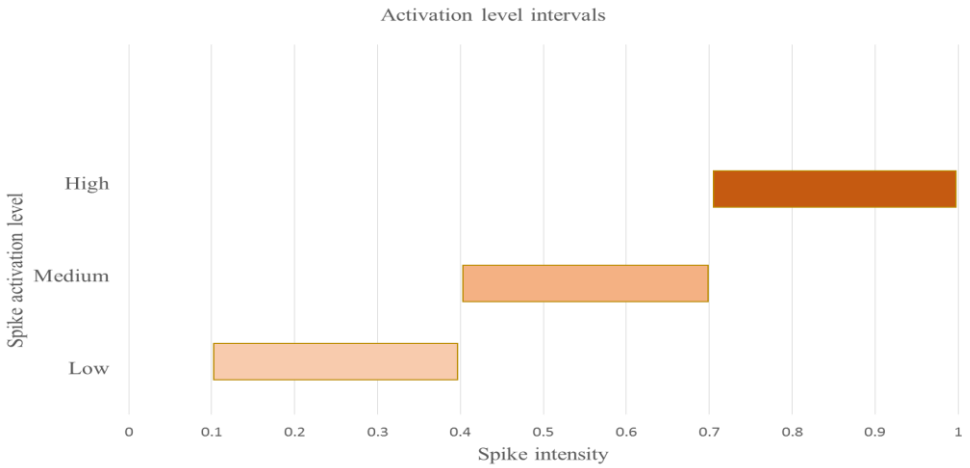

Figure 5-10 the levels of spike activation

During the STDP learning process, the intensity of the spikes in a cluster of neurons around each EEG channel is measured. The intensity is measured as a percentage of the number of neurons that fired among all the neurons that are connected to an EEG channel. The spike intensity is reported in Appendix B- 5. In Table 5-4, the activated areas in the SNN models are labelled as low, medium and strong levels of activation with respect to the number of spiking *neurons* involved at each time frame. As defined in Figure 5-10, the activation

level is categorised to low (from 0.1 to 0.4) medium (from 0.4 to 0.7) and high (from 0.7 to 1) representing the percentage of the fired neurons among all the connected neurons to an input neuron. The spike intensity in a cluster of neurons around each EEG channel *i* is defined as a percentage of the number of fired neurons divided by the number of connected neurons to *i*. The maximum level of activation at each time frame *t* is 1 which means all the connected neurons to *i* fire, while 0 refers to the minimum level of activation which means no neuron fires. This interval was partitioned to three levels as shown in Figure 5-10. This confirms the clear discrimination between perceptions of familiar versus unfamiliar logos at the subconscious level.

When the unsupervised training of the SNN models was completed, an SNN supervised learning algorithm was applied to train a classifier to identify whether SNN model activity was generated in response to the familiar or unfamiliar logo. As described in the ERP data acquisition section, twenty participants each performed a three-block cognitive task that involved the presentation of both familiar and unfamiliar stimuli. Therefore, for each participant, there are three EEG samples per class (6 samples per participant).

In total, 120 EEG data samples were used for the classification problem using a LOOCV method. This method involves the creation of 120 models, one for each sample of data, training the model using the remaining 119 samples, and testing the accuracy of each of these models for the left-out sample (unseen sample). For optimisation, an exhaustive grid search was performed on the combination of parameters for every model. Each parameter was searched within a range, specified by the minimum and maximum, through several iterations related to the number of steps for moving from minimum to maximum. For every model created out of 120 models, three main parameters (STDP learning rate, neuron firing threshold, and classifier parameter *mod*) were chosen to be optimised. The parameters were selected by assigning 10 steps between the minimum and maximum values of each parameter. Therefore, for every model creation, 1000 iterations of training (using 119 samples) and testing (using the single holdout sample) were performed using a different combination of these three parameters. Then the parameters that resulted in the best accuracy in most of the iterations, have been reported as the optimal parameters. When the optimisation procedure was completed, the most selected values for the parameters across all the 120 models were selected as: STDP learning rate= 0.01; neuron firing threshold= 0.5; deSNN classifier parameter mod= 0.4. Table 5-5 presents the overall classification accuracy for the two classes of stimuli. To perform a comparative analysis, conventional methods of MLP, MLR, and SVM were used for classification of EEG data as reported in Table 5-6. The classification problem was performed using LOOCV.

Table 5-4. The activated brain areas are reported according to the numbers of activated neurons in the SNN models during learning, over time steps: 50, 100, 150 and 200ms. The level of activation is denoted as low, medium and strong.

	Brain areas involved at different time frames				
Classes	**Activity intensity**	**50ms**	**100ms**	**150ms**	**200ms**
Familiar	**Low**	T4	P3	F7, Fp1	O1,F7,Fp1
	Medium	O2	Pz, O2, T6	Pz, P3, P4,Cz	F8
	Strong	-	-	-	O2, T4,Pz,P4, Fp2
Unfamiliar	**Low**	O2	O1, O2, T6	P3, T4	O2, T6
	Medium	-	-	-	O1, P4
	Strong	-	-	-	T4, Fp2

Table 5-5. The classification accuracy of 120 EEG samples of familiar logos (class 1) and unfamiliar logos (class 2) are obtained using leave-one-out cross validation in a SNN model. In the confusion table, the rows are the real values and the columns are the predicted values.

	The SNN-based methodology					
Real \ Predicted	**Familiar Stimuli (C1)**	**Unfamiliar Stimuli (C2)**	**Total accuracy %**	**F-Score %**	**Sensitivity %**	**Specificity %**
Familiar Stimuli (class C1)	**52**	8	**83.00**	84.00	84.00	86.00
Unfamiliar Stimuli (class C2)	10	**50**				

Table 5-6. The classification accuracy of EEG data using Multilayer Perceptron (MLP), Multiple Linear Regression (MLR) and Support Vector Machine (SVM) through leave-one-out cross validation (computed using NeuCom at www.theneucom.com). The MLP configuration is: Number of Hidden Units: 9; Number of Training Cycles: 1800; Output Value Precision: 0.0001; Output Function Precision: 0.0001; Output Activation Function: linear. The SVM configuration is: SVM kernel: Polynomial, Degree Gamma: 1.

	Traditional Machine Learning Methods		
Methods	**MLP (Multi-Layer Perceptron)**	**MLR (Multiple Linear Regression)**	**SVM (Support Vector Machine)**
Accuracy in %	47.50	37.50	37.50
F-Score	40.00	39.50	41.00

5.5 Discussion

This chapter presented a designed SNN architecture for modelling and learning from ERP data to capture differences in the dynamic brain activity patterns corresponding to peri-perceptual processes in response to familiar and unfamiliar stimuli, exemplified here as marketing logos.

As illustrated in Figure 5-2, Table 5-1, the ERP analysis indicates that familiar items are associated with larger response amplitudes over the posterior regions. This might mean that both kinds of stimuli drive activity over the same regions, but familiar items drive more activity. Beyond the ERP results, the designed SNN models discovered the

differences in the scalp areas involvement between familiar and unfamiliar logos at different time points. It means that SNN models can learn and identify which areas of the brain contribute to an increase in ERP and also - how does it happen over time. Such a conclusion could not be drawn from the ERP analysis only. In the current chapter, the SNN-based methodology is used in integrating the temporal and scalp topographic information, such that a better understanding of the pathways of information processing was obtained, in addition to have discrete measurements of neuronal response (e.g. ERP component amplitudes). The SNN models trained on familiar logos suggest stronger connections (Figure 5-6) even at early processing stages (e.g., 200ms), and across the EEG channels compared to the SNN models for unfamiliar logos. For unfamiliar logos (Figure 5-7), connections are generally uniform and cannot be differentiated between the channels at any processing stage in the SNN model.

Given that perceptual speed increases as individuals adapt to features of the environment, the current findings might reflect a more rapid spread of activation in response to familiar stimuli because they are more commonplace in individuals' environments. Alternatively, it could be that certain characteristic features of the familiar stimuli lead to greater activation across brain regions through activation of schemas (those cognitive frameworks or concepts that are used for organising and perceiving new information) (DiMaggio, 1997). Consumers pay more attention to the stimuli that assimilate into their schema while re-interpreting conflicts to the schema as exceptions or reshaping them to assimilate (Nadkarni & Narayanan, 2007). Indeed, consumers continuously operate with some degree of automaticity. The more familiar the stimuli, the more routine the behaviour (Ouellette & Wood, 1998). In contrast, the more novel the stimuli or environment, the more the conscious mind attends to the circumstances (Wood & Neal, 2009). Whilst these two hypotheses are not mutually exclusive, their

differentiation would require further support experimentally in relation to the SNN output as a function of familiarity schema activation.

Whilst differences in spatiotemporal activation patterns were most prominent when data from the 200ms epoch were streamed for the training process, more subtle differences were observed at earlier time points, supporting the SNN models as being able to distinguish brands of varying familiarity in brain activation patterns at a peri-perceptual stage. For example, as shown in Figure 5-8 at the 50ms time point (T1), activation is observed over occipital and temporal regions for familiar logos but is restricted to occipital sites for unfamiliar stimuli. This may reflect top-down input to the perception of temporal regions, for example from those governing memory and or emotion (Sumich, Kumari, & Sharma, 2003) for familiar logos. Activation for familiar logos then takes more widespread parallel dorsal and ventral routes to activate frontal regions, with possible feedback loops to the occipital cortex. Whether these routes relate to the "where/how" (dorsal) and "what" (ventral) pathways for visual perception (Goodale & Milner, 1992) should be investigated in future research. Such work would provide insight into whether the greater restriction of the response to unfamiliar logos to the ventral pathway is due to a primary goal of the observer in object recognition (i.e., processing "what" the object is). In comparison, larger semantic networks may be activated in response to the familiar logo.

Experimental results are illustrated here mainly to represent the visual exploration of the SNN models, but numerical information (such as connection weights and spiking intensity) is also facilitated and can be exported from the models. For comparative analysis, the average value of connection weights was calculated in each trained SNN model Figure 5-6 and Figure 5-7 reported this number as activation level towards each stimulus (familiar and unfamiliar). A higher activation level of 1.01 in the trained SNN

model was obtained that corresponds to familiar stimuli at 200ms post-stimulus. Findings of this chapter suggest that stronger functional connectivity may indicate increased interplay of activated brain areas underlying cognitive functions. More information can be obtained from Appendix Table B-4 in which the averaged connection weights for every single EEG channel are reported for both familiar and unfamiliar stimuli. It shows a higher average of connection weights towards familiar stimuli at every time frame (0.35, 0.70 and 1.01 at 100, 150 and 200ms respectively).

Figure 5-9 illustrates the sequential spikes in the SNN models for familiar and unfamiliar logos from 50ms to 200ms. This figure is supported by numerical information which represents the number of spikes emitted at each time frame. It shows more neurons fired and sent out spikes in the SNN model of familiar than unfamiliar in all time frames. This information is also reported in Table 5-3 that shows, for instance, the intensity of spike activation for familiar is 3.7 times greater than unfamiliar. In order to interpret which EEG channels were mostly involved in the spiking activity at each frame, Table 5-4 was presented with respect to the intensity of activation measured for each EEG channel. This intensity was computed with respect to the percentage of the number of spikes in a cluster of neurons around an input neuron (connected neurons to input neuron). It shows that the Pz, P4, T4, Fp2 and O2 channels at 200ms post-stimulus had a greater intensity of spikes emitted during the learning process for familiar stimuli than unfamiliar ones. Table 5-5 summarises the classification accuracy achieved from the SNN method while Table 5-6 represents the results of conventional learning techniques.

In Table 5-5 a confusion table is reported to show the miss-classified samples versus the correctly classified ones. The conventional machine learning methods presented in Table 5-6 deal with vector-based data and do not model the spatiotemporal interactions related to the processes that generated the data as it is in the SNN models. Table 5-5 shows

that applying SNN for classification of spatiotemporal data resulted in significantly higher accuracy as compared with conventional methods such as MLP, MLR, and SVM. This can be justified with respect to a vital aspect of SNN that can preserve time information along with the spatial information of the sources of temporal data. In the SNN model, each data sample for training and for testing the model represents the intensity of all EEG channels within a whole-time interval, e.g. 200msec. During the training process, the temporal information of all channels is entered as a data stream to the SNN model through the spatially mapped input neurons and the spiking neurons were dynamically processing these inputs. However, in the conventional machine learning methods, each sample is a single input vector, where neither temporal- nor spatial information of the data is adequately represented.

5.6 Chapter Summary

Familiarity of marketing stimuli may affect consumer behaviour at a peri-perceptual processing level. The current chapter designed a method for detecting patterns of ERP data using an SNN approach that reveals the complexity of peri-perceptual processes of familiarity. The method was applied to data from 20 participants viewing familiar and unfamiliar logos. The results support the potential of SNN models as novel tools in the exploration of peri-perceptual mechanisms that respond differentially to familiar and unfamiliar stimuli. Specifically, the activation pattern of the time-locked response identified by the designed SNN model at approximately 200ms post-stimulus suggests greater connectivity and more widespread dynamic spatiotemporal patterns for familiar than unfamiliar logos. The designed SNN approach can be applied to study other peri-perceptual or perceptual brain processes in cognitive and computational neuroscience.

5.7 Contribution

In this chapter, I have made the following contributions:

---

1. Design of the cognitive task.
2. ERP data recording and conducting all the requirements including interacting with human participants and ethical approval producers.
3. Design of the experiments.
4. A designed SNN architecture, as a specific framework for a model of consumers' behaviour for detection and prediction of preference.
5. Conducting the statistical analysis of the data.
6. Conducting the SNN models and results.
7. Interpretation of the SNN models and results.
8. Publishing part of the study in a journal paper as the leading author:

Doborjeh, Z. G., Kasabov, N., Doborjeh, M. G., & Sumich, A. (2018). Modelling peri-perceptual brain processes in a deep learning spiking neural network architecture. *Nature, Scientific Reports*, 8(1), 8912.

“We are shaped by our thoughts; we become what we think. When the mind is pure, joy follows like a shadow that never leaves”.

Buddha

Chapter 6 Study 2 in Psychology - Mindfulness Training

6.1 Introduction

There has been substantial interest in Mindfulness Training (MT) to understand how it can benefit healthy individuals as well as people with a broad range of health conditions. Research has begun to delineate associated changes in brain function. However, whether measures of brain function can be used to identify individuals who are more likely to respond to MT remains unclear. This chapter reviews the mindfulness and brain neural changes (section 6.2) and develops and applies a brain-inspired SNN model for efficient comparative analysis of brain activities before and after Mindfulness training. Section 6.3 represents the design of the experiment for both pattern recognition and prediction in a real-life EEG data that measured as a function of depression and response to mindfulness training in the general population. Section 6.4 explained the EEG data recording. Finally, section 6.5 reports the analytical results that include both statistical analysis and the SNN modelling of EEG.

6.2 Mindfulness Training and Brain Mental States

A substantial literature, including systematic reviews, supports mindfulness-based practices in the management of emotions and improved cognition (Creswell, 2017; Keng, Smoski, & Robins, 2011; Lomas, Ivtzan, & Fu, 2015; Long, Briggs, & Astin, 2017). Mindfulness training (MT) has thus been adopted by many sectors across a wide range of contexts including education, workplace, health care practices, and rehabilitation centres (Gouda, Luong, Schmidt, & Bauer, 2016; Weare, 2014) . Self-report measures of state and trait mindfulness are commonly used as outcome measures. However, there has been a growing need to better understand associated neural mechanisms given the potential

health benefits (Tang, Hölzel, & Posner, 2015; Vignaud, Donde, Sadki, Poulet, & Brunelin, 2018). It is widely accepted that the human brain is capable of reorganisation and the generation of functional connections to compensate for deficits caused by injury, disease, and aging (Markus et al., 2005; Stein & Firl, 1976; Wall, Xu, & Wang, 2002) and advances in neuroimaging have contributed to understanding the underpinning mechanisms of neuroplasticity and skill learning (Chang, 2014; Keller & Just, 2016). Accordingly, neuroimaging offers an opportunity to investigate the neural reorganisation associated with mindfulness training.

A recent systematic review supported Mindfulness-Based Interventions (MBIs) in modulating several brain regions implicated in the pathophysiology of depression, (e.g., prefrontal cortex, basal ganglia, cingulate and parietal cortices) and cognitive processes, such as self-awareness, sustained attention, visual-spatial memory, working memory and emotion regulation (Creswell, 2017; Vignaud et al., 2018). Neuroimaging studies also suggest that consistent mindfulness practice results in increased thickness of various cortical regions linked with auditory, visual, and somatosensory processing functions (Lazar et al., 2005; Luders, Toga, Lepore, & Gaser, 2009; Vestergaard-Poulsen et al., 2009). Subdomains of mindfulness may rely on distinct brain networks. For example, reduced nodal strength in the left posterior cingulate gyrus, bilateral paracentral lobule, and middle cingulate gyrus following MT may reflect self-detachment (Cotier, Zhang, & Lee, 2017). Zhuang et al., (2017) found that Describing, Non-judging, and Non-reactivity facets of mindfulness were selectively associated with the cortical volume, thickness and surface area of multiple prefrontal regions and the inferior parietal lobule (Zhuang et al., 2017). Changes in the hippocampal-cortisol association following compassion and mindfulness-based meditation were dependent on changes in awareness of experience subscores (Lau, Leung, Chan, Wong, & Lee, 2015).

EEG offers high temporal resolution and provides a useful tool in investigating neural oscillations and connectivity (W. O. Tatum IV, 2014). EEG studies have shown alterations in several frequency bands that may be dependent on the type of meditation practice: focused attention, open-monitoring, transcendental meditation, and loving-kindness (D. J. Lee, Kulubya, Goldin, Goodarzi, & Girgis, 2018). In the last several decades, the power spectrum of EEG has been found to provide information on a depressive state as well as recovery. Numerous studies have found significant differences in depressive patient EEG sub-bands compared to healthy control (Fitzgerald & Watson, 2018; Hinrikus et al., 2010; Kalev & Bachmann, 2015; Wu et al., 2018). For example, synchronisation of alpha and beta band frequencies from right inferior frontal and primary sensory areas may reflect increases in controlled attention (Tang et al., 2015), also associated with increased theta (anterior and posterior (D. J. Lee et al., 2018; Lomas et al., 2015)).

Given the complexity of various interacting networks that underpin behaviour (Reimann et al., 2017; Weber, 2017), a challenge in understanding brain function, measured by STBD, is the integration of both spatial and temporal components. Hence, a proper unifying computational model is required to effectively model the integrated spatiotemporal relationship in such multivariate data. Employing an SNN-based methodology, this chapter aims to investigate the effects of mindfulness training on EEG data (Z. Doborjeh et al., 2019). The methodology was applied to address the following objectives:

(1) To recognise the patterns of changes in EEG, measured at before and after mindfulness training across participants with a different level of depression.

(2) To investigate whether EEG can identify if a person is likely to benefit from mindfulness training.

The population study contains three groups of participants who underwent mindfulness training, characterised by (a) non-depressed (denoted as ND); (b) high depression scores prior to training who showed a reduced level of depression scores post-mindfulness training (denoted as D^+); and (c) high depression pre-mindfulness training scores who declared no changes in depression scores post-mindfulness training (denoted as D^-).

For a deeper analysis of the effects of mindfulness training on EEG data, rhythms of delta (δ), theta (θ), alpha (α) and beta (β) bands were extracted and separately analysed. These EEG frequency sub-bands were visualised by paying special attention to the underpinning brain activity changes among the D+ group. Finally, the SNN-based methodology was used for prediction of response to mindfulness training in depressed individuals, when only the EEG data from the pre-mindfulness stage was used.

6.3 Method and Experimental design

The SNN architecture applied to this study includes several algorithms that allow for aspects of EEG data to be comprehensively evaluated. For this case study, the SNN architecture is designed as the following six steps and shown graphically in Figure 6-1.

1) **Data encoding:** Spatiotemporal EEG data were measured as temporal sequences of continues real values, which in our study were converted (encoded) into discrete spikes. In the example shown in Figure 6-1 a threshold-based method was used (Chan et al., 2007) for EEG encoding (This method is fully explained in section 3.1.1).

2) **Mapping:** For the mapping of EEG data into a 3D SNN reservoir, the Talairach brain template (Giacometti et al., 2014; Talairach & Tournoux, 1988) was used. The input EEG data variables were positioned in the SNN model as input

neurons with respect to their (x, y, z) coordinates as located in the Talairach brain atlas.

3) **Learning:** After an SNN model was spatially mapped, the model was trained in an unsupervised learning mode by using a spike-timing learning rule (in this case, using the STDP learning rule) (Masquelier et al., 2009). In this study, different SNN models were trained with the EEG data related to different mental states, e.g. before (Time T1) and after (Time T2) mindfulness training, across groups of participants. The SNN models of T1 and T2 were subtracted to capture the differences between the two states as a result of MT.

4) **Pattern visualisation:** To better understand the modification of spatiotemporal interactions between brain areas (62 EEG channels) in relation to mindfulness training, the SNN models were visualised into a 3D space. Six SNN models were visualised, each of them was trained separately by the EEG data of one group (ND, D^+ and D^-) at T1 and T2. The quantitative information of the visualised models was statistically analysed to investigate the effects of mindfulness on EEG data.

5) **Pattern classification:** To perform a classification task, an output layer classifier was trained, at a supervised mode, to learn the association between the trained SNN connectivity and the class label information. This is performed here using the deSNN classifier (N. Kasabov et al., 2013). This procedure was performed here for classification of EEG data (frequency sub-bands) into two classes T1 and T2 to investigate how the EEG were changed after the MT.

6) **Prediction:** In order to predict whether an individual is likely to respond to MT at T2, a classification task on the EEG data (from T1) into two classes D+ and D- (assessed at T2) was performed.

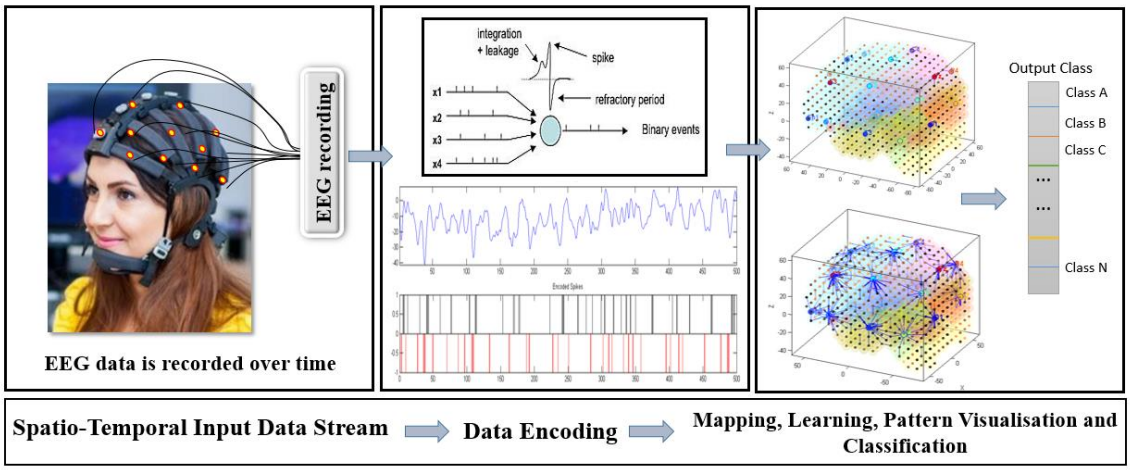

Figure 6-1. A block diagram of the methodology, consisting of: encoding EEG data into spike sequences; a brain-inspired 3D SNN structure for data mapping; learning; visualisation in 3D SNN; and output classification of patterns.

6.3.1 EEG Data Acquisition and Mindfulness Training

Ethical approval was obtained by the Auckland University of Technology (AUT) Ethics Committee (AUTEC) New Zealand and written informed consent was signed by all participants.

Forty participants underwent clinical assessment, including (BDI-II) (Beck & Alford, 2009). To model changes in brain function as a result of the MT, specific participants were selected according to their scores on the depression subscales. A total of 18 participants (6 males with a mean age of 27.50 (SD=7.34) years and 12 females with a mean age of 28 (SD=10.43) years) were selected for the EEG data analysis.

In this dataset, three classes were defined: Non-depressed subjects (ND), Depressed subjects who responded to mindfulness (D^+), and Depressed subjects who did not respond to mindfulness (D^-), which were labelled according to the BDI-II test results reported in Appendix Table C-1.

In class 1, seven participants who scored lower than 10 in BDI test were selected. In class 2, six participants affected by a moderate level of depression who have responded to the training were selected. In class 3, five participants with the clinical and severe level of depression who have not responded to the training were selected. Two stages of EEG

data recording were conducted in this chapter. The first stage was related to EEG data acquisition at baseline (denoted as T1) and the second one was recorded after a 6-week webinar MT programme (denoted as T2) from all the participants.

Descriptive information of all participants including age, gender, mean age, range, mean score and the standard deviation along with descriptive information of BDI test, including mean and standard deviation are reported in the Appendix Tables C- 2 and C-3. The mindfulness program was modified from an educational mindfulness program called Pause, Breathe and Smile (Devcich, Rix, Bernay, & Graham, 2017). Each session lasted 90-110 minutes and predominantly comprised a brief guided meditation exercise and a mindful tasting exercise. A detailed description of the program and the effect on mood has been explained in previous research (Krägeloh et al., 2018).

EEG was recorded in two sessions (1) before participants began training in MT and (2) following 6 weeks of MT. In each session, resting state data were recorded for 2 minutes with eyes-closed.

Recordings were carried out using a SynAmps amplifier and 62-channel QuikCap with electrode placements based on a standard 10-20 international system. The EEG channels are: FP1, FPZ, FP2, AF3, AF4, F7, F5, F3, F1, FZ, F2, F4, F6, F8, FT7, FC5, FC3, FC1, FCZ, FC2, FC4, FC6, FT8, T7, C5, C3, C1, CZ, C2, C4, C6, T8, TP7, CP5, CP3, CP1, CPZ, CP2, CP4, CP6, TP8, P7, P5, P3, P1, PZ, P2, P4, P6, P8, PO7, PO5, PO3, POZ, PO4, PO6, PO8, CB1, O1, OZ, O2, CB2. Data was recorded at a sampling rate of 1000 Hz. Off-line ICA computerised artefact correction was used to remove detectable eye movement or muscles potentials.

The EEG data were divided into two conditions (T1 and T2) across all 18 participants (11 depressed participants and 7 non-depressed participants). The EEG data were

processed by down sampling to 500 Hz and using a 30-second sliding temporal data window, creating 60 samples per each of the two conditions.

To investigate the effects of mindfulness on the EEG frequency sub-bands, the EEG signals were divided into bands of type δ, θ, α and β by using a set of power-pass filtering in MATLAB through Fast Fourier Transform (FFT) (Van Loan, 1992). Appendix Table C-1 reports the participants' information and their BDI scores from three groups: either D^+ participants or D^- and ND group. For example, participant Id: S1 (from D^+ group) scored 20, at T1, and 8, at T2 in the BDI- II test. This indicates a clinically significant improvement in the depression scores with changes from a moderate level of depression to a normal healthy level. On the other hand, participant Id: S#2 (from D^- group) scored 36 at T1, and 22 at T2 in the BDI subscale. This indicates the participant scores remained at the depressed level despite it changing from severe to moderate.

6.4 Results

The results are organised in a two-phase analysis as follows:

(1) Pattern recognition and prediction using SNN architecture to investigate the effects of mindfulness training across participants with different mental health conditions.

(2) Statistical analysis of the results to evaluate the model significance.

These steps are explained in the following sections 6.4.1 and 6.4.2

6.4.1 Pattern Recognition/ Prediction Using SNN Architecture

The 62 EEG channels were mapped into a 3D space of 1471 artificial spiking neurons, where the spatial locations of the input neurons were the same as their (x, y, z) coordinates in the Talairach brain template (Giacometti et al., 2014; Talairach & Tournoux, 1988). Figure 6-2 illustrates the SNN models were trained on EEG data related to before and

after mindfulness training (T1 and T2) across three groups of participants. It shows differences in the development of spatiotemporal connections in the SNN models as a function of group (ND, D^+, and D^-).

To better scrutinise the differences between the SNN models of different mental states, the connection weights (W_{ij}) of the difference between two correspondingly trained SNN models (T1, T2) was calculated for each group $Wij(D) = (W_{ij}\ (T2) - W_{ij}\ (T1)$. The total connection weight of each SNN model in three groups is reported in Table 6-1.

The subtracted connectivity model is depicted in Figure 6-3 which shows the involved brain areas, activated in response to the MT. The differences between the SNN models of T1 and T2 can be also studied by computing the number of spatiotemporal interactions between the EEG variables using a Feature Interaction Network (FIN). In Figure 6-4 the total temporal spike interaction among 62 input neuronal areas (corresponding to 62 EEG channels) is shown in the FIN, where nodes represent the input neuronal areas (neuronal clusters) and each line, that links two nodes, corresponds to the amount of spike transmission between the clusters during the SNN learning model.

6.4.1.1 Analysis of Functional Changes across Power Band-Frequency

For a deeper examination of the effect of mindfulness on the depressed participants, the SNN models of different EEG frequency sub-bands were developed, including delta (δ: 0.4-4 Hz), theta (θ: 4-8 Hz), alpha (α: 8-12 Hz), and beta (β: 12- 28 Hz), shown in Figure 6-5, Figure 6-6, Figure 6-7, Figure 6-8. The visualisation of EEG sub-bands as a function of time (T1, T2) in depressed participants, suggested that alpha and beta bands were most affected by the mindfulness training as shown in Figure 6-7 and Figure 6-8. Table 6-2 reports the connection weight of four sub-bands SNN models. Further quantitative information of the differences between the SNN models of these four EEG frequency sub-bands are plotted in Figure 6-9. This illustrates the SNN models'

histograms, defined by the number of connections as well as the connection weight in the SNN models of different sub-bands related to before and after the mindfulness training.

6.4.1.2. Pattern Classification of EEG Data Measuring Brain States Before and After Mindfulness Training in the Designed SNN Model

Here, an output classifier was trained to investigate how well a brain-inspired SNN model can classify the EEG patterns of T1 and T2 stages. There was a total number of 120 EEG samples (60 samples per class) for the classification task, which was here based on the LOOCV method. The classification experiment was performed four times, separately for each EEG frequency sub-bands as reported in Table 6-3. An essential step in finding optimal results from the SNN model is the optimisation of its parameters. Therefore, SNN training and validation procedures were repeated in a LOOCV mode with different combinations of parameter values in a grid-search, with an objective function being the highest classification accuracy. Table 6-3 indicates the total classification accuracy of EEG frequency sub-bands as a function of time (T1, T2).

6.4.1.3 Prediction of Response to Mindfulness Training

To investigate whether the SNN architecture can be used for prediction of response to mindfulness training, an SNN model was trained (using only the EEG data collected at T1) to predict the output classes at time T2. The predictive outcomes were here the two groups of participants (D+ and D-). For each participant, 10 samples in EEG data were extracted, each of them had a length of 1000 time points (one second EEG recording at resting state at T1). In total, the classification task was performed using 110 EEG samples, which belonged to six D^+ participants as class 1 and five D- participants as class 2. The classification was based on the LOOCV method and the results are reported in Table 6-4.

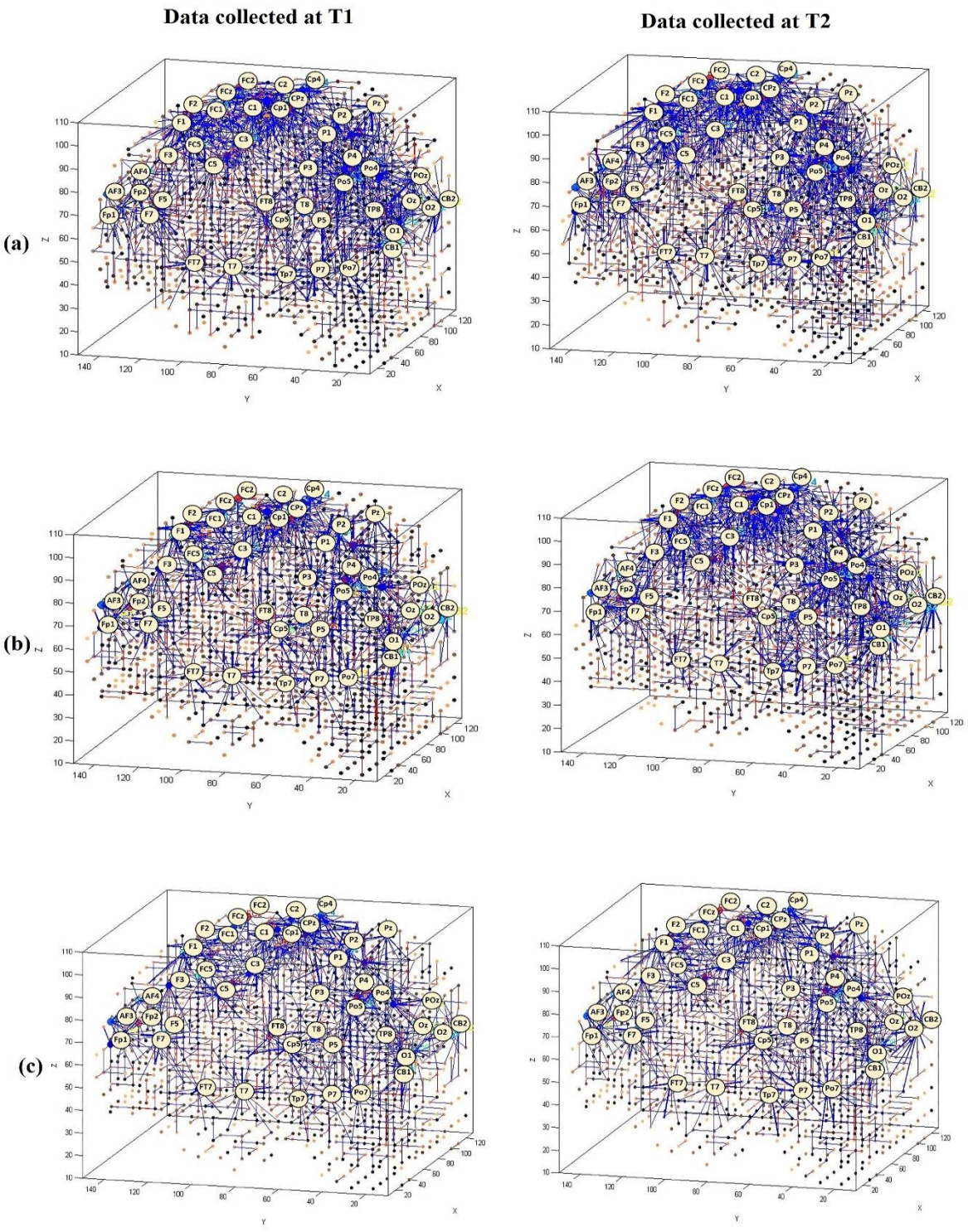

Figure 6-2. SNN connectivity trained on EEG samples that measured at T1 (before MT) and T2 (after MT), related to (a) non-depressed group (ND), (b) responsive-depressed group (D^+) and (c) unresponsive-depressed group (D^-).

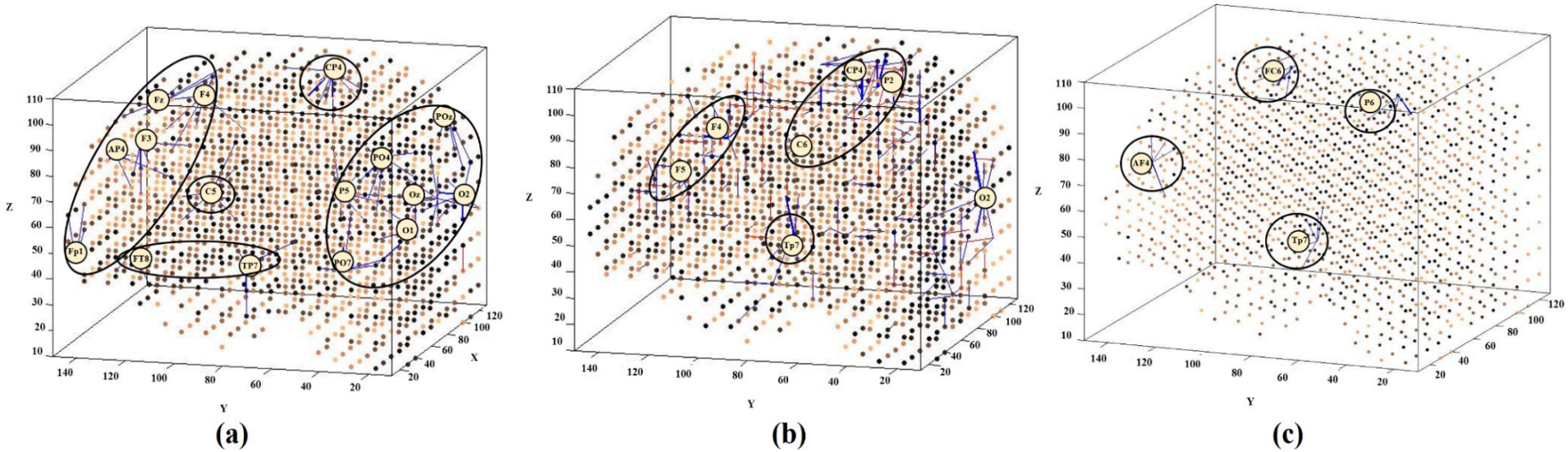

Figure 6-3. Differences between the connectivity in the trained SNN models of T1 (prior to MT) and T2 (post-training) in (a) non-depressed (ND) group, (b) responsive-depressed (D+) group, and (c) unresponsive-depressed (D-) group. The connections in each neural cluster represent the areas of main changes in the EEG data at post-MT.

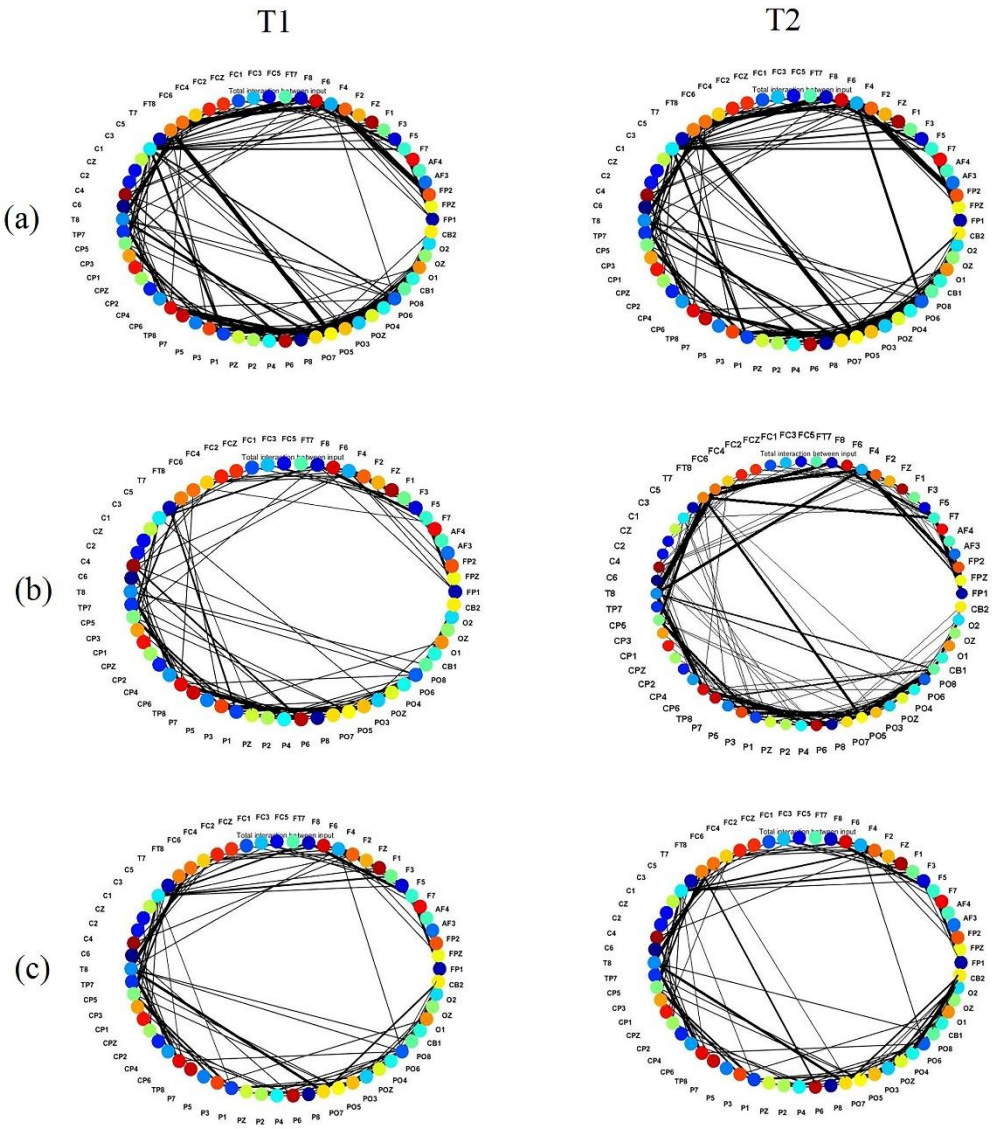

Figure 6-4. The Feature Interaction Network (FIN) captured the total spike interaction between the areas in the SNN models representing 62 EEG channels as input neurons during the STDP learning for: (a) non-depressed (ND); (b) responsive-depressed (D^+); and (c) unresponsive depressed (D^-). FIN nodes represent the input neuronal areas of the SNN model and lines represent the amount of spike transmission between these areas (clusters) of neurons that correspond to the input neurons (EEG channels.

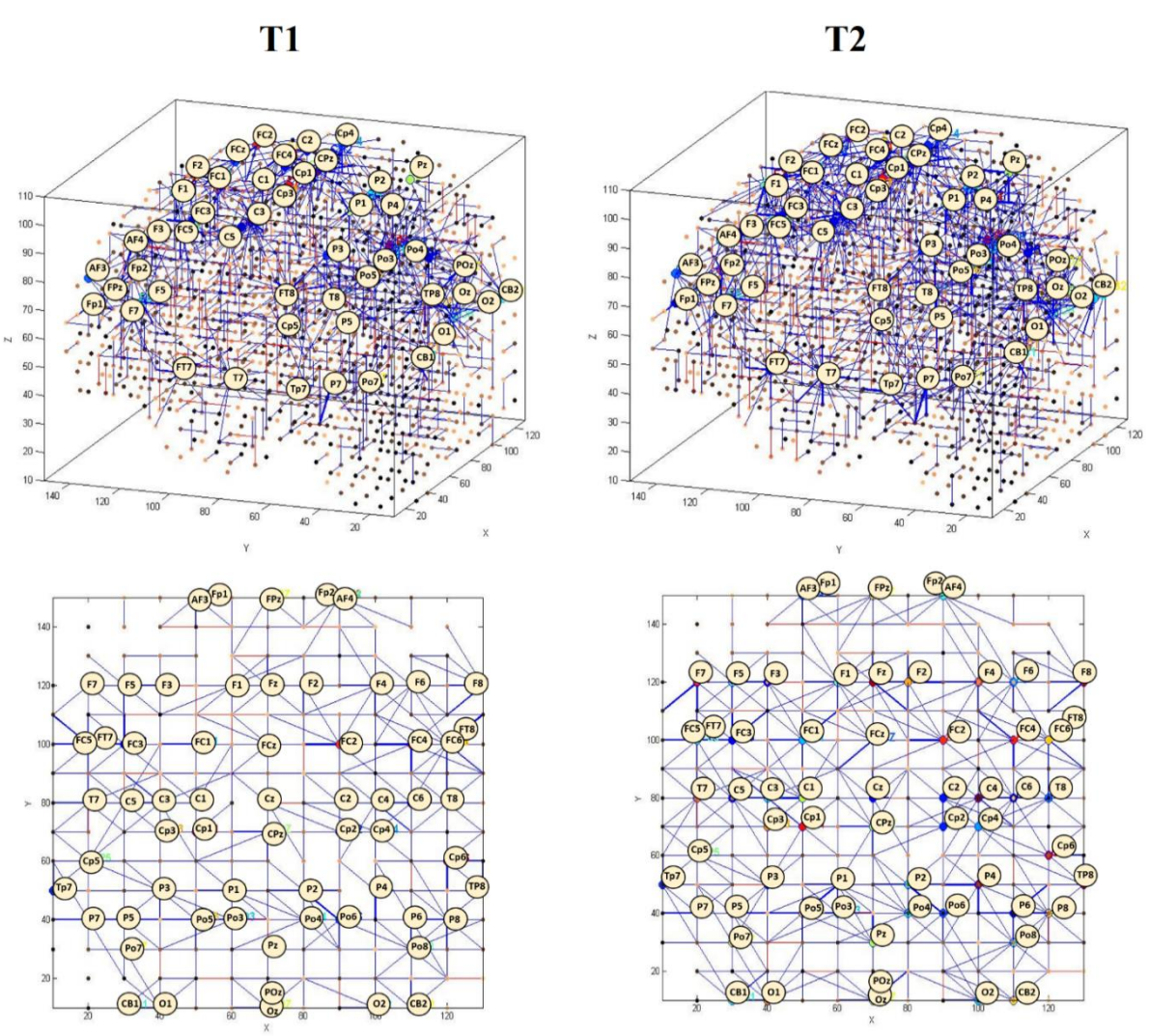

Figure 6-5 Spatiotemporal connectivity generated in the SNN models for responsive-depressed (D+) participants. The SNN models are visualised in both 3D (x, y, z) and 2-D (x, y) projections for the Delta frequency sub-band at T1 and delta at T2.

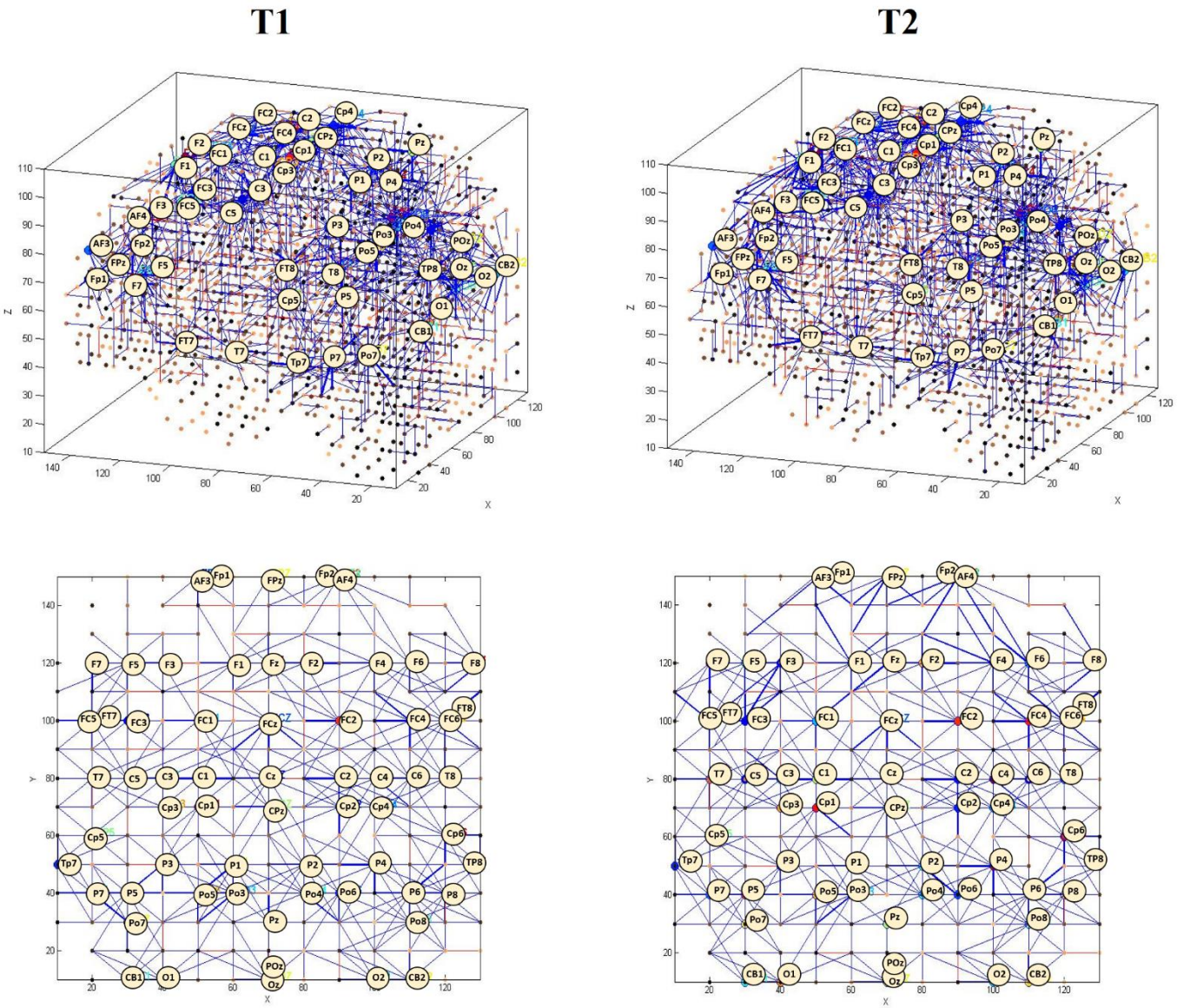

Figure 6-6. Spatiotemporal connectivity generated in the SNN models for responsive-depressed (D+) participants. The SNN models are visualised in both 3D (x, y, z) and 2-D (x, y) projections for the Theta frequency sub-band at T1 and theta at T2.

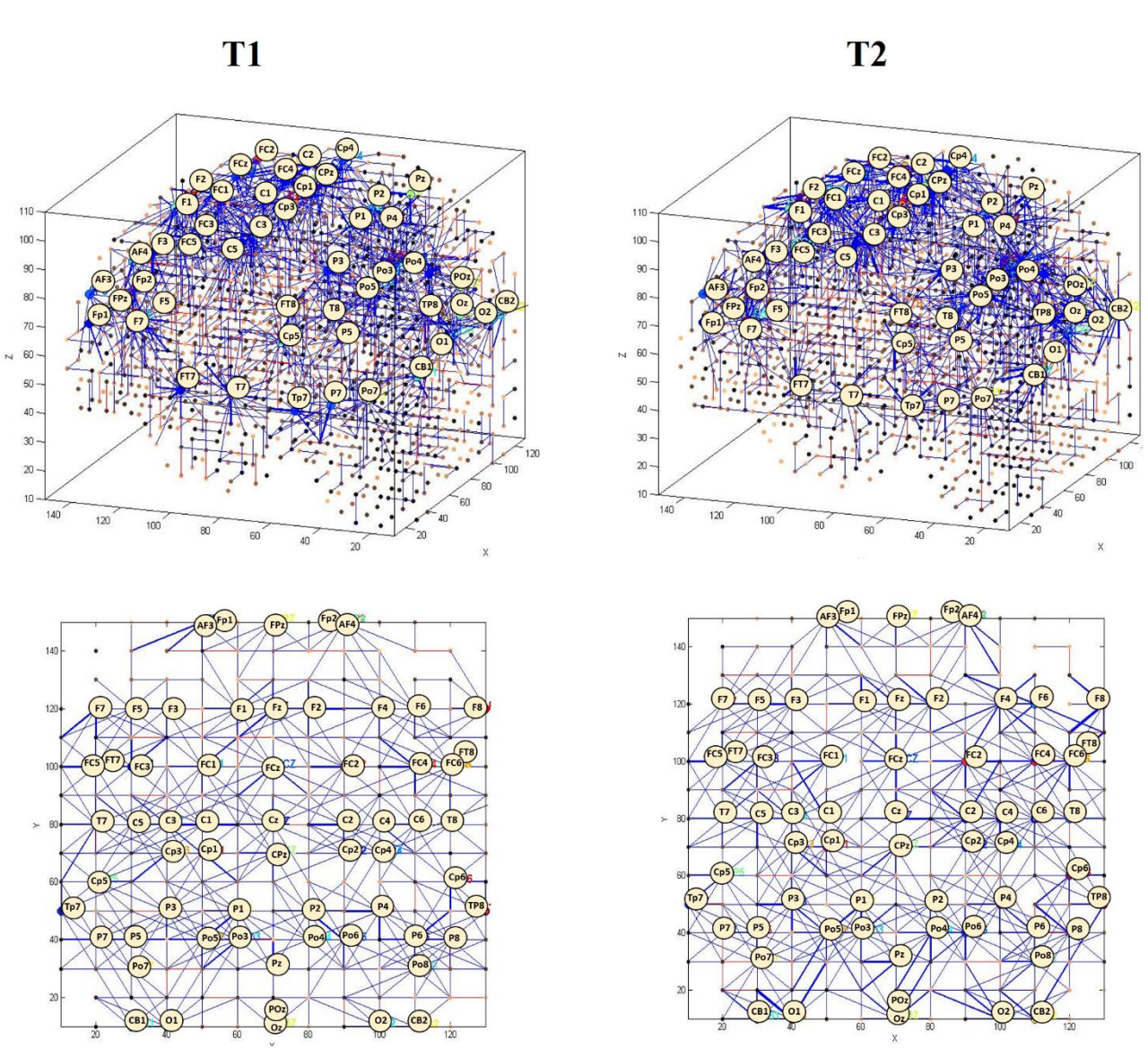

Figure 6-7. Spatiotemporal connectivity generated in the SNN models for responsive-depressed (D+) participants. The SNN models are visualised in both 3D (x, y, z) and 2-D (x, y) projections for the Alpha frequency sub-band at T1 and alpha at T2.

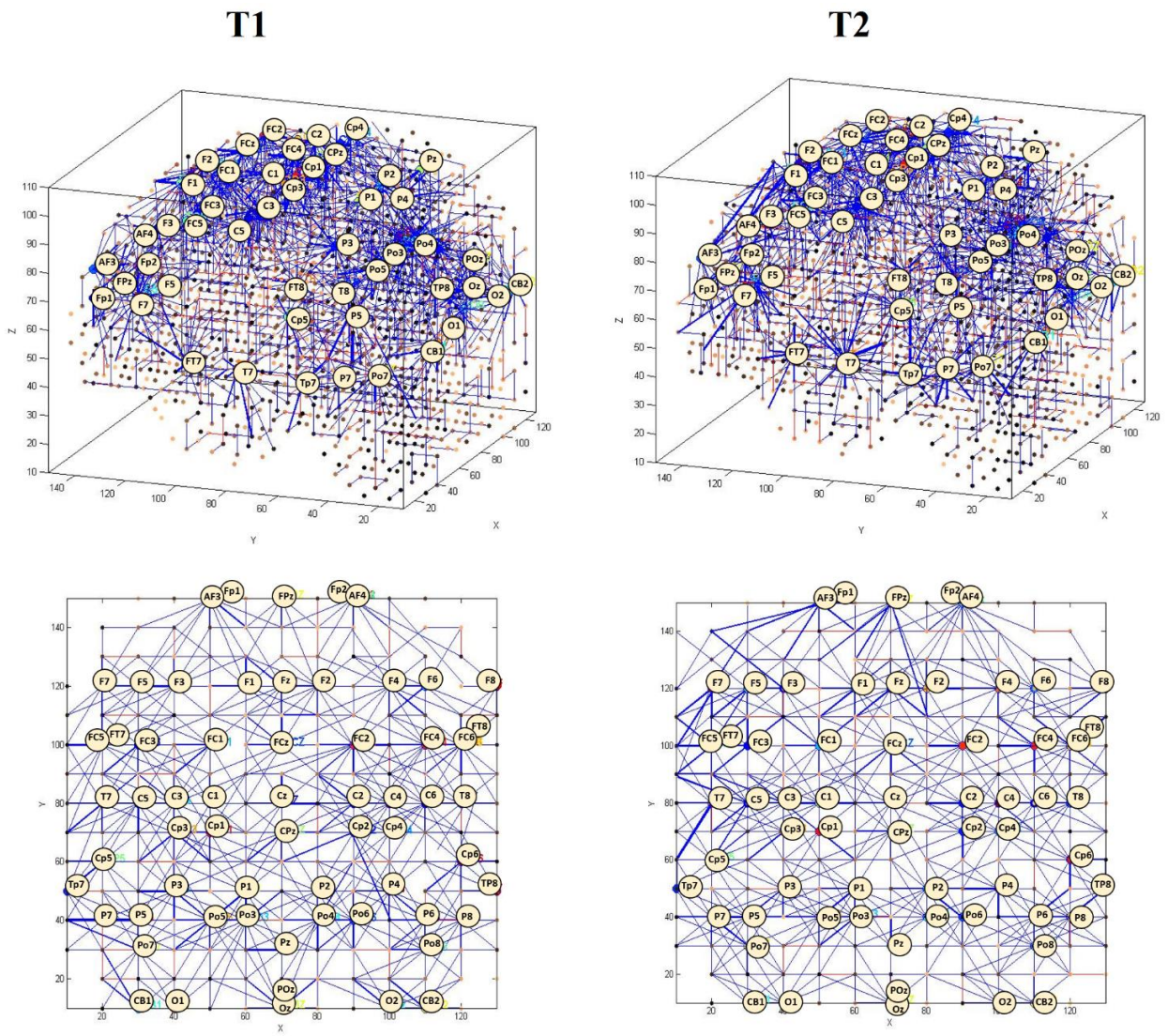

Figure 6-8. Spatiotemporal connectivity generated in the SNN models for responsive-depressed (D+) participants. The SNN models are visualised in both 3D (x, y, z) and 2-D (x, y) projections for the Beta frequency sub-band at T1 and alpha at T2.

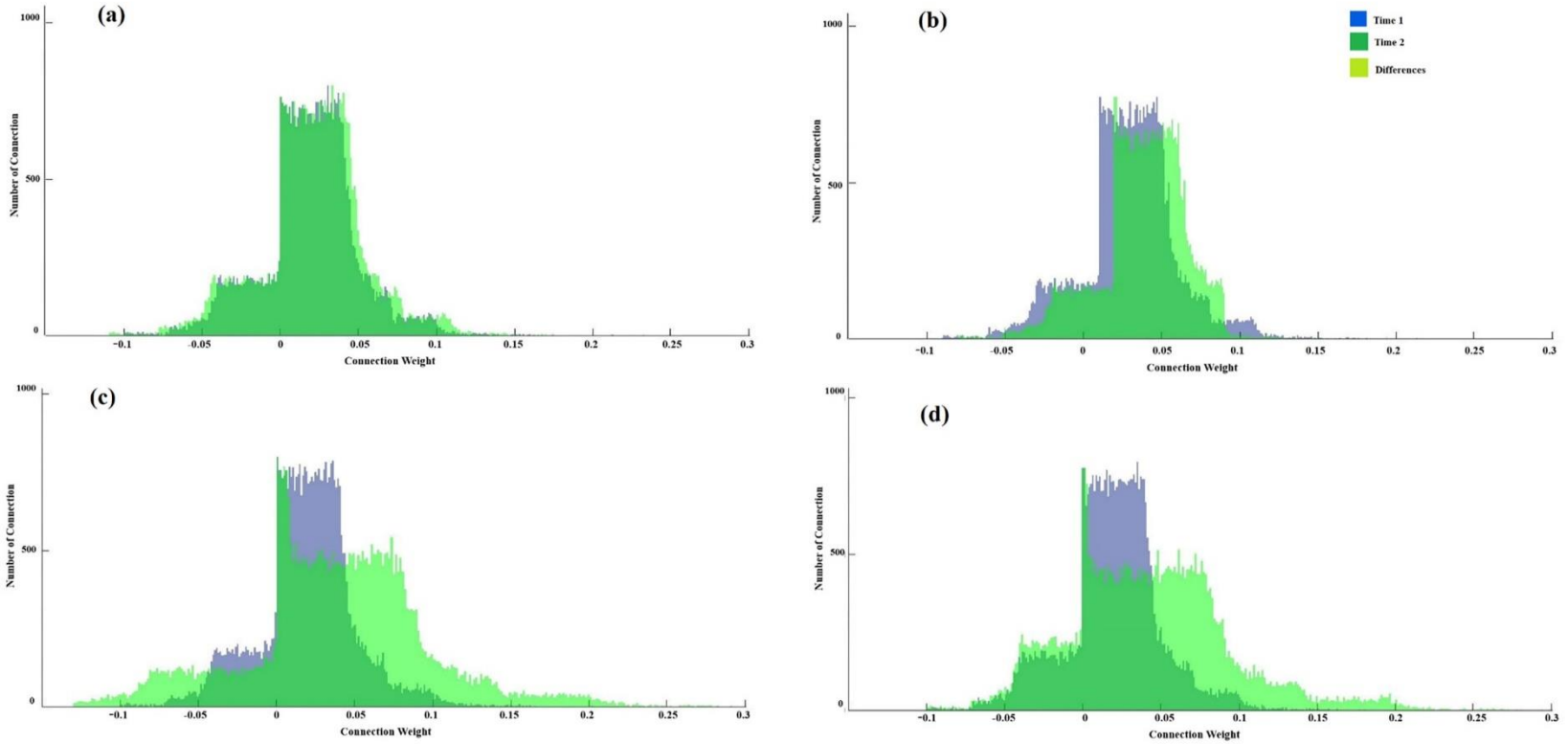

Figure 6-9. Histogram of the number of connections and the connection weights in the SNN models for the D^+ group trained on data corresponding to four EEG frequency sub-bands before (T1) and after (T2) mindfulness training. (a) Delta, (b) Theta, (c) Alpha, and (d) Beta.

Table 6-1. The average of the connection weights for each SNN model as an activation metric for three groups of participants: non-depressed (ND); responsive-depressed (D^+); and unresponsive depressed (D^-) over two time points: before training (T1) and after training (T2).

Average Connection weight of the SNN models		
Group	**Time point**	
	T1	**T2**
ND	0.84	1.04
D+	0.74	0.89
D-	0.54	0.64

Table 6-2. The average of the connection weights for each SNN model of sub-bands frequency for the responsive-depressed (D^+) group before training (T1) and after training (T2).

Average Connection weight of the sub-bands SNN models			
		Time point	
Group	bands	**T1**	**T2**
D+	Delta	0.7	0.7
	Theta	0.79	0.98
	Alpha	1.02	1.26
	Beta	1.03	1.17

Table 6-3. Classification accuracy of 120 EEG samples (10 samples per participant) from six D^+ participants at T1 (class 1) and T2 (class 2), performed using four EEG frequency sub-bands (modelled separately). The diagonals on the confusion tables represent the correctly classified samples. Highest classification accuracy is seen for alpha (91%) and beta (85%).

EEG frequency sub-bands			**Accuracy**	**F-score**
Delta				
EEG Data Classes	Delta (T1)	Delta (T2)		
Delta (T1)	**36**	24	0.75	75%
Delta (T2)	5	**55**		
Theta			**Accuracy**	
EEG Data Classes	Theta (T1)	Theta (T2)		
Theta (T1)	**42**	18	0.81	81%
Theta (T2)	4	**56**		
Alpha			**Accuracy**	
EEG Data Classes	Alpha (T1)	Alpha (T2)		
Alpha (T1)	**51**	11	0.91	90%
Alpha (T2)	1	**59**		
Beta			**Accuracy**	
EEG Data Classes	Beta (T1)	Beta (T2)		
Beta (T1)	**44**	16	0.85	85%
Beta (T2)	1	**59**		

Table 6-4. Classification accuracy of 110 EEG samples from T1 (10 samples per participant) into two classes D^+ and D- . There were six D^+ participants as class 1 and five D^- participants as class 2. This is to predict which participant is likely to response to the mindfulness at time T2 (after training) when the SNN model was only trained by the EEG data from T1. The diagonal on the confusion table represents the correctly predicted samples. Classification accuracy is also obtained via traditional machine learning methods. The parameters of the MLP model are: number of hidden neurons 3; number of training cycles 300; output value precision 0.0001; output function precision 0.0001; output activation function - linear. The SVM model uses polynomial kernel.

Predicted / Real	D^+ at T1	D^- at T1	**Accuracy Per Class**	**Total Accuracy in SNN**	**F-score**
D^+ at T1	**54**	6	0.90	**0.87**	**89%**
D^- at T1	5	**42**	0.84		

Classification accuracy obtained via traditional machine learning methods using NeuCom

Methods	**MLP**	**MLR**	**SVM**
Accuracy in %	69.50	68.50	68.50

6.4.2 Statistical Analysis of the SNN Results

The average weight of the connections for each of the trained SNN models calculated and reported this activation level as a function of group and time point (Table 6-1). As shown in Table 6-1, the SNN models of ND participants represented the strongest average activation levels (T1=.84, T2=1.04), compared to D^+ participants (T1=.74, T2=.89), and D^- participants (T1=.54, T2=.64).

The EEG channels were then clustered into five sites with respect to their topography (Figure 6-10): frontal, frontocentral, temporal, centroparietal and occipitoparietal. Appendix Table C-4 reported the average weight of the connections that were formed in each site of the SNN models, again as a function of group and time point. Appendix Figures C-7, C-8, show the line graphs of average activation levels for each EEG channels as a function of Group, Site and Time.

For each participant from the three groups (ND, D^+, D^-), one SNN model was developed and trained it with the EEG data of this participant. Repeated-measures Analysis of Variance (ANOVA) tested for differences in activation levels as a function of three within-subjects variables, including, *Hemisphere* (left, right), *Time* (T1, T2) and

Site (frontal, frontocentral, temporal, centroparietal and occipitoparietal), and *Group* (ND, D^+, D^-).

Figure 6-11 shows the line graphs of average activation levels as a function of *Group*, *Site* and *Time*. Appendix Tables C- 5 and C- 6 show descriptive (means, SDs) as a function of *Group*, *Site*, *Hemisphere* and *Time.*

Results of the repeated-measures ANOVA are presented in Table 6-5, which shows a significant main effect of *Time* (T1<T2) and *Group* (ND>D^+> D^-). The significant *Site*Group* interaction suggested that ND participants had higher activation values than D^+ at frontal and occipitoparietal sites. Higher activation values were seen for ND and D^+ compared to D^- at all sites. The significant *Site*Time*Group* interaction appeared to be due to an increase in activation levels at T2 compared to T1 across frontal, centroparietal and occipitoparietal for the ND group. For D^+ group, the effect of *Time* (T2>T1) was seen at all sites except occipitoparietal. For D^- group, the effect of *Time* (T2>T1) was seen at all sites except centroparietal and occipitoparietal. Also, there was a *Site*Group* interaction at T2, but not at T1. This was because the effect of *Group* (ND>D^+>D^-) at T1 was present at all sites. However, at T2 ND>D+ was only seen at frontal and Occipitoparietal sites; and at temporal sites, no difference was seen between ND and D^+.

Table 6-5. Repeated-measures ANOVA

	Lower order Conditions	F-value	Degree of freedom	p-value	Eta^2	Post Hoc Tests
Time		176.90	1,15	<.001	.92	T2>T1
Group		44.81	2, 15	<.001	.86	ND>D+>D-
Site*Group		2.64	5.86, 43.93	.029	.26	(F): ND>D+>D- (FC): ND=D+>D- (T): ND=D+>D- (CP): ND<D+>D- (OP): ND>D+>D-
Site*Time*Group		2.89	6.52, 48.90	.015	.28	
Site*Time	ND	6.88	2.67, 16.02	.004	.53	Effect of Time (T2>T1) (F): [F(1,6)=82.90, p<.001, eta^2=.93] (CP): [F(1,6)=11.72, p.014, eta^2=.66] (OP): [F(1,6)=21.50, p=.004, eta^2=.78] Other sites: Not Significant
	D+	1.45	2.65, 13.24	.273	.22	T2>T1 at all sites, except (OP)
	D-	1.36	1.66,6.63	.312	.25	T2>T1 at all sites, except (CP)and (OP)
Site*Group	T1	1.57	5.35, 40.12	.153	.17	ND>D+>D- at all sites
	T2	3.57	5.84, 43.78	.006	.32	(F): ND>D+>D- (FC): ND=D+>D- (T): ND=D+=D- (CP): ND=D+>D- (OP): ND>D+>D-
Time*Group	F	2.03	2,15	.165	.21	
	FC	3.41	2,15	.060	.31	
	T	2.90	2,15	.086	.28	
	CP	3.27	2,15	.066	.30	
	OP	3.62	2,15	.052	.32	Effect of Time (T2>T1) ND [F (1,6)=21.51, p=.004, eta^2=.78] D- [F (1,4) =28.24, p=.006, eta^2=.88] D+ Not Significant

*p<.05

Frontal (F), Frontocentral (FC), Temporal (T), Centroparietal (CP) and Occipitoparietal (OP)

Not depressed group (ND), participants in depressed group who responded to the training (D^+), participants in depressed group who did not respond to the training (D^-).

Before training (T1) and after training (T2).

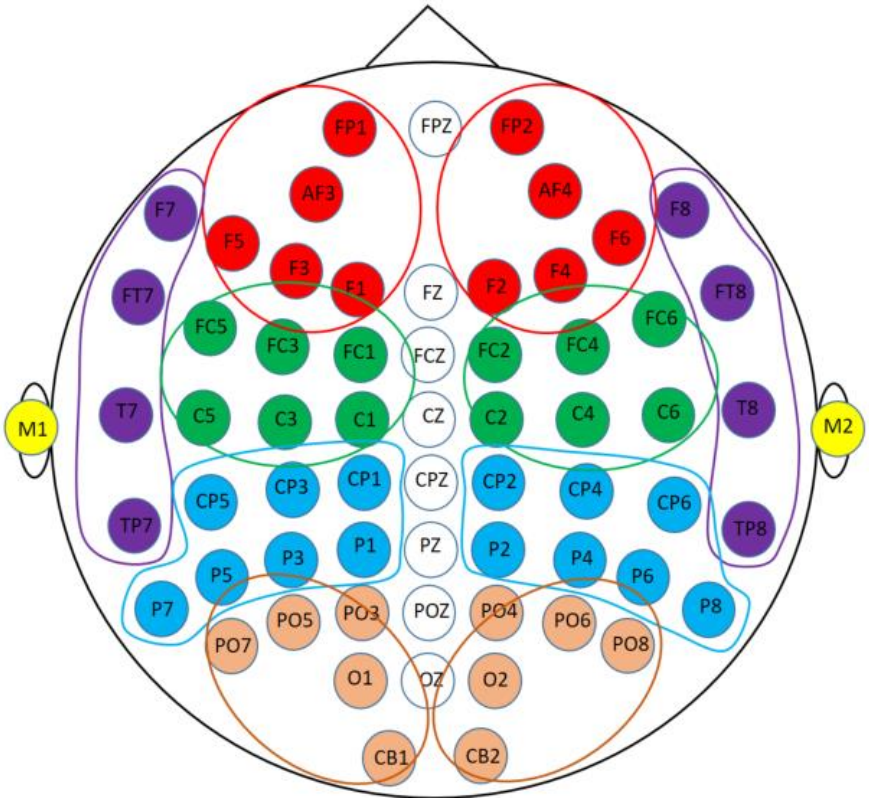

Figure 6-10. Clustering of EEG channels into five sites for both hemisphere (left and right) with respect to their topological information including: Left Frontal (Fp1, AF3, F5,F3 and F1); Right Frontal (Fp2, AF4, F6, F4 and F2); Left Frontocentral (FC5, FC3, FC1, C5, C3 and C1); Right Frontocentral (FC6, FC4, FC2, C6, C4 and C2); Left Temporal (F7, FT7, T7 and TP7); Right Temporal (F8, FT8, T8, TP8); Left Centroparietal (CP5, CP3, CP1, P7, P5, P3, P1); Right Centroparietal (CP6, CP4, CP2, P8, P6, P4 and P2); Left Occipitoparietal (PO7, PO5, PO3,O1 and CB1); and Right Occipitoparietal (PO8, PO6, PO4, O2 and CB2).

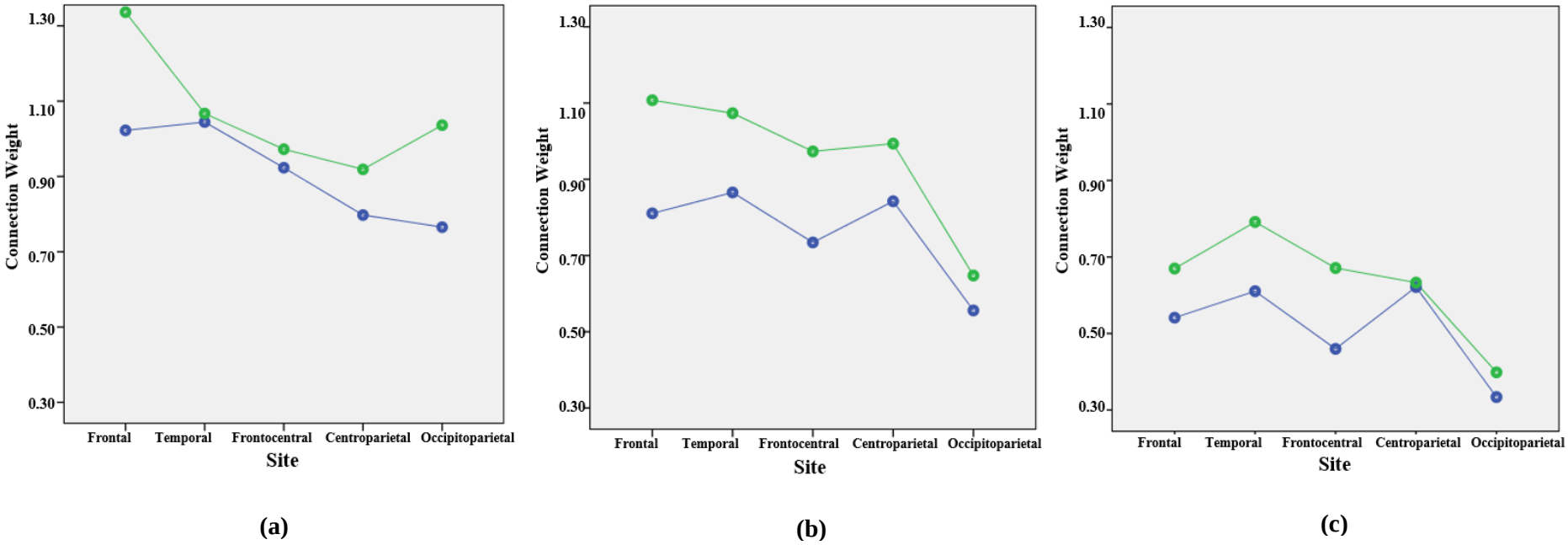

Figure 6-11. The SNN connection weights prior to MT (T1) and after following 6 weeks of training (T2) in (a) ND group, (b) D^+ group and (c) D^- group at Frontal, Temporal, Frontocentral, Centroparietal and Occipitoparietal clusters. Blue line represents the connectivity values in the SNN model of T1 (before mindfulness training) and green line represents T2 (after the mindfulness training).

6.5 Discussion

The present chapter designed a brain-inspired SNN architecture for investigating neural activity as a function of depression and response to MT in a nonclinical population. The SNN models are used to determine the discriminative patterns in the EEG samples that recorded prior to and following a 6-week MT programme in three participant groups.

The chapter outcomes took into account the following sections 6.5.1 and 6.5.2:

6.5.1 SNN Architecture for Modelling of Brain Mental States Followed by Mindfulness Training

To begin with, six SNN models were separately trained using different EEG data sample sets corresponding to ND group at T1 and T2, D^+ group at T1 and T2, and D^- group at T1 and T2. Figure 6-2 illustrates that the SNN connections have been evolved differently during unsupervised learning with EEG data related to different brain mental states. The SNN models trained in each group revealed information about the involvement of particular brain areas after the MT.

To perform a better analysis of EEG changes after MT, the differences between the SNN models of pre-MT and post-MT were computed for each group through subtracting the two correspondingly trained SNN models (T1, T2). This allows visualising the changes in neural connectivity as a result of MT over time. As shown in Figure 6-3, findings suggested that mindfulness resulted in a similar pattern of changes in some regional activation (frontal, frontocentral, and temporal) across all the three groups. However, the size of the activated connectivity was higher in the ND group, compared to D^+ and D^-, and that of D^+ was higher than D^-.

A within-group examination suggests that in ND group, MT was found to increase the spatiotemporal connectivity over the frontal (AF4, Fp1, F3, F4, Fz,), centroparietal (C5, CP4) and occipitoparietal areas (POz, PO7, PO4, O1, O2, Oz) at T2. For the D^+ group, stronger connectivity at T2 was seen over posterior temporal areas (Tp7). However, the intensity of this connectivity was minor when compared with the ND group. Greater activation appeared over centroparietal regions (C6, CP4, and P2), whilst very little change was seen posteriorly (O2). For the D^- group, slight changes in SNN connectivity over frontal (AF4, F6), frontocentral (FC6) and temporoparietal (TP6) regions were observed. In total, the SNN model of D^- group has shown minimal changes after the MT. The fact that these participants did not perceive and/or did not report that the training had any effect on them and yet there were clear brain connectivity changes according to our modelling, may indicate that neural changes are not resulting in a subjective change in depression (Berridge, 2003; Braun, Jackson, & Wiley, 2001). That is, it has been theorised that core processes of implicit reactions may occur independently of conscious awareness (Braun et al., 2001), but are detectable using brain imaging. SNN appears to be useful in this respect. In order to analyse the information interaction between the brain areas in response to MT across the three groups, the total temporal interactions (in terms of spike communication) between 62 input neurons was depicted. Figure 6-4 shows the average one-to-one interaction between the input's neurons (EEG channels). As illustrated by the FIN graph in 6-4(a), broader interaction lines were formed between the 62 EEG channels of ND participants when compared with the D+ and D- groups in 6-4(b) and (c). In FIN graph of D+ group, there were thicker interaction lines at T2, especially between the EEG channels positioned at frontal areas (Fp1, Fp2, AF3, AF4, and F7), when compared with the graph at T1 (before training). Thicker lines indicate more interaction between the inputs. These connections were established strongly because of more spikes transmitted between the neurons located in these areas, reflecting more changes in the corresponding

EEG signals. In 6-4(c), it was revealed that although D- participants reported that they did not respond to the MT (based on BDI-II scores), the FIN of the corresponding SNN model at T2 (after training) showed stronger interactions than T1 in brain areas in frontal, frontocentral and temporal.

In the current chapter, to precisely evaluate how MT influenced the level of depression in D+ group, the EEG frequency sub-bands were examined. As can be seen from Figure 6-5 to Figure 6-8, the SNN models of alpha and beta bands were more affected by the MT at T2 when compared with other frequency bands. The SNN connectivity of alpha and beta bands at T2 show that stronger activity was observed at T2 (activation level = 1.26 and 1.17) than T1 (activation level = 1.02 and 1.03) in comparison with other bands. There was a significant difference at the electrode channels of F8, F4, O1, O2 and OZ in the SNN connectivity of alpha brainwaves at T2 as compared to the T1. These electrode channels located at the right frontal and occipital lobes. These areas involve in motor planning, emotional expression, visual and sensory input processing from the environment. Lower SNN connectivity of alpha at T1 than T2 in these areas could be due to the less attentiveness to the outer environment. This finding is supported by previous empirical studies (Brzezicka, Kamiński, Kamińska, Wołyńczyk-Gmaj, & Sedek, 2017; Kan & Lee, 2015; Segrave et al., 2011) that suggested depressed people tend to more focus inward on own negative emotions. Therefore, they pay less attention to receiving the information from the outer world. The SNN model of beta band at T2 illustrate stronger connectivity around channels of F5, F7, AF3, Fp1 and T7 than other areas. These channels located at the left frontal and left temporal regions that are involved in the verbal and emotional expression, attention and emotional memory (Walker, Kozlowski, & Lawson, 2007). The SNN model of theta sub-band at T2 (Figure 6-6b) shows that the spatiotemporal connectivity slightly increased over F3 and C3 channels that are located

in left frontal and left central as compared with T1. These areas are engaged in motor planning and sensorimotor integration.

For the delta sub-band (Figure 6-5a), all the connections in the SNN models of T1 and T2 were approximately uniform. Therefore, we could not distinguish specifically modified connections in many parts of the SNN model of T2 that could suggest a response to the MT. The results are in line with the findings in the literature that showed regional hemispheric asymmetries are associated with less activity in left frontal and right posterior regions in depression (Fingelkurts et al., 2007; Y. Li et al., 2016; Manna et al., 2010). Decreased connectivity of the frontal regions has been suggested to account for the loss of interest, motivation, and pleasure. These symptoms are typical characteristics of depression. Interactions among regions in this network have been shown to be attenuated in patients with depression, that all can be control of negative thoughts and emotions in depressed individuals (B. J. Li et al., 2018; Sahay & Hen, 2007).

In this study, after MT, SNN connectivity of the frontal regions significantly increased. Stronger functional connectivity indicates an increased interplay of activated brain areas underlying cognitive functions (Bazanova & Vernon, 2014).

To validate the visualised changes in the SNN models that depict the variation in EEG sub-bands from T1 to T2, a quantitative analysis on the SNN connection weights was performed. Eight histograms of the connection weights in the SNN models were plotted, each of which was separately trained by the EEG frequency sub-bands from T1 and T2 of the D^+ group. Figure 6-9(a) represents that the SNN connection weight histograms related to the delta sub-band at T1 and T2 were overlapped. This supports the previous argument (shown in Figure 6-2 and Table 6-2) that no significant changes were observed

after the MT in the delta sub-band. However, the connection weight histograms of the other sub-bands varied to a different degree from T1 to T2 as shown in Figure 6-9(b-d).

A classification task also was performed on the EEG data sub-bands to examine if the SNN model can classify the EEG patterns of T1 and T2 stages. Table 6-3 shows that applying SNN for classification of spatiotemporal data resulted in significantly high accuracy for both alpha and beta sub-bands. This indicates that alpha and beta were the most affected EEG sub-bands after MT; therefore, the correspondingly trained SNN models could accurately classify between T1 and T2.

The SNN architecture was also applied in this chapter for prediction of response to MT. At this point, the SNN models were only trained by the EEG data from T1 (prior to training) to detect, in an earlier stage, whether a participant is likely to respond to the MT at T2. This was performed by classifying the EEG data of T1 into two classes of participants (D^+ and D^- which were assessed at T2). Table 6-4 summarises the classification accuracy obtained using the SNN-based methodology versus the traditional machine learning methods. The confusion table shows that the classification accuracy of EEG samples to D^+ and D^- groups was 87%, which suggested the existence of discriminative patterns between the groups at T1. Also, significantly higher classification accuracy was obtained compared to the traditional machine learning methods. Through assessment of both spatiotemporal patterns has led to the detection of important discriminative features in the SNN models. Hence using only the selected informative features for a classification task, an average of 20% increase in accuracy has been achieved. This finding indicates that the designed SNN-based methodology can be potentially explored and used in the future to predict response to treatment for depressed individuals before training is applied.

6.5.2 Statistical Analysis of the SNN Results

For statistical analysis, the average value of connection weights in each trained SNN model was calculated and reported as an activation level towards each mental state (prior to and after MT). The ANOVA statistical analysis is then applied to represent the significance of the models. As reported in Table 6-1, we obtained a higher activation level of 1.04 in the trained SNN model that corresponds to the ND group at post-training evaluation. Further information regarding this analysis can be obtained from the Appendix C-4 in which the average connection weights for every single site are reported for factors of the *hemisphere* (left, right) and *Time* (before, after training) across all *groups* of participants. It shows a higher average of connection weights over the right hemisphere at T2 for all the three groups of participants (1.15, 0.95 and 0.62) when compared to the right hemisphere at T1 (0.95, 0.76 and 0.51).

ANOVA analysis of the SNN models identified common changes under the MT across participants, but also those that varied as a function of group and responsiveness to training. As shown in Figure 6-11 greater initial activation levels were observed in ND compared to depressed groups, and this difference was maintained at frontal and occipitoparietal regions following MT. At baseline, D^+ had great activation than D^-. Following MT, frontocentral and temporal activation reached ND levels in D^+ but remained low in D^-.

The statistical analysis indicates that MT is associated with the larger response over the anterior regions for all three groups. This might mean that MT drive activity over the same regions but drive more and stronger activity for the ND group. The results were consistent with the recent meta-analysis that found the Mindfulness-Based Stress Reduction (MBSR) significantly reduced many parameters, including depression, stress

and anxiety scores in those healthy subjects who attended mindfulness programmes compared to waiting list controls (Astin, 1997; Chiesa & Serretti, 2009).

Beyond the ANOVA results, the designed SNN models discovered the differences in the scalp areas involvement between T1 and T2 for three groups. It means that SNN models can learn and identify which areas of the brain contribute to an increase in EEG (at T2) and also how does it happen over time. In the current chapter, the SNN-based methodology is used in integrating the temporal and scalp topographic information, such that a better understanding of the pathways of information processing was obtained, in addition to have discrete measurements of neuronal response.

Although numerous researchers are dedicated to unravelling the functional and structural changes associated with MT, the understanding of the underlying psychological and neural mechanisms is currently limited. The SNN models can be used to obtain new findings, such as tracing a trajectory of neural brain activities, which could not be obtained with the use of traditional statistical methods. The results of previous mindfulness research suggest that meditation improves executive and attentional functioning. The designed SNN methodology for modelling mindfulness data confirms these findings but further extends them to reveal the connectivity intensity across different brain regions affected by mindfulness practice.

6.6 Chapter Summary

The present chapter applied a recently developed brain-inspired SNN model to EEG data to provide novel insights into: i) brain function in depression; ii) the effect of MT on depressed and non-depressed individuals; and iii) neurobiological characteristics of depressed individuals who respond to mindfulness. Resting state EEG was recorded from before and after a 6-week MT programme in 18 participants. Based on self-report, 3 groups were formed: non-depressed (ND), depressed before but not after MT (responsive, D^+) and depressed both before and after MT (unresponsive, D^-). The designed SNN, which utilises a standard brain-template, was used to model EEG data and assess connectivity, as indicated by activation levels across scalp regions (frontal, frontocentral, temporal, centroparietal and occipitoparietal), at baseline and follow-up. Results suggest an increase in activation following MT that was site-specific as a function of the group. Greater initial activation levels were seen in ND compared to depressed groups, and this difference was maintained at frontal and occipitoparietal regions following MT. At baseline, D^+ had great activation than D^-. Following MT, frontocentral and temporal activation reached ND levels in D^+ but remained low in D^-. Findings support the SNN approach in distinguishing brain states associated with depression and responsiveness to MT. The results also demonstrated that the SNN approach can be used to predict the effect of mindfulness on an individual basis before it is even applied.

6.7 Contribution

In this chapter, I have made the following contributions:

---

1. Participating in EEG data collection
2. Design of the experiments.
3. A designed SNN architecture, as a specific framework for a mental wellbeing application for detection and prediction of mindfulness effects on STBD.
4. Conducting the statistical analysis of the data.
5. Conducting the SNN models and results.
6. Interpretation of the SNN models and results.
7. Publishing part of the study in a journal paper as the leading author:

   Doborjeh, Z., Doborjeh, M., Taylor, T., Kasabov, N., Wang, G., Siegert, R.., & Sumich, A. (2019). Spiking Neural Network Modelling Approach Reveals How Mindfulness Training Rewires the Brain. *Nature, Scientific Reports*, 9(1), 6367.

“Life is a circle. The end of one journey is the beginning of the next”

Joseph M. Marshal

Chapter 7 Conclusion and Recommendations for Future Work

7.1 Introduction

This thesis aimed to improve modelling and understanding of spatiotemporal brain data underpinning human behaviour with the use of a brain-inspired computational framework. The method utilised one of the most promising recent trends of artificial intelligence research, called spiking neural networks. These networks incorporate both *space* and *time* information of brain data into one unifying model, allowing to capture spatiotemporal relationships and the trajectory of sequentially activated brain areas in response to different types of stimuli under different mental states.

This chapter begins with an overview of the thesis in section 7.2. Section 7.3 addresses the main thesis's findings, followed by section 7.4 that describes three major contributions into the science. The constraints and limitations of the thesis are summarised in section 7.5, whereas section 7.6 outlines a recommendation for future research.

7.2 Overview of the Thesis

In this thesis, chapter 1 presented the aims, motivation, and significance of the research. Brief information about spatiotemporal brain data measurements such as EEG, ERP, and fMRI were given, followed by referring to several extant analytical tools. In Section 1.1, it was explained that the analysis of STBD is a challenging task, as temporal features may manifest complex interactions that may also change dynamically over time. Most the extant analytical techniques create models by separately processing the *spatial* and *temporal* information. They also lack biological plausibility as well as model's

interpretability. To overcome these limitations when dealing with spatiotemporal data, SNN architecture was suggested as a brain-inspired analytic that incorporates both *spatial* and *temporal* characteristics of data into the computation. SNN models were used in this thesis for both *dynamic pattern recognition* and *pattern prediction* in two real-life empirical scenarios from neuroinformatics: (1) neuromarketing and (2) mindfulness training. Finally, chapter 1 pointed to three aspects of the thesis's contribution. The first contribution was in terms of designing a generic framework of SNN-based methodology to perform an empirical study on different types of STBD (EEG and ERP). The second contribution was to the field of neuromarketing by designing SNN architecture as a model of consumers' behaviour for detection and prediction of preference. The third contribution was designing SNN architecture as a mental wellbeing application for detection and prediction of mindfulness effects on STBD.

Chapter 2 provided literature reviews on three major scopes of interest: (1) the brain, as a complex information processing system; (2) EEG and ERPs as two measurement techniques of neural information processing; and (3) data analysis techniques for STBD. The analytical methods that were reviewed in chapter 2 are commonly used statistical approaches (ICA, SPSS), AI methods (Machine learning, brain-inspired artificial neural networks, and spiking neural network) and software packages (EEGLAB, SPSS, Weka, Neucom, NeuCube) for data mining processes. Finally, section 2.5.2 suggested SNN as a promising approach to bridge the gap between neuroscience study and machine learning techniques, using biologically-realistic models of neurons to carry out computations.

In chapter 3, the principles of SNN architecture were presented. Then an SNN-based methodology was introduced as a computational framework that visualises the brain data in a 3D space of artificial neurons and elucidates the connectivity and interaction between data variables. Section 3.1.1 to 3.1.4 depicted the main functional modules of the SNN

framework, which are: (1) input data encoding and mapping; (2) unsupervised learning in a 3D SNN model; (3) supervised learning and classification; and (4) knowledge extraction.

Chapter 4 presented the designed novel methodology and framework based on SNN architecture for both *dynamic pattern recognition* and *prediction* tasks using EEG and ERP data. This generic framework includes several steps: cognitive task preparation, data collection, defining samples, data mapping, learning, visualising, classifying, and validating the results. The designed SNN-based framework was then applied to two case studies: neuromarketing (Chapter 5) and mindfulness (Chapter 6).

By using the developed in this study novel SNN methods for dynamic pattern recognition and pattern prediction, findings in Psychology are made that improve the understanding of brain datasets (EEG and ERP) in relation to brain activities as presented in the section below.

7.3 Key Findings in Psychology

7.3.1 Dynamic pattern recognition in Neuromarketing

To address the research question: *"How can brain-inspired SNN architecture be used to investigate the spatiotemporal information flow in ERP data related to viewing familiar vs unfamiliar marketing logos? Are familiar and unfamiliar logos distinguished at a peri-perceptual stage of processing?"* Chapter 5 represented a feasibility analysis of the SNN for modelling a real-life ERP data from neuromarketing. This chapter demonstrated, for the first time, that the designed SNN models could capture spatiotemporal patterns of ERP data, reflecting peri-perceptual brain processes during a neuromarketing experiment in which familiar and unfamiliar logos were presented. The designed SNN architecture revealed unstudied components of perception of familiar and unfamiliar marketing

stimuli at a peri-perceptual level. The trained SNN models developed significantly different spatiotemporal neural connections illustrated in a 3D brain-inspired space for different marketing products. The results suggested that familiar logos elicited more widespread brain responses than unfamiliar logos. The SNN models of familiar versus unfamiliar logos generated discriminative spatiotemporal patterns. This resulted in obtaining a high classification accuracy of 83% which represented an average improvement of 40% when compared with conventional machine learning methods such as SVM, MLP, and MLR classification techniques.

The differences between SNN models of familiar and unfamiliar logos were most prominent around 200ms, but variations in brain activity could be picked up as early as 100ms after a familiar logo was shown. This finding achieved through tracking the trajectory of sequential activated neural areas in the SNN models, reflecting the importance of the STBD variables with respect to the time at which these areas were activated. The repeated ANOVA measure ($F=100.51$, $p=0.001$) confirmed that the SNN models of familiar versus unfamiliar logos were statistically significant.

Insights into this early window of neurocognitive processing have been technically infeasible in the extant neuromarketing studies. In comparison with state-of-the-art neuromarketing studies, the employed SNN models for ERP analysis in this thesis resulted in improved detection of brain peri-perceptual regions affected by marketing stimuli. This was supported by capturing the activation time and spiking intensity of neural areas involved in perceiving of marketing stimuli.

7.3.2 Discriminative Patterns in Mindfulness Study

To address the research question: "*How SNN architecture can be applied to identify discriminative patterns in EEG data related to before and after mindfulness training*

across individuals with different mental states?", Chapter 6 presented a brain-inspired SNN architecture for investigating neural activity as a function of depression and response to mindfulness training in a nonclinical population. Findings suggested that mindfulness resulted in a similar pattern of changes in some regional activation across all the three groups. However, the size of the activated connectivity was higher in the ND group (T1=.84, T2=1.04), compared to D^+ (T1=.74, T2=.89) and D^- (T1=.54, T2=.64) and that of D^+ was higher than D^-. The repeated ANOVA measure (F= 44.81, P<.001) also confirmed significant differences. Beyond the statistical findings, the designed SNN models illustrated the differences in brain data variables involvement between T1 and T2 for three groups. The SNN models identified which areas of the brain contributed to an increase in EEG (at T2) and also how did it happen over time after the intervention. Findings support the SNN approach in distinguishing brain states associated with depression and responsiveness to mindfulness training. The designed SNN-based methodology considered both spatial and temporal information together in an SNN model and dynamically detects the evolving spatiotemporal patterns over time.

7.3.3 Event prediction in Neuromarketing and Mindfulness Study

To address the research question: *Can SNN models lead to knowledge discovery by making a predictive system of brain mental states?* Both Chapter 5 and Chapter 6 revealed the potential of SNN architecture for the early detection of spatiotemporal patterns in two studies: neuromarketing and mindfulness training.

The finding in neuromarketing presented a model of consumer behaviour that represents how early marketing materials are perceived at an unconscious level of information processing (around 200ms). This model is potential to be further developed to recognise patterns of choice behaviour and as such could be used to direct marketing strategies.

The findings in mindfulness study demonstrated that the SNN approach can be used to predict the effect of mindfulness on an individual before it (the intervention) is applied. The classification accuracy of EEG samples to D^+ and D^- groups was 87%, which showed an average improvement of 20% as compared to conventional classifiers. This accuracy improvement suggested the existence of discriminative patterns between these groups at T1 (before mindfulness training), which was not captured using conventional machine learning methods. This research indicates that the designed SNN-based methodology is potential to be explored and used in the future to predict response to treatment (e.g., mindfulness or other types of interventions) for individuals, even before the training is applied. The model can be also used to predict which individuals are more likely to respond to the training.

7.4 Empirical and Theoretical Contributions

This thesis contributed to the field of Neuroinformatics and Psychology through the following three empirical studies:

- A designed SNN-based methodology, as a generic framework for a precise analysis of different types of STBD (EEG and ERP).
- A designed SNN architecture, as a model of consumers' behaviour for detection and prediction of preference.
- A designed SNN architecture, as a mental wellbeing application for detection and prediction of mindfulness effects on STBD.

7.4.1 A Generic Framework for Precise Analysis of Different Types of STBD (EEG and ERP)

The designed SNN architecture is performed through an empirical study that involved the following steps:

- Mapping the spatial information of EEG variables (channels), to a 3D brain-inspired SNN model, pre-structured with the use of a standard brain template;
- Unsupervised learning of the spatially mapped EEG data in the SNN model using spike time dependent plasticity learning algorithm;
- Visualising and interpreting of the trained spatiotemporal connectivity of the SNN model;
- Classification, prediction, and validation of the SNN models;
- Statistical analysis of the SNN models to evaluate the level of significance.

When compared with traditional machine learning techniques or deep learning neural networks, an SNN model has the following advantages: 1) it preserves the *spatial* and *temporal* information both together in one model and can be interpreted as this model is spatially structured according to a brain template; 2) It learns spatiotemporal patterns from data through biologically plausible learning rules; 3) It allows for interpretation of the interactions and relationships between the brain data variables.

7.4.2 Model of Consumers' Behaviour for Detection and Prediction of Preference.

This thesis developed a model of consumer behaviour that represents how early marketing materials are perceived at an unconscious level of information processing and elucidated the underpinning dynamics of these processes. Understanding how these early stages of processing are affected by familiarity (e.g. by familiar logos) has important theoretical implications in the models of memory in general and applications to neuromarketing in terms of objective evaluation of product presentation and development.

The contribution of this study is in cognitive system development, understanding human choice behaviour, preference and decision making in respect to new designs and social behaviour, and new knowledge discovery. The designed methodology is promising and suitable for pattern recognition of peri-perceptual brain activity in various environments for early detection of brain responses towards stimuli. For example, the model might be further developed to recognise patterns of human choice behaviour, and as such could be used to improve product design, the design of the environment we all live in. In general, it can help researchers and social scientists understand better how biased or prejudiced perceived at a sub-consciousness level, when we make decisions, what are our true preferences in life, how can we communicate better, how we learn better.

From a sale and neuromarketing perspective, this research also suggests a basis in neuroscience for the "subconscious biased and content marketing". Content marketing can be different based on the target audience (Z. G. Doborjeh, Doborjeh, & Kasabov, 2018). For example, one aspect can be used in marketing by engaging consumers' emotions in the content marketing process. The emotional state often influences attention and consumers tend to pay more attention to the contents that emotionally stimulate them. The more consumers are touched emotionally, whether that be in a positive or negative manner, the more they will focus explicitly on this emotional stimulus over any other aspects available to them. In total, chapter 5 provided a proof of principle for the role of "sub-conscious biases" on perception in directing human choice behaviour. It represents knowledge discovery in the prediction of consumers' behaviour in the field of neuromarketing.

7.4.2. Mental Wellbeing Application for Detection and Prediction of Mindfulness Effects on STBD

The findings in mindfulness study are centred on two main empirical contributions:

- Theoretical: understanding the mechanisms of neural changes of individuals with different mental states followed by mindfulness training; and

- Methodological: identifying improved brain functions as a result of intervention in the designed SNN architecture; identifying neural activation patterns that predict treatment response at the individual-levels.

This study pursued these two intertwined lines of research in the hope to further our understanding of typical and disordered brains, with the overall goal to facilitate personalised approaches to intervention. There are hundreds of thousands of people in New Zealand suffering from depression, stress, anxiety. This research will benefit the affected population in NZ and lead to discovering how their depression can be diagnosed at an early stage; therefore, suggesting an early intervention. This will result to change that upward trend of high prevalence of depression in NZ.

7.5 Limitations of the Thesis

It should be borne in mind that the study has a number of limitations:

- Participants: The data collected from human participants. A continuing challenge in the acquisition and analysis of human EEG data is the presence of artefacts–electrical activity generated outside of cerebral sources of primary interest. Although I aimed to record the brain data as artefact free data as possible, some brain data of participants were not acceptable due to physiological artefact and were excluded to prevent missing information through artefacts rejection process. Therefore, the evaluation was performed on a small size dataset, so the

trained models can only be valid on the defined data scope and this is not yet generalised to be tested on any new person's STBD stream. On the other hand, an individual's brain architecture is determined largely by genetic and environmental influences. Individual differences in adult human brain structure have been found to reveal a great deal of information about variability in behaviours, cognitive abilities, and mental and physical health. Cultural and historical impact on individuals has not been measured.

- Methodological point of view: EEG data relays dipole activity from the superficial areas of cortex. Therefore, the spatial locations of the activity (this is the inverse problem) due to different strengths, the electrode specify, and skull scattering may not be obtained accurately.

7.6 Future Direction and Implications

Future direction and implications are presented into two "methodological" and "applications" sections as follows:

7.6.1 Methodological

Source localisation has been one of the primary goals of solving the inverse problem in EEG. What this means is identifying where in the brain a particular type of activity originates based on the surface EEG recording. This is particularly would be useful to figure out where a response is being initiated. However, it may also be useful to understand from where different stimulus responses come from. Identifying the source within the brain from which an EEG signal element originates is a complex problem that requires a model of a brain-inspired framework. To this end, the SNN based methodology can be further developed for source localisation by taking into account the following improvement in the model: (1) high spatial resolution (the resolution of images has to be

increased as the low spatial resolution is undesirable in feature extraction of spatiotemporal pattern recognition; (2) low computational time (it can be solved through reducing the complexity of algorithms and mathematical calculation as they cause high computational time and chance of losing the data due to continuous iteration of weight matrix); (3) low localisation error (better estimation can be obtained with low localisation error or exact zero error); and (4) validation on real-time data (the results from the model should not be evaluated on simulated data, but through real-time data).

Another direction for further research is deep knowledge representation from trained SNN models as suggested in (Kasabov, 2018). This research will continue the trend of knowledge engineering that was established and developed in (Kasabov, 1996; Kasabov, 2003, 2007), where neural network structures are analysed and rules are extracted that present the essence of the data in a concise and understandable way.

7.6.2 Applications

7.6.2.1 Marketing-related applications

The current results illustrate that the designed methodology is promising and suitable for pattern recognition of peri-perceptual brain activity in response to marketing stimuli. Future work will investigate whether it could be used as a tool in the early detection of spatiotemporal patterns generated by other stimuli in relation to neuromarketing. For example, the model might be further developed to recognise patterns of choice behaviour, and as such could be used to direct marketing strategies. Thus, future studies should evaluate the potential for refinement of the model and application of peri-perceptual processing measures to neuromarketing, as an objective measure of consumer preference for logos and product presentation. Although the present thesis has investigated familiarity to logos, the current findings might not be restricted to such stimuli. Thus,

future research should investigate whether similar effects are seen in relation to familiarity to other stimuli, for example, faces.

Human choice behaviour results from a complex interplay of cultural, social, personal, and psychological factors. Human feelings, motives, and decisions are influenced by their past experiences and stored in the unconscious. Therefore, it is important to analyse the behavioural and neurological states of these psychological biases as they might impact consumers' choices and decision making. Based on the findings in this thesis, future work should investigate brain activation patterns using the SNN model in terms of psychosocial factors, personality variables and inter-individual differences that may affect a person's cognitive response to familiar logos and, indeed, brand preference. For example, future studies should investigate the early and late ERP components in relation to brand attachment and brand attitude. One might expect the earlier components to relate to an empathic attachment to the brand. The research has applications beyond marketing, however. It could be revolutionary in police line-ups, allowing a victim who has blocked out a traumatic experience to pick out the offender. It could also be used to detect criminal activity; if a suspect claimed not to recognise a crime scene or object, this could be tested on a preconscious level.

7.6.2.2 Health-related Applications

Future application could focus on the clinical setting utilising this model in a practical way to develop optimal and individualised treatment plans that were tailored specifically to the psychological profile and brain architecture of an individual. The designed SNN-based methodology can be potentially used in the future to predict response to any treatment for patients before intervention is even applied. Moreover, in this thesis, identification of the improved brain functions in relation to mindfulness training can lead to propose a new computerised cognitive therapy to reduce the level of depression and

improve cognitive performance. In New Zealand, health statistics suggest that Māori face a high level of depression; therefore, this study offers the potential to provide new information that could contribute to improving Māori mental health and wellbeing. The plan in future is to disseminate any relevant information that may help reduce health inequities directly to stakeholders involved in Māori healthcare service delivery, including Māori Health Boards and health providers.

References

Abdullah, A., Khan, I. H., Basuhail, A., & Hussain, A. (2015). A Novel Near-Infrared Spectroscopy Based Spatiotemporal Cognition Study of the Human Brain Using Clustering. *Cognitive Computation, 7*(6), 693-705.

Ackerman, S. (1992). *Discovering the brain*: National Academies Press.

Agatonovic-Kustrin, S., & Beresford, R. (2000). Basic concepts of artificial neural network (ANN) modeling and its application in pharmaceutical research. *Journal of pharmaceutical and biomedical analysis, 22*(5), 717-727.

Alpaydin, E. (2009). *Introduction to machine learning*: MIT press.

Amari, S. (2003). *The handbook of brain theory and neural networks*: MIT press.

Ashburner, J. (2012). SPM: a history. *Neuroimage, 62*(2), 791-800.

Astin, J. A. (1997). Stress reduction through mindfulness meditation. *Psychotherapy and psychosomatics, 66*(2), 97-106.

Bargh, J. A. (2002). Losing consciousness: Automatic influences on consumer judgment, behavior, and motivation. *Journal of consumer research, 29*(2), 280-285.

Bargh, J. A., Chen, M., & Burrows, L. (1996). Automaticity of social behavior: Direct effects of trait construct and stereotype activation on action. *Journal of personality and social psychology, 71*(2), 230.

Bazanova, O., & Vernon, D. (2014). Interpreting EEG alpha activity. *Neuroscience & Biobehavioral Reviews, 44*, 94-110.

Beck, A. T., & Alford, B. A. (2009). *Depression: Causes and treatment*: University of Pennsylvania Press.

Bengio, Y. (2009). Learning deep architectures for AI. *Foundations and trends® in Machine Learning, 2*(1), 1-127.

Berridge, K. C. (2003). Pleasures of the brain. *Brain and cognition, 52*(1), 106-128.

Braitenberg, V., & Schüz, A. (2013). *Cortex: statistics and geometry of neuronal connectivity*: Springer Science & Business Media.

Brammer, M. (2004). Brain scam? *Nature Neuroscience, 7*(10), 1015.

Braun, H. I., Jackson, D. N., & Wiley, D. E. (2001). Socially desirable responding: The evolution of a construct *The role of constructs in psychological and educational measurement* (pp. 61-84): Routledge.

Brzezicka, A., Kamiński, J., Kamińska, O. K., Wołyńczyk-Gmaj, D., & Sedek, G. (2017). Frontal EEG alpha band asymmetry as a predictor of reasoning deficiency in depressed people. *Cognition and emotion, 31*(5), 868-878.

Bullmore, E., & Sporns, O. (2009). Complex brain networks: graph theoretical analysis of structural and functional systems. *Nature Reviews Neuroscience, 10*(3), 186.

Carter, R. (2014). *The human brain book*: Penguin.

Caruana, R., & Niculescu-Mizil, A. (2006). *An empirical comparison of supervised learning algorithms.* Paper presented at the Proceedings of the 23rd international conference on Machine learning.

Chan, V., Liu, S.-C., & van Schaik, A. (2007). AER EAR: A matched silicon cochlea pair with address event representation interface. *IEEE Transactions on Circuits and Systems I: Regular Papers, 54*(1), 48-59.

Chang, Y. (2014). Reorganization and plastic changes of the human brain associated with skill learning and expertise. *Frontiers in human neuroscience, 8*, 35.

Charron, S., Fuchs, A., & Oullier, O. (2008). Exploring brain activity in neuroeconomics. *Revue d'économie politique, 118*(1), 97-124.

Chiesa, A., & Serretti, A. (2009). Mindfulness-based stress reduction for stress management in healthy people: a review and meta-analysis. *The journal of alternative and complementary medicine, 15*(5), 593-600.

Costantini, G., Todisco, M., Casali, D., Carota, M., Saggio, G., Bianchi, L., . . . Quitadamo, L. (2009). SVM Classification of EEG Signals for Brain Computer Interface. *Frontiers in Artificial Intelligence and Applications*, 229-233.

Costantini, G., Todisco, M., Casali, D., Carota, M., Saggio, G., Bianchi, L., . . . Quitadamo, L. (2009). *SVM Classification of EEG Signals for Brain Computer Interface.* Paper presented at the Proceedings of the 2009 conference on Neural Nets WIRN09: Proceedings of the 19th Italian Workshop on Neural Nets, Vietri sul Mare, Salerno, Italy, May 28--30 2009.

Cotier, F. A., Zhang, R., & Lee, T. M. (2017). A longitudinal study of the effect of short-term meditation training on functional network organization of the aging brain. *Scientific reports, 7*(1), 598.

Cox, R. W. (1996). AFNI: software for analysis and visualization of functional magnetic resonance neuroimages. *Computers and Biomedical research, 29*(3), 162-173.

Creswell, J. D. (2017). Mindfulness interventions. *Annual review of psychology, 68*, 491-516.

Delorme, A., & Makeig, S. (2004). EEGLAB: an open source toolbox for analysis of single-trial EEG dynamics including independent component analysis. *Journal of neuroscience methods, 134*(1), 9-21.

Devcich, D. A., Rix, G., Bernay, R., & Graham, E. (2017). Effectiveness of a Mindfulness-Based Program on School Children's Self-Reported Well-Being: A

Pilot Study Comparing Effects With An Emotional Literacy Program. *Journal of Applied School Psychology, 33*(4), 309-330.

Dijksterhuis, A., & Nordgren, L. F. (2006). A theory of unconscious thought. *Perspectives on Psychological science, 1*(2), 95-109.

DiMaggio, P. (1997). Culture and cognition. *Annual review of sociology, 23*(1), 263-287.

Djuwari, D., Kumar, D. K., & Palaniswami, M. (2006). *Limitations of ica for artefact removal.* Paper presented at the 2005 IEEE Engineering in Medicine and Biology 27th Annual Conference.

Doborjeh, Z., Doborjeh, M., Taylor, T., Kasabov, N., Wang, G. Y., Siegert, R., & Sumich, A. (2019). Spiking Neural Network Modelling Approach Reveals How Mindfulness Training Rewires the Brain. *Scientific reports, 9*(1), 6367. doi:10.1038/s41598-019-42863-x

Doborjeh, Z. G., Doborjeh, M. G., & Kasabov, N. (2018). Attentional bias pattern recognition in spiking neural networks from spatio-temporal EEG data. *Cognitive Computation, 10*(1), 35-48.

Doborjeh, Z. G., Kasabov, N., Doborjeh, M. G., & Sumich, A. (2018). Modelling peri-perceptual brain processes in a deep learning spiking neural network architecture. *Scientific reports, 8*(1), 8912.

Duffy, F. H., Burchfiel, J. L., & Lombroso, C. T. (1979). Brain electrical activity mapping (BEAM): a method for extending the clinical utility of EEG and evoked potential data. *Annals of Neurology: Official Journal of the American Neurological Association and the Child Neurology Society, 5*(4), 309-321.

Falkenstein, M., Hoormann, J., & Hohnsbein, J. (1999). ERP components in Go/Nogo tasks and their relation to inhibition. *Acta psychologica, 101*(2-3), 267-291.

Field, A. (2013). *Discovering statistics using IBM SPSS statistics*: sage.

Fingelkurts, A. A., Fingelkurts, A. A., Rytsälä, H., Suominen, K., Isometsä, E., & Kähkönen, S. (2007). Impaired functional connectivity at EEG alpha and theta frequency bands in major depression. *Human brain mapping, 28*(3), 247-261.

Fitzgerald, P. J., & Watson, B. O. (2018). Gamma oscillations as a biomarker for major depression: an emerging topic. *Translational psychiatry, 8*(1), 177.

Freeman, W., & Quiroga, R. Q. (2012). *Imaging brain function with EEG: advanced temporal and spatial analysis of electroencephalographic signals*: Springer Science & Business Media.

Friston, K. J., Jezzard, P., & Turner, R. (1994). Analysis of functional MRI time-series. *Human brain mapping, 1*(2), 153-171.

García-Larrea, L., Lukaszewicz, A.-C., & Mauguiére, F. (1992). Revisiting the oddball paradigm. Non-target vs neutral stimuli and the evaluation of ERP attentional effects. *Neuropsychologia, 30*(8), 723-741.

Gardner, M. W., & Dorling, S. (1998). Artificial neural networks (the multilayer perceptron)—a review of applications in the atmospheric sciences. *Atmospheric environment, 32*(14-15), 2627-2636.

Gevins, A. S., & Rémond, A. (1987). *Methods of analysis of brain electrical and magnetic signals* (Vol. 1): Elsevier Science Limited.

Giacometti, P., Perdue, K. L., & Diamond, S. G. (2014). Algorithm to find high density EEG scalp coordinates and analysis of their correspondence to structural and functional regions of the brain. *Journal of neuroscience methods, 229*, 84-96.

Goodale, M. A., & Milner, A. D. (1992). Separate visual pathways for perception and action. *Trends in neurosciences, 15*(1), 20-25.

Gouda, S., Luong, M. T., Schmidt, S., & Bauer, J. (2016). Students and teachers benefit from mindfulness-based stress reduction in a school-embedded pilot study. *Frontiers in psychology, 7*, 590.

Hinrikus, H., Suhhova, A., Bachmann, M., Aadamsoo, K., Võhma, Ü., Pehlak, H., & Lass, J. (2010). Spectral features of EEG in depression. *Biomedizinische Technik/Biomedical Engineering, 55*(3), 155-161.

Hinton, G. E. (2007). Learning multiple layers of representation. *Trends in cognitive sciences, 11*(10), 428-434.

Hinton, G. E., & Salakhutdinov, R. R. (2006). Reducing the dimensionality of data with neural networks. *Science, 313*(5786), 504-507.

Holmes, G., Donkin, A., & Witten, I. H. (1994). *Weka: A machine learning workbench.* Paper presented at the Intelligent Information Systems, 1994. Proceedings of the 1994 Second Australian and New Zealand Conference on.

Holzinger, A. (2016). *Machine Learning for Health Informatics: State-of-the-Art and Future Challenges* (Vol. 9605): Springer.

Humphries, M. D., Gurney, K., & Prescott, T. J. (2006). The brainstem reticular formation is a small-world, not scale-free, network. *Proceedings of the Royal Society of London B: Biological Sciences, 273*(1585), 503-511.

Hyvärinen, A., Karhunen, J., & Oja, E. (2001). Independent Component Analysis. Series on Adaptive and Learning Systems for Signal Processing, Communications, and Control: Wiley.

Indiveri, G., Corradi, F., & Qiao, N. (2015). *Neuromorphic architectures for spiking deep neural networks.* Paper presented at the Electron Devices Meeting (IEDM), 2015 IEEE International.

Isomura, T., & Toyoizumi, T. (2016). A local learning rule for independent component analysis. *Scientific reports, 6*, 28073.

Izhikevich, E. M. (2006). Polychronization: computation with spikes. *Neural computation, 18*(2), 245-282.

Jasper, H. H. (1958). The ten-twenty electrode system of the International Federation. *Electroencephalogr. Clin. Neurophysiol., 10*, 370-375.

Jongsma, M. L., van Rijn, C. M., Gerrits, N. J., Eichele, T., Steenbergen, B., Maes, J. H., & Quiroga, R. Q. (2013). The learning-oddball paradigm: Data of 24 separate individuals illustrate its potential usefulness as a new clinical tool. *Clinical Neurophysiology, 124*(3), 514-521.

Kalev, K., & Bachmann, M. (2015). *Selection of EEG Frequency Bands for Detection of Depression.* Paper presented at the 16th Nordic-Baltic Conference on Biomedical Engineering.

Kan, D., & Lee, P. (2015). *Decrease alpha waves in depression: An electroencephalogram (EEG) study.* Paper presented at the 2015 International Conference on BioSignal Analysis, Processing and Systems (ICBAPS).

Kasabov, N., Dhoble, K., Nuntalid, N., & Indiveri, G. (2013). Dynamic evolving spiking neural networks for on-line spatio-and spectro-temporal pattern recognition. *Neural Networks, 41*, 188-201.

Kasabov, N. K. (2014). NeuCube: A spiking neural network architecture for mapping, learning and understanding of spatio-temporal brain data. *Neural Networks, 52*, 62-76.

Keller, T. A., & Just, M. A. (2016). Structural and functional neuroplasticity in human learning of spatial routes. *Neuroimage, 125*, 256-266.

Kelly, R. B. (1993). Storage and release of neurotransmitters. *Cell, 72*, 43-53.

Keng, S.-L., Smoski, M. J., & Robins, C. J. (2011). Effects of mindfulness on psychological health: A review of empirical studies. *Clinical psychology review, 31*(6), 1041-1056.

Kim, S. G., Richter, W., & Uğurbil, K. (1997). Limitations of temporal resolution in functional MRI. *Magnetic resonance in medicine, 37*(4), 631-636.

Knight, B. W. (1972). Dynamics of Encoding in a Population of Neurons. *The Journal of General Physiology, 59*(6), 734-766.

Krägeloh, C. U., Medvedev, O. N., Taylor, T., Wrapson, W., Rix, G., Sumich, A., . . . Ranta, J. T. (2018). A pilot randomized controlled trial for a videoconference-delivered mindfulness-based group intervention in a nonclinical setting. *Mindfulness*, 1-12.

Latora, V., & Marchiori, M. (2001). Efficient behavior of small-world networks. *Physical review letters, 87*(19), 198701.

Lau, W. K., Leung, M.-K., Chan, C. C., Wong, S. S., & Lee, T. M. (2015). Can the neural–cortisol association be moderated by experience-induced changes in awareness? *Scientific reports, 5*, 16620.

Lauder, J. M. (1993). Neurotransmitters as growth regulatory signals: role of receptors and second messengers. *Trends in neurosciences, 16*(6), 233-240.

Lazar, S. W., Kerr, C. E., Wasserman, R. H., Gray, J. R., Greve, D. N., Treadway, M. T., . . . Benson, H. (2005). Meditation experience is associated with increased cortical thickness. *Neuroreport, 16*(17), 1893.

Lee, D. J., Kulubya, E., Goldin, P., Goodarzi, A., & Girgis, F. (2018). Review of the Neural Oscillations Underlying Meditation. *Frontiers in neuroscience, 12*, 178.

Lee, N., Broderick, A. J., & Chamberlain, L. (2007). What is 'neuromarketing'? A discussion and agenda for future research. *International journal of psychophysiology, 63*(2), 199-204.

Li, B. J., Friston, K., Mody, M., Wang, H. N., Lu, H. B., & Hu, D. W. (2018). A brain network model for depression: From symptom understanding to disease intervention. *CNS neuroscience & therapeutics, 24*(11), 1004-1019.

Li, Y., Kang, C., Qu, X., Zhou, Y., Wang, W., & Hu, Y. (2016). Depression-related brain connectivity analyzed by EEG event-related phase synchrony measure. *Frontiers in human neuroscience, 10*, 477.

Liao, X., Vasilakos, A. V., & He, Y. (2017). Small-world human brain networks: perspectives and challenges. *Neuroscience & Biobehavioral Reviews, 77*, 286-300.

Lodish, H., Berk, A., Zipursky, S. L., Matsudaira, P., Baltimore, D., & Darnell, J. (2000). Neurotransmitters, synapses, and impulse transmission.

Lomas, T., Ivtzan, I., & Fu, C. H. (2015). A systematic review of the neurophysiology of mindfulness on EEG oscillations. *Neuroscience & Biobehavioral Reviews, 57*, 401-410.

Long, J., Briggs, M., & Astin, F. (2017). Overview of Systematic Reviews of Mindfulness Meditation-based Interventions for People With Long-term Conditions. *Advances in mind-body medicine, 31*(4), 26-36.

Luck, S. J. (2014). *An introduction to the event-related potential technique*: MIT press.

Luck, S. J., & Kappenman, E. S. (2011). *The Oxford handbook of event-related potential components*: Oxford university press.

Luck, S. J., & Kappenman, E. S. (2012). ERP components and selective attention. *The Oxford handbook of event-related potential components*, 295-327.

Luders, E., Toga, A. W., Lepore, N., & Gaser, C. (2009). The underlying anatomical correlates of long-term meditation: larger hippocampal and frontal volumes of gray matter. *Neuroimage, 45*(3), 672-678.

Maass, W. (1997). Networks of spiking neurons: the third generation of neural network models. *Neural Networks, 10*(9), 1659-1671.

Manna, C. B., Tenke, C. E., Gates, N. A., Kayser, J., Borod, J. C., Stewart, J. W., . . . Bruder, G. E. (2010). EEG hemispheric asymmetries during cognitive tasks in depressed patients with high versus low trait anxiety. *Clinical EEG and neuroscience, 41*(4), 196-202.

Mannila, H. (1996). *Data mining: machine learning, statistics, and databases.* Paper presented at the ssdbm.

Markus, T. M., Tsai, S. Y., Bollnow, M. R., Farrer, R. G., O'Brien, T. E., Kindler-Baumann, D. R., . . . Mir, A. K. (2005). Recovery and brain reorganization after stroke in adult and aged rats. *Annals of Neurology: Official Journal of the American Neurological Association and the Child Neurology Society, 58*(6), 950-953.

Martin, N., & Morich, K. (2011). Unconscious mental processes in consumer choice: Toward a new model of consumer behavior. *Journal of Brand Management, 18*(7), 483-505.

Masquelier, T., Guyonneau, R., & Thorpe, S. J. (2009). Competitive STDP-based spike pattern learning. *Neural computation, 21*(5), 1259-1276.

Murtagh, F. (1991). Multilayer perceptrons for classification and regression. *Neurocomputing, 2*(5-6), 183-197.

Nadkarni, S., & Narayanan, V. K. (2007). Strategic schemas, strategic flexibility, and firm performance: The moderating role of industry clockspeed. *Strategic management journal, 28*(3), 243-270.

Natu, V., & O'Toole, A. J. (2011). The neural processing of familiar and unfamiliar faces: a review and synopsis. *British Journal of Psychology, 102*(4), 726-747.

Niedermeyer, E., & da Silva, F. L. (2005). *Electroencephalography: basic principles, clinical applications, and related fields*: Lippincott Williams & Wilkins.

Nuwer, M. R., Lehman, D., Lopes da Silva, F., Matsuoka, S., Sutherling, V., & Vibert, J. (1999). IFCN guidelines for topographic and frequency analysis of EEGs and EPs. *Report of an IFCM committee*.

Olofsson, J. K., Nordin, S., Sequeira, H., & Polich, J. (2008). Affective picture processing: an integrative review of ERP findings. *Biological psychology, 77*(3), 247-265.

Ouellette, J. A., & Wood, W. (1998). Habit and intention in everyday life: The multiple processes by which past behavior predicts future behavior. *Psychological bulletin, 124*(1), 54.

Perry, M., Li, Q., & Kennedy, R. T. (2009). Review of recent advances in analytical techniques for the determination of neurotransmitters. *Analytica chimica acta, 653*(1), 1-22.

Platkiewicz, J., & Brette, R. (2010). A threshold equation for action potential initiation. *PLoS computational biology, 6*(7), e1000850.

Polich, J. (2007). Updating P300: an integrative theory of P3a and P3b. *Clinical Neurophysiology, 118*(10), 2128-2148.

Quiroga, R. Q., & Schürmann, M. (1999). Functions and sources of event-related EEG alpha oscillations studied with the Wavelet Transform. *Clinical Neurophysiology, 110*(4), 643-654.

Rätsch, G., Sonnenburg, S., & Schäfer, C. (2006). *Learning interpretable SVMs for biological sequence classification.* Paper presented at the BMC bioinformatics.

Reimann, M. W., Nolte, M., Scolamiero, M., Turner, K., Perin, R., Chindemi, G., . . . Markram, H. (2017). Cliques of neurons bound into cavities provide a missing link between structure and function. *Frontiers in computational neuroscience, 11*, 48.

Rosenblatt, F. (1957). The Perceptron, A Perceiving and Recognizing Automaton Project Para. *Report: Cornell Aeronautical Laboratory, 85*(460-461).

Russell, S. J., & Norvig, P. (2016). *Artificial intelligence: a modern approach*: Malaysia; Pearson Education Limited.

Sahay, A., & Hen, R. (2007). Adult hippocampal neurogenesis in depression. *Nature Neuroscience, 10*(9), 1110.

Schmidhuber, J. (2015). Deep learning in neural networks: An overview. *Neural Networks, 61*, 85-117.

Segrave, R. A., Cooper, N., Thomson, R., Croft, R. J., Sheppard, D., & Fitzgerald, P. (2011). Individualized alpha activity and frontal asymmetry in major depression. *Clinical EEG and neuroscience, 42*(1), 45-52.

Simard, D., Nadeau, L., & Kröger, H. (2005). Fastest learning in small-world neural networks. *Physics Letters A, 336*(1), 8-15.

Song, S., Miller, K. D., & Abbott, L. F. (2000). Competitive Hebbian learning through spike-timing-dependent synaptic plasticity. *Nature Neuroscience, 3*(9), 919.

Sporns, O., Chialvo, D. R., Kaiser, M., & Hilgetag, C. C. (2004). Organization, development and function of complex brain networks. *Trends in cognitive sciences, 8*(9), 418-425.

Sporns, O., Tononi, G., & Kötter, R. (2005). The human connectome: a structural description of the human brain. *PLoS computational biology, 1*(4), e42.

Stein, D. G., & Firl, A. C. (1976). Brain damage and reorganization of function in old age. *Experimental neurology, 52*(1), 157-167.

Stone, J. V. (2004). *Independent component analysis: a tutorial introduction*: MIT press.

Subasi, A., & Gursoy, M. I. (2010). EEG Signal Classification Using PCA, ICA, LDA and Support Vector Machines. *Expert Systems with Applications, 37*(12), 8659-8666.

Sumich, A., Kumari, V., & Sharma, T. (2003). Neuroimaging of sexual arousal: research and clinical utility. *Hospital Medicine, 64*(1), 28-33.

Talairach, J., & Tournoux, P. (1988). Co-planar stereotaxic atlas of the human brain: 3-dimensional proportional system: an approach to cerebral imaging.

Tang, Y.-Y., Hölzel, B. K., & Posner, M. I. (2015). The neuroscience of mindfulness meditation. *Nature Reviews Neuroscience, 16*(4), 213.

Tatum IV, W., Hausain, A., Banbadis, S., & Kaplan, P. Handbook of EEG interpretation. Demos Medical Publishing; 2008.

Tatum IV, W. O. (2014). *Handbook of EEG interpretation*: Demos Medical Publishing.

Telesford, Q. K., Simpson, S. L., Burdette, J. H., Hayasaka, S., & Laurienti, P. J. (2011). The brain as a complex system: using network science as a tool for understanding the brain. *Brain connectivity, 1*(4), 295-308.

Thatcher, R. (2008). NeuroGuide Manual and Tutorial. *St. Petersburg, FL: Applied Neuroscience*.

Thorpe, S., & Gautrais, J. (1998). Rank order coding *Computational neuroscience* (pp. 113-118): Springer.

Touhami, Z. O., Benlafkih, L., Jiddane, M., Cherrah, Y., Malki, H. O. E., & Benomar, A. (2011). Neuromarketing: Where marketing and neuroscience meet. *African Journal of Business Management, 5*(5), 1528-1532.

Tu, E., Kasabov, N., & Yang, J. (2017). Mapping temporal variables into the neucube for improved pattern recognition, predictive modeling, and understanding of stream data. *IEEE transactions on neural networks and learning systems, 28*(6), 1305-1317.

van Gerven, M., & Bohte, S. (2018). *Artificial neural networks as models of neural information processing*: Frontiers Media SA.

Van Loan, C. (1992). *Computational frameworks for the fast Fourier transform* (Vol. 10): Siam.

Vestergaard-Poulsen, P., van Beek, M., Skewes, J., Bjarkam, C. R., Stubberup, M., Bertelsen, J., & Roepstorff, A. (2009). Long-term meditation is associated with increased gray matter density in the brain stem. *Neuroreport, 20*(2), 170-174.

Vignaud, P., Donde, C., Sadki, T., Poulet, E., & Brunelin, J. (2018). Neural effects of mindfulness-based interventions on patients with major depressive disorder: A systematic review. *Neuroscience & Biobehavioral Reviews*.

von Bartheld, C. S., Bahney, J., & Herculano-Houzel, S. (2016). The search for true numbers of neurons and glial cells in the human brain: a review of 150 years of cell counting. *Journal of Comparative Neurology, 524*(18), 3865-3895.

Walker, J. E., Kozlowski, G. P., & Lawson, R. (2007). A modular activation/coherence approach to evaluating clinical/QEEG correlations and for guiding neurofeedback training: modular insufficiencies, modular excesses, disconnections, and hyperconnections. *Journal of Neurotherapy, 11*(1), 25-44.

Wall, J., Xu, J., & Wang, X. (2002). Human brain plasticity: an emerging view of the multiple substrates and mechanisms that cause cortical changes and related sensory dysfunctions after injuries of sensory inputs from the body. *Brain Research Reviews, 39*(2-3), 181-215.

Weare, K. (2014). Evidence for mindfulness: Impacts on the wellbeing and performance of school staff. *Mindfulness in Schools*.

Weber, B. (2017). Neuroscience: Connectivity mapping and behaviour. *Nature Human Behaviour, 1*(8), 0164.

Wood, W., & Neal, D. T. (2009). The habitual consumer. *Journal of Consumer Psychology, 19*(4), 579-592.

Wu, C.-T., Dillon, D., Hsu, H.-C., Huang, S., Barrick, E., & Liu, Y.-H. (2018). Depression Detection Using Relative EEG Power Induced by Emotionally Positive Images and a Conformal Kernel Support Vector Machine. *Applied Sciences, 8*(8), 1244.

Yao, X., Panaye, A., Doucet, J.-P., Zhang, R., Chen, H., Liu, M., . . . Fan, B. T. (2004). Comparative study of QSAR/QSPR correlations using support vector machines, radial basis function neural networks, and multiple linear regression. *Journal of chemical information and computer sciences, 44*(4), 1257-1266.

Yu, S., Huang, D., Singer, W., & Nikolić, D. (2008). A small world of neuronal synchrony. *Cerebral cortex, 18*(12), 2891-2901.

Zhuang, K., Bi, M., Li, Y., Xia, Y., Guo, X., Chen, Q., . . . Yin, H. (2017). A distinction between two instruments measuring dispositional mindfulness and the correlations between those measurements and the neuroanatomical structure. *Scientific reports, 7*(1), 6252.

Zurada, J. M. (1992). *Introduction to artificial neural systems* (Vol. 8): West publishing company St. Paul.

Zurawicki, L. (2010). *Neuromarketing: Exploring the brain of the consumer*: Springer Science & Business Media.

Appendix A

Table A- 1. Anatomical locations of cortical projections. The BA column represents the id of the corresponding Brodmann areas.

Labels	Talairach coordinates			Brodmann Area and Number	
	***x* avg (mm)**	***y* avg (mm)**	***z* avg (mm)**		
FP1	− 21.2 ± 4.7	66.9 ± 3.8	12.1 ± 6.6	Superior frontal G	10
FPz	1.4 ± 2.9	65.1 ± 5.6	11.3 ± 6.8	Bilat. medial	10
FP2	24.3 ± 3.2	66.3 ± 3.5	12.5 ± 6.1	Superior frontal G	10
AF7	− 41.7 ± 4.5	52.8 ± 5.4	11.3 ± 6.8	Middle frontal G	10
AF3	− 32.7 ± 4.9	48.4 ± 6.7	32.8 ± 6.4	Superior frontal G	9
AFz	1.8 ± 3.8	54.8 ± 7.3	37.9 ± 8.6	Bilat. medial	9
AF4	35.1 ± 3.9	50.1 ± 5.3	31.1 ± 7.5	Superior frontal G	9
AF8	43.9 ± 3.3	52.7 ± 5.0	9.3 ± 6.5	Middle frontal G	10
F7	− 52.1 ± 3.0	28.6 ± 6.4	3.8 ± 5.6	Inferior frontal G	45
F5	− 51.4 ± 3.8	26.7 ± 7.2	24.7 ± 9.4	Middle frontal G	46
F3	− 39.7 ± 5.0	25.3 ± 7.5	44.7 ± 7.9	Middle frontal G	8
F1	− 22.1 ± 6.1	26.8 ± 7.2	54.9 ± 6.7	Superior frontal G	6
Fz	0.0 ± 6.4	26.8 ± 7.9	60.6 ± 6.5	Bilat. medial	6
F2	23.6 ± 5.0	28.2 ± 7.4	55.6 ± 6.2	Superior frontal G	6
F4	41.9 ± 4.8	27.5 ± 7.3	43.9 ± 7.6	Middle frontal G	8
F6	52.9 ± 3.6	28.7 ± 7.2	25.2 ± 7.4	Middle frontal G	46
F8	53.2 ± 2.8	28.4 ± 6.3	3.1 ± 6.9	Inferior frontal G	45
FT9	− 53.8 ± 3.3	− 2.1 ± 6.0	− 29.1 ± 6.3	Inferior temporal G	20
FT7	− 59.2 ± 3.1	3.4 ± 5.6	− 2.1 ± 7.5	Superior temporal G	22
FC5	− 59.1 ± 3.7	3.0 ± 6.1	26.1 ± 5.8	Precentral G	6
FC3	− 45.5 ± 5.5	2.4 ± 8.3	51.3 ± 6.2	Middle frontal G	6
FC1	− 24.7 ± 5.7	0.3 ± 8.5	66.4 ± 4.6	Superior frontal G	6
FCz	1.0 ± 5.1	1.0 ± 8.4	72.8 ± 6.6	Superior frontal G	6
FC2	26.1 ± 4.9	3.2 ± 9.0	66.0 ± 5.6	Superior frontal G	6
FC4	47.5 ± 4.4	4.6 ± 7.6	49.7 ± 6.7	Middle frontal G	6
FC6	60.5 ± 2.8	4.9 ± 7.3	25.5 ± 7.8	Precentral G	6
FT8	60.2 ± 2.5	4.7 ± 5.1	− 2.8 ± 6.3	Superior temporal G	22
FT10	55.0 ± 3.2	− 3.6 ± 5.6	− 31.0 ± 7.9	Inferior temporal G	20
T7	− 65.8 ± 3.3	− 17.8 ± 6.8	− 2.9 ± 6.1	Middle temporal G	21
C5	− 63.6 ± 3.3	− 18.9 ± 7.8	25.8 ± 5.8	Postcentral G	123
C3	− 49.1 ± 5.5	− 20.7 ± 9.1	53.2 ± 6.1	Postcentral G	123
C1	− 25.1 ± 5.6	− 22.5 ± 9.2	70.1 ± 5.3	Precentral G	4
Cz	0.8 ± 4.9	− 21.9 ± 9.4	77.4 ± 6.7	Precentral G	4
C2	26.7 ± 5.3	− 20.9 ± 9.1	69.5 ± 5.2	Precentral G	4
C4	50.3 ± 4.6	− 18.8 ± 8.3	53.0 ± 6.4	Postcentral G	123
C6	65.2 ± 2.6	− 18.0 ± 7.1	26.4 ± 6.4	Postcentral G	123
T8	67.4 ± 2.3	− 18.5 ± 6.9	− 3.4 ± 7.0	Middle temporal G	21
TP7	− 63.6 ± 4.5	− 44.7 ± 7.2	− 4.0 ± 6.6	Middle temporal G	21
CP5	− 61.8 ± 4.7	− 46.2 ± 8.0	22.5 ± 7.6	Supramarginal G	40
CP3	− 46.9 ± 5.8	− 47.7 ± 9.3	49.7 ± 7.7	Inferior parietal G	40
CP1	− 24.0 ± 6.4	− 49.1 ± 9.9	66.1 ± 8.0	Postcentral G	7
CPz	0.7 ± 4.9	− 47.9 ± 9.3	72.6 ± 7.7	Postcentral G	7
CP2	25.8 ± 6.2	− 47.1 ± 9.2	66.0 ± 7.5	Postcentral G	7
CP4	49.5 ± 5.9	− 45.5 ± 7.9	50.7 ± 7.1	Inferior parietal G	40
CP6	62.9 ± 3.7	− 44.6 ± 6.8	24.4 ± 8.4	Supramarginal G	40
TP8	64.6 ± 3.3	− 45.4 ± 6.6	− 3.7 ± 7.3	Middle temporal G	21
P9	− 50.8 ± 4.7	− 51.3 ± 8.6	− 37.7 ± 8.3	Tonsil	NP
P7	− 55.9 ± 4.5	− 64.8 ± 5.3	0.0 ± 9.3	Inferior temporal G	37
P5	− 52.7 ± 5.0	− 67.1 ± 6.8	19.9 ± 10.4	Middle temporal G	39
P3	− 41.4 ± 5.7	− 67.8 ± 8.4	42.4 ± 9.5	Precuneus	19

P1	− 21.6 ± 5.8	− 71.3 ± 9.3	52.6 ± 10.1	Precuneus	7
Pz	0.7 ± 6.3	− 69.3 ± 8.4	56.9 ± 9.9	Superior parietal L	7
P2	24.4 ± 6.3	− 69.9 ± 8.5	53.5 ± 9.4	Precuneus	7
P4	44.2 ± 6.5	− 65.8 ± 8.1	42.7 ± 8.5	Inferior parietal L	7
P6	54.4 ± 4.3	− 65.3 ± 6.0	20.2 ± 9.4	Middle temporal G	39
P8	56.4 ± 3.7	− 64.4 ± 5.6	0.1 ± 8.5	Inferior temporal G	19
P10	51.0 ± 3.5	− 53.9 ± 8.7	− 36.5 ± 10.0	Tonsil	NP
PO7	− 44.0 ± 4.7	− 81.7 ± 4.9	1.6 ± 10.6	Middle occipital G	18
PO3	− 33.3 ± 6.3	− 84.3 ± 5.7	26.5 ± 11.4	Superior occipital G	19
POz	0.0 ± 6.5	− 87.9 ± 6.9	33.5 ± 11.9	Cuneus	19
PO4	35.2 ± 6.5	− 82.6 ± 6.4	26.1 ± 9.7	Superior occipital G	19
PO8	43.3 ± 4.0	− 82.0 ± 5.5	0.7 ± 10.7	Middle occipital G	18
O1	− 25.8 ± 6.3	− 93.3 ± 4.6	7.7 ± 12.3	Middle occipital G	18
Oz	0.3 ± 5.9	− 97.1 ± 5.2	8.7 ± 11.6	Cuneus	18
O2	25.0 ± 5.7	− 95.2 ± 5.8	6.2 ± 11.4	Middle occipital G	18

Appendix B

B- 1. Descriptive statistics of Mean and Std. Deviation values of P1 ERP components for the variables of the research: Hemisphere (left and right), Sites (frontal, parietal, central, temporal and occipital), and conditions (familiar and unfamiliar) across 20 participants. Highlighted in blue show the highest mean values among other sites. * Fam: Familiar, UnFam: Unfamiliar.

Descriptive Statistics			
Variables	Mean	Std. Deviation	N
Left_Frontal_P1_Fam*	3.1205	.91198	20
Left_Frontal_P1_UnFam	1.4655	.39451	20
Left_Parietal_P1_Fam	3.7770	.73806	20
Left_Parietal_P1_UnFam	2.0200	1.07867	20
Left_Central_P1_Fam	2.3750	1.11756	20
Left_Central_P1_UnFam	1.2160	.49311	20
Left_Temporal_P1_Fam	2.1578	.71316	20
Left_Temporal_P1_UnFam	1.5300	.63533	20
Left_Occipital_P1_Fam	3.2700	.62789	20
Left_Occipital_P1_UnFam	2.7015	1.30496	20
Right_Frontal_P1_Fam	2.5740	.74654	20
Right_Frontal_P1_UnFam	1.7063	.41942	20
Right_Parietal_P1_Fam	4.0240	.73203	20
Right_Parietal_P1_UnFam	1.8890	1.01932	20
Right_Central_P1_Fam	2.6615	1.32956	20
Right_Central_P1_UnFam	1.5240	.79164	20
Right_Temporal_P1_Fam	2.7398	1.13426	20
Right_Temporal_P1_UnFam	2.4040	.65450	20
Right_Occipital_P1_Fam	3.6615	.58251	20
Right_Occipital_P1_UnFam	1.9855	.71663	20

B- 2. Descriptive statistics of Mean and Std. Deviation values of P2 ERP components for the variables of the research: Hemisphere (left and right), Sites (frontal, parietal, central, temporal and occipital), and conditions (familiar and unfamiliar) across 20 participants. Highlighted in blue show the highest mean values among other sites. * Fam: Familiar, UnFam: Unfamiliar.

Descriptive Statistics			
Variables	Mean	Std. Deviation	N
Left_Frontal_P2_Fam	2.1998	.71907	20
Left_Frontal_P2_UnFam	1.4988	.50059	20
Left_Parietal_P2_Fam	4.3330	.84388	20
Left_Parietal_P2_UnFam	4.2535	.89139	20
Left_Central_P2_Fam	1.8830	1.23405	20
Left_Central_P2_UnFam	1.2530	.76792	20
Left_Temporal_P2_Fam	2.1685	.76478	20
Left_Temporal_P2_UnFam	1.3128	.49649	20
Left_Occipital_P2_Fam	6.2065	.66768	20
Left_Occipital_P2_UnFam	5.4065	.79287	20
Right_Frontal_P2_Fam	1.5580	.47954	20
Right_Frontal_P2_UnFam	1.2645	.42270	20
Right_Parietal_P2_Fam	4.3820	.85341	20
Right_Parietal_P2_UnFam	4.1990	.87884	20
Right_Central_P2_Fam	1.6555	1.07540	20
Right_Central_P2_UnFam	1.2530	.76792	20
Right_Temporal_P2_Fam	2.4408	.64864	20
Right_Temporal_P2_UnFam	2.0983	.56442	20
Right_Occipital_P2_Fam	6.0940	.61007	20
Right_Occipital_P2_UnFam	5.9575	.55052	20

B- 3. Descriptive statistics of Mean and Std. Deviation values of N1 ERP components for the variables of the research: Hemisphere (left and right), Sites (frontal, parietal, central, temporal and occipital), and conditions (familiar and unfamiliar) across 20 participants. Highlighted in blue show the highest mean values among other sites. * Fam: Familiar, UnFam: Unfamiliar.

Descriptive Statistics			
Variables	Mean	Std. Deviation	N
Left_Frontal_N1_Fam	.8485	.35046	20
Left_Frontal_N1_UnFam	.4588	.33940	20
Left_Parietal_N1_Fam	1.8795	.54083	20
Left_Parietal_N1_UnFam	1.6460	.42424	20
Left_Central_N1_Fam	1.8795	.54083	20
Left_Central_N1_UnFam	1.6460	.42424	20
Left_Temporal_N1_Fam	.3855	.13027	20
Left_Temporal_N1_UnFam	.3828	.08135	20
Left_Occipital_N1_Fam	3.9600	.69932	20
Left_Occipital_N1_UnFam	2.4765	1.20008	20
Right_Frontal_N1_Fam	.5203	.41882	20
Right_Frontal_N1_UnFam	.4160	.33072	20
Right_Parietal_N1_Fam	.7640	.49868	20
Right_Parietal_N1_UnFam	.8665	.53197	20
Right_Central_N1_Fam	.5440	.43189	20
Right_Central_N1_UnFam	.4175	.29340	20
Right_Temporal_N1_Fam	1.0378	.38480	20
Right_Temporal_N1_UnFam	1.0275	.33203	20
Right_Occipital_N1_Fam	5.8025	.58247	20
Right_Occipital_N1_UnFam	2.5630	.92889	20

B- 4. The average of the connection weights between each input neuron (EEG channel) and a cluster of neighbouring neurons that are connected to it during the learning process with EEG epochs of 100ms, 150ms and 200ms. The last column represents the average of the connection weights across all the EEG channels.

Time frame	class	C3	Cz	C4	F7	F3	Fz	F4	F8	P3	Pz	P4	T3	T4	T5	T6	FP1	FP2	O1	O2	AVG
100ms	Familiar	0.23	0.18	0.26	0.52	0.68	0.73	0.09	0.32	0.22	0.29	0.37	0.11	0.98	0.73	0.38	0.15	0.11	0.05	0.36	0.35
	Unfamiliar	0.32	0.08	0.23	0.43	0.78	0.23	0.05	0.28	0.04	0.03	0.37	0.05	0.8	0.19	0.03	0.14	0.13	0.15	0.12	0.23
150ms	Familiar	0.84	0.93	1.04	0.43	0.73	0.93	0.58	0.3	0.54	0.34	1.02	0.85	0.8	0.8	0.87	0.6	0.54	0.89	0.32	0.70
	Unfamiliar	0.3	0.27	0.84	0.07	0.66	0.2	0.11	0.19	0.13	0.06	0.78	0.76	0.03	0.74	0.99	0.06	0.32	0.04	0.79	0.38
200ms	Familiar	1.3	1.33	0.76	1.03	1.05	0.65	0.32	1.05	1.01	0.97	1.12	1.12	1.19	1.06	1.04	0.89	1.03	1.32	1.02	1.01
	Unfamiliar	0.93	1.07	0.11	0.49	0.68	0.48	0.01	0.48	0.54	0.58	0.51	0.88	0.6	0.41	1.03	0.42	0.83	0.45	0.73	0.59

B- 5. Intensity of the spikes emitted in clusters of neurons that surrounding EEG channels (input neurons) during the learning process with EEG epochs of 50ms, 150ms and 200ms. The activation level is highlighted into 3 colours that are explained in
Figure 5-10.

Time frame	class	C3	Cz	C4	F7	F3	Fz	F4	F8	P3	Pz	P4	T3	T4	T5	T6	FP1	FP2	O1	O2
50ms	Familiar	0	0	0	0	0	0	0	0	0	0	0	0	0.2	0	0	0	0	0	0.5
	Unfamiliar	0	0	0	0	0	0	0	0	0	0	0	0	0	0	0	0	0	0	0.3
100ms	Familiar	0	0	0	0	0	0	0	0	0.2	0.5	0	0	0	0	0.6	0	0	0	0.6
	Unfamiliar	0	0	0	0	0	0	0	0	0	0	0	0	0	0	0.3	0	0	0.3	0.3
150ms	Familiar	0	0.5	0	0.2	0	0	0	0	0.6	0.5	0.5	0	0	0.1	0	0.2	0	0	0
	Unfamiliar	0	0	0	0	0	0	0	0	0.2	0	0	0	0.2	0	0	0	0	0.1	0
200ms	Familiar	0	0	0	0.3	0	0	0	0.6	0	0.7	0.8	0	0.9	0	0	0.2	0.9	0.2	0.8
	Unfamiliar	0	0	0	0	0	0	0	0	0	0	0.5	0	0.7	0	0.2	0	0.7	0.6	0.2

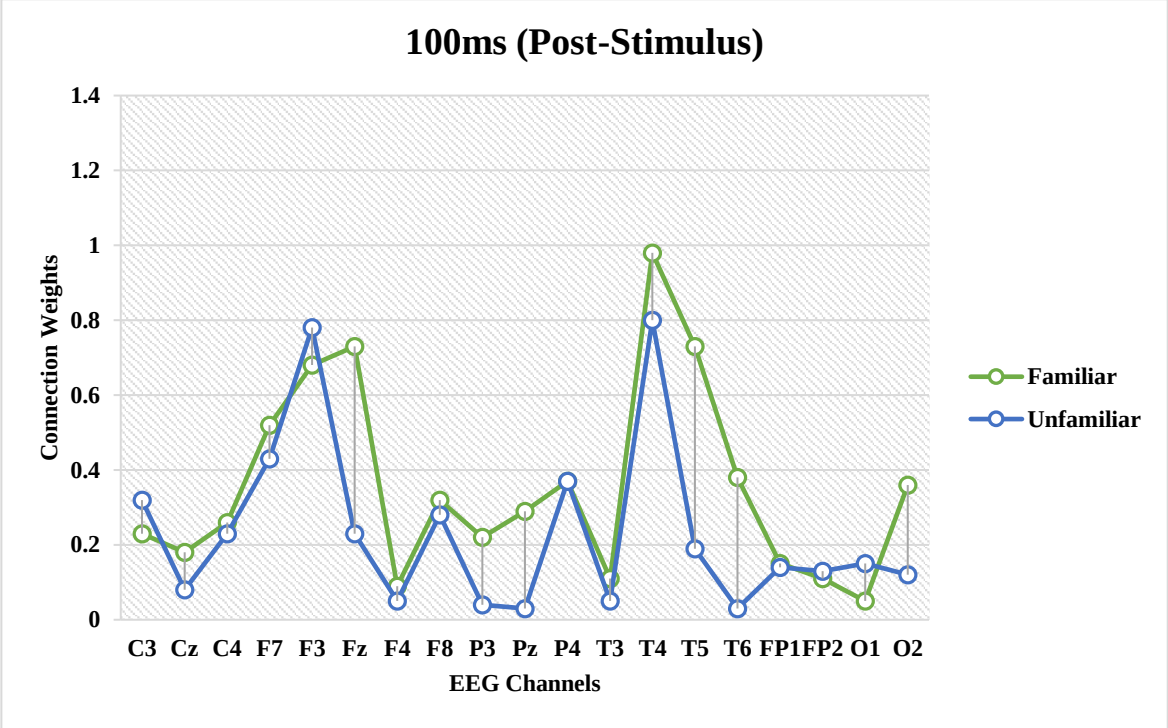

B- 6 . The average of the connection weights created by each of the input neurons (representing an EEG channel) in the SNN models trained on EEG data related to 100ms post stimulus showing changes towards familiar and unfamiliar marketing stimuli. Green line represents the connectivity values in the SNN model of familiar marketing stimuli and blue line represents unfamiliar marketing stimuli.

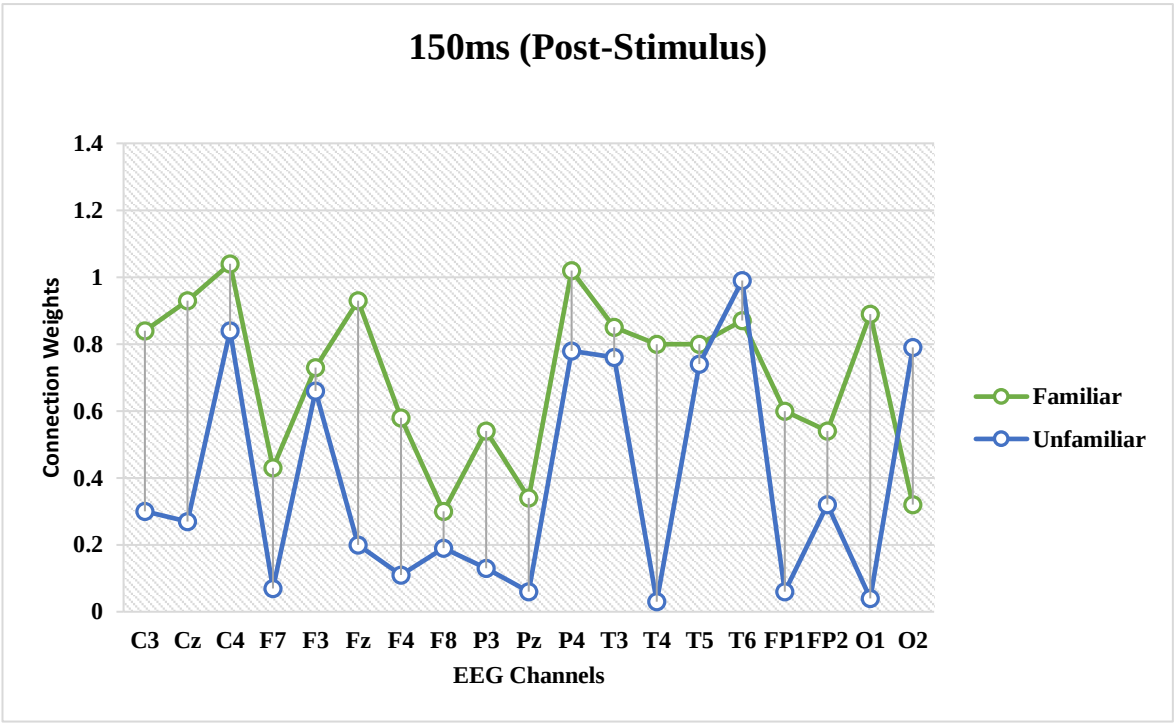

B- 7. The average of the connection weights created by each of the input neurons (representing an EEG channel) in the SNN models trained on EEG data related to 150ms post stimulus showing changes towards familiar and unfamiliar marketing stimuli. Green line represents the connectivity values in the SNN model of familiar marketing stimuli and blue line represents unfamiliar marketing stimuli.

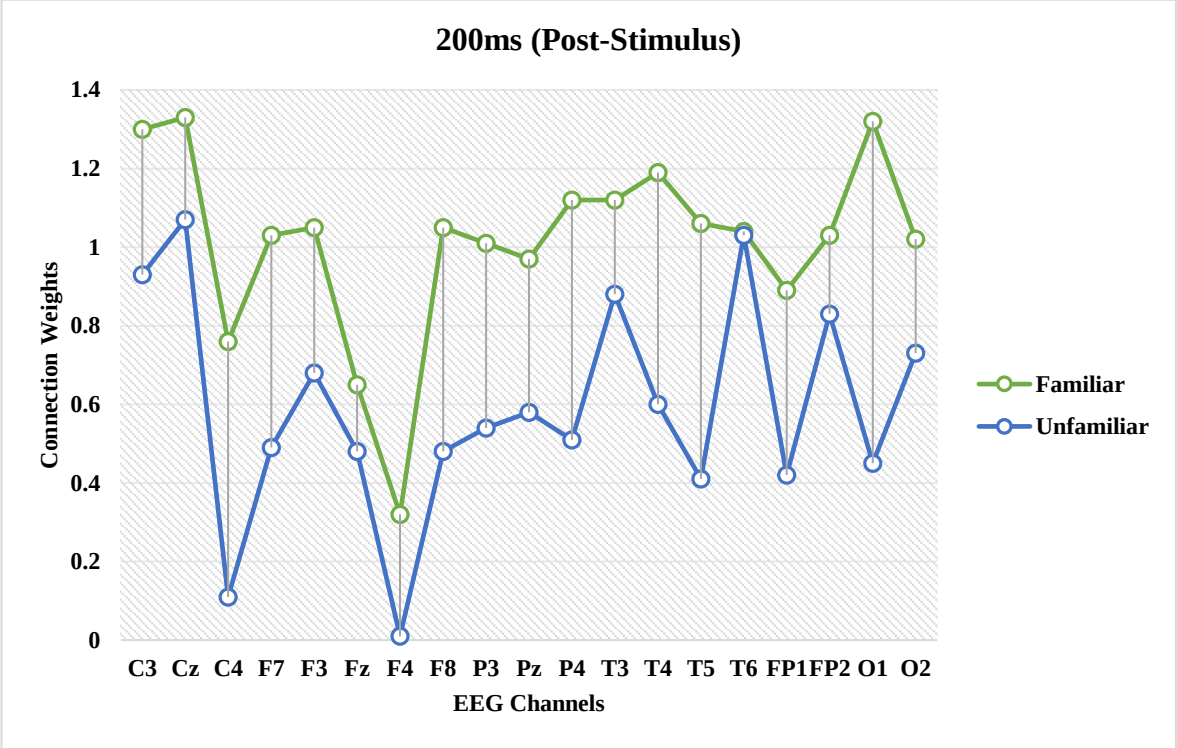

B- 8. The average of the connection weights created by each of the input neurons (representing an EEG channel) in the SNN models trained on EEG data related to 200ms post stimulus showing changes towards familiar and unfamiliar marketing stimuli. Green line represents the connectivity values in the SNN model of familiar marketing stimuli and blue line represents unfamiliar marketing stimuli.

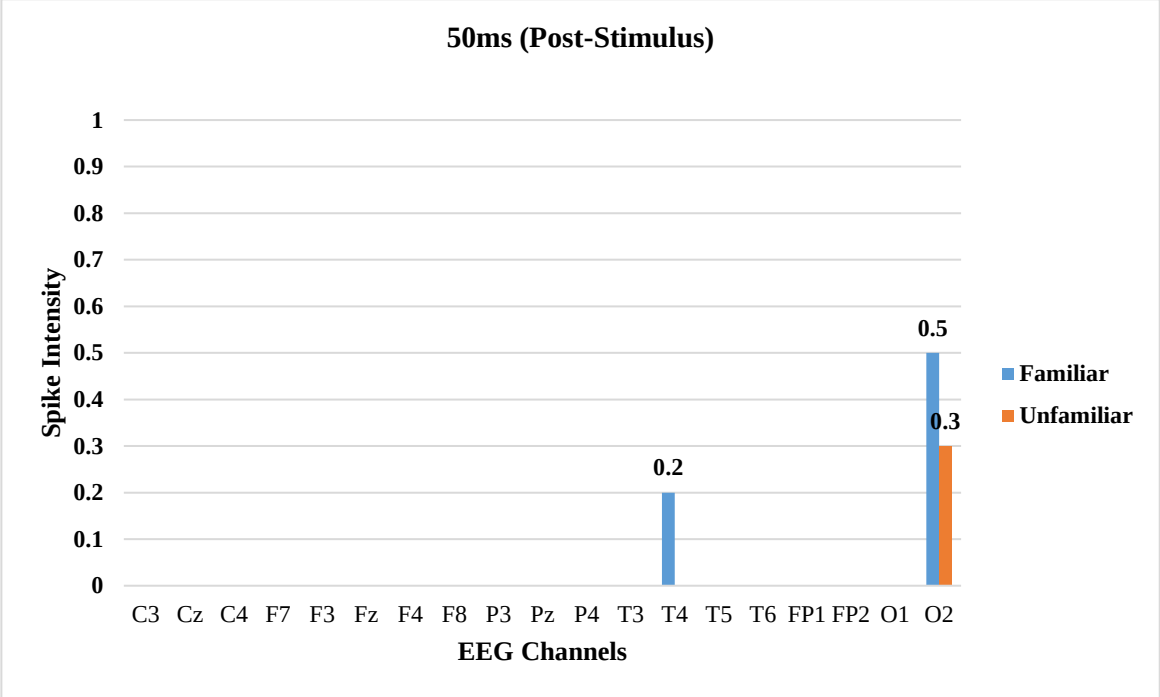

B- 9. The activated brain areas according to the numbers of activated neurons in the SNN models during learning, over 50ms post stimulus towards familiar and unfamiliar marketing stimuli. The level of activation for O2 channel towards familiar stimuli is 0.5 which denoted as medium intensity versus 0.3 towards unfamiliar ones which is denoted as low intensity. T4 channel with 0.2 level of intensity is activated towards familiar stimuli at this time but not for unfamiliar ones.

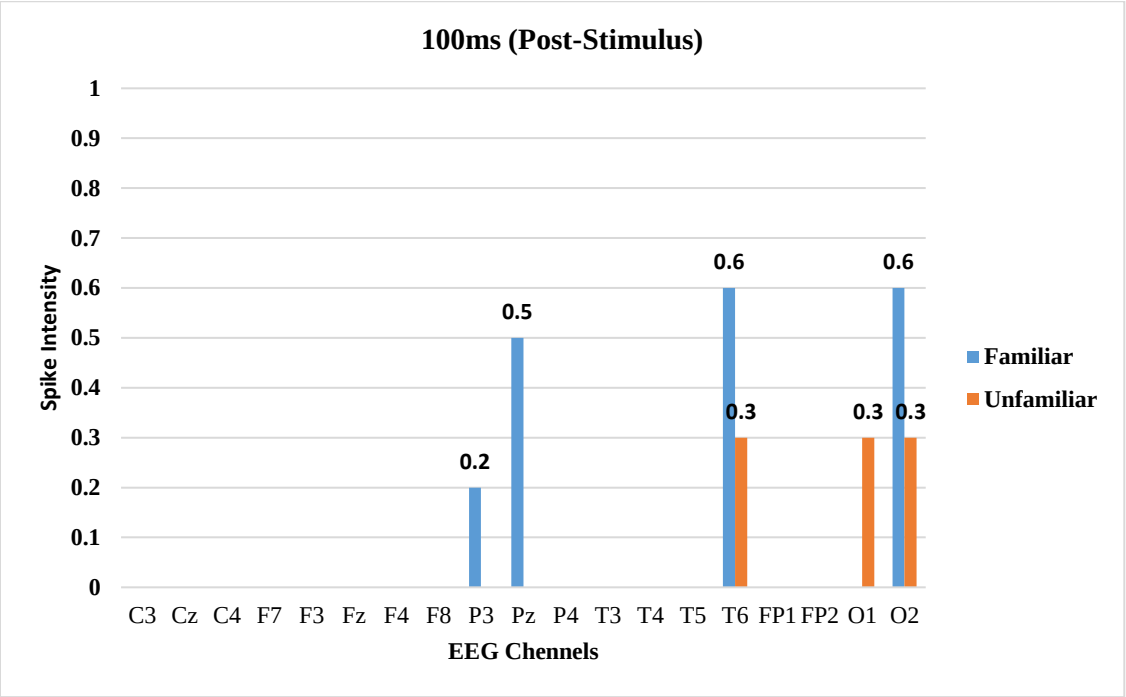

B- 10. The activated brain areas according to the numbers of activated neurons in the SNN models during learning, over 100ms post stimulus towards familiar and unfamiliar marketing stimuli. The level of activation for O2 and T6 channels towards familiar stimuli is 0.6 which denoted as medium intensity versus 0.3 towards unfamiliar ones which is denoted as low intensity. Some other areas were also activated at this time towards familiar stimuli but were not seen towards unfamiliar ones such as (Pz and P3).

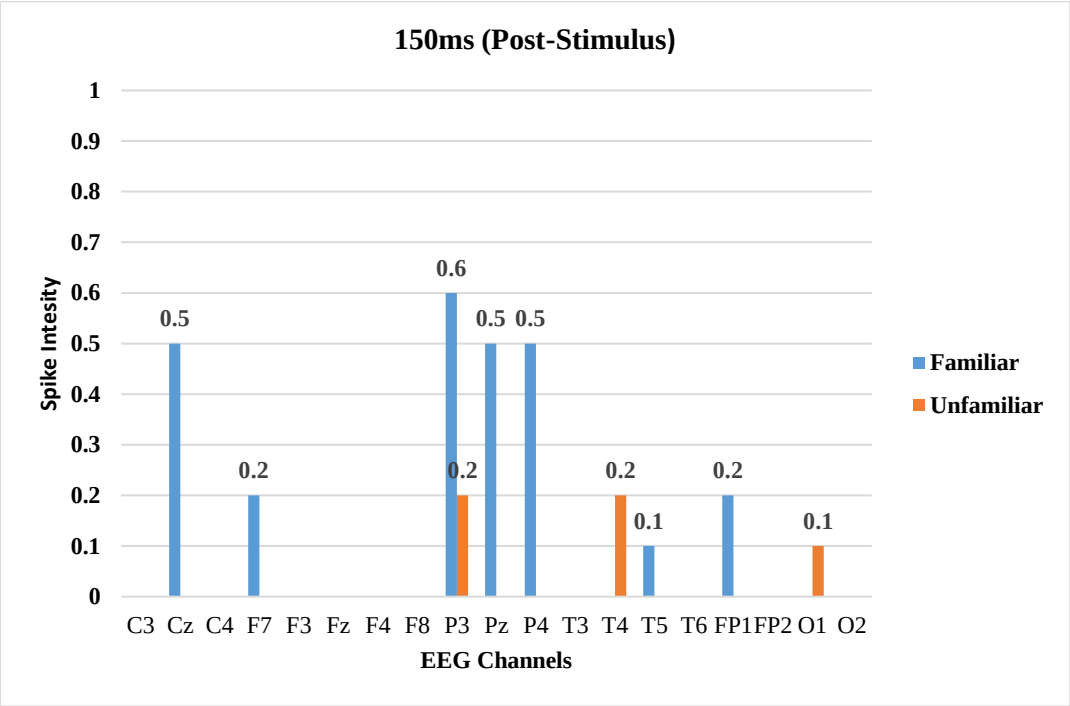

B- 11. The activated brain areas according to the numbers of activated neurons in the SNN models during learning, over 150ms post stimulus towards familiar and unfamiliar marketing stimuli. The level of activation for P3 channel towards familiar stimuli is 0.6 which denoted as medium intensity versus 0.2 towards unfamiliar ones which is denoted as low intensity. Some other areas were also activated at this time towards familiar stimuli but were not seen for unfamiliar ones such as (Pz, P4, Cz, F7, and Fp1). Some areas which was activated earlier in time towards familiar stimuli, now is activated towards unfamiliar ones such as T4 channel.

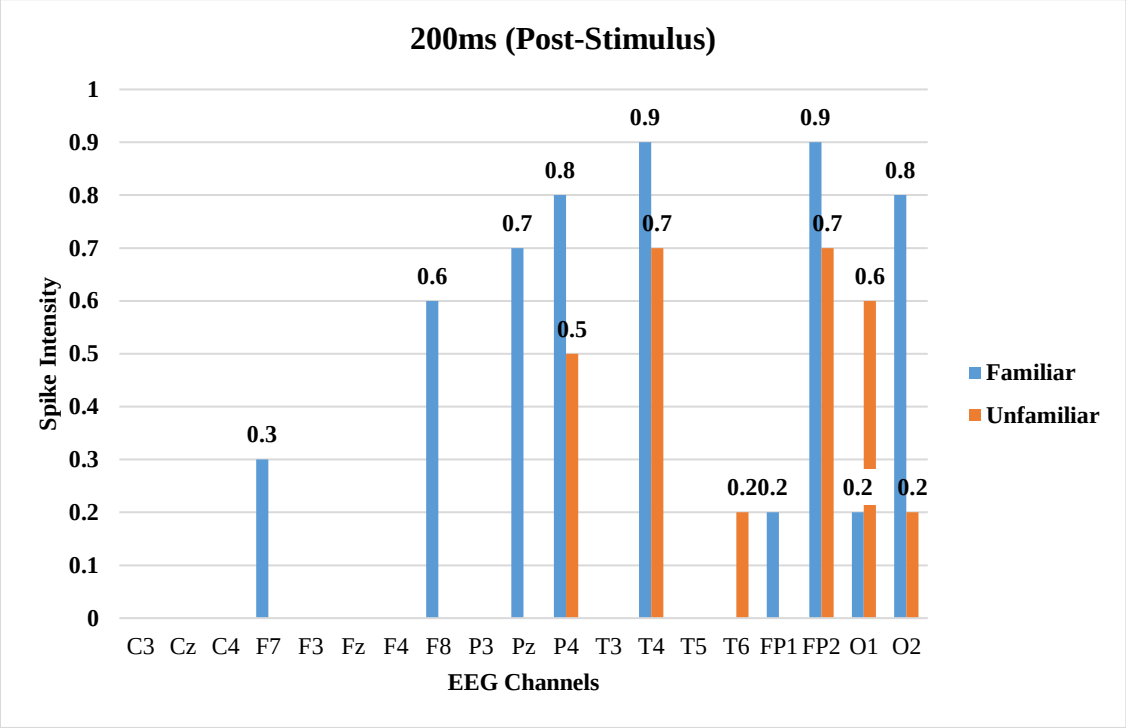

B- 12. The activated brain areas according to the numbers of activated neurons in the SNN models during learning, at 200ms post stimulus towards familiar and unfamiliar marketing stimuli. The level of activation for P4, T4, Fp2, and O2 channels towards familiar stimuli is considerably higher than unfamiliar ones. Some other areas were also activated at this time towards familiar stimuli but were not seen towards unfamiliar ones such as (F7, F8, Fp1 and Pz). The highest intensity belongs to T4 and Fp2 channels towards familiar stimuli and corresponding to memory formation, storage and emotional attention functions.

Appendix C

C- 1. Information of 18 participants who were affected by different levels of depression from minimal (non-depressed) to severe, according to the Beck Depression Inventory (BDI-II) assessment. Based on BDI-II profile, the severity rating for depression subscale labelled as normal (between 1-10), Mild (between 11-16), clinical depression (between 17-20), Moderate depression (between 21-30), severe depression (between 31-40) and extreme depression (over 40). 1) Non-Depressed group (denoted as ND), 2) depressed group who responded to the training (denoted as D+) and 3) depressed group who did not respond to the training (denoted as D-). Descriptive information such as age, gender, mean age, range, mean score and the standard deviation are also reported in the Appendix C-2 and C-3.

Participants	Id	Age	Gender	BDI score at T1	BDI score at T2
ND Group	**S##1**	34	F	10	8
	S##2	18	F	5	5
	S##3	43	F	6	5
	S##4	19	F	3	4
	S##5	37	F	10	9
	S##6	33	F	2	3
	S##7	20	F	8	9
D^+	**S1**	20	M	20	8
	S2	21	F	18	6
	S3	30	M	22	3
	S4	26	F	18	2
	S5	25	M	21	8
	S6	24	F	18	6
D^-	**S#1**	29	M	22	18
	S#2	29	F	36	22
	S#3	21	M	20	19
	S#4	19	F	22	18
	S#5	40	M	22	23

C- 2. Descriptive information of all participants including age, gender, mean age, range, mean score and the standard deviation.

Descriptive Statistics			
		Male	**Female**
N	**Valid**	6	12
	Missing	0	0
Mean		27.5	26.9167
Std. Deviation		7.342	8.25126
Variance		53.9	68.083
Range		20	25
Minimum age		20	18
Maximum age		40	43

C- 3. Descriptive information of BDI test, including mean and standard deviation.

Descriptive Statistics			
		BDI score at T1	**BDI score at T2**
N	**Valid**	18	18
	Missing	0	0
Mean score		15.72	9.78
Std. Deviation		8.857	6.924

C- 4. The average of the connection weights between each input neuron and a cluster of neighbouring neurons that are connected to it during the learning process across both left and right sides of five sites: F (Frontal), FC (Frontocentral), T (Temoporal), CP (Cenroparietal) and OP (Occipitoparietal) at T1 (before the treatment) and at T2 (after the treatment) for all the 3 groups: a) non-depressed (ND); b) depressed group who responded to the treatment (D+); and c) depressed group who did not respond to the treatment (D-). The mean and standard deviation (SD) of both hemispheres at T1 and T2 are also reported.

Groups	**Sites**	**T1**		**T2**	
		Left	**Right**	**Left**	**Right**
a) ND	**F**	0.97	1.07	1.24	1.44
	FC	0.83	1.02	0.99	0.95
	T	0.95	1.14	0.99	1.15
	CP	0.68	0.91	0.72	1.12
	OP	0.9	0.63	0.97	1.1
Mean (SD)		0.86(0.11)	0.95(0.11)	0.98(0.18)	1.15(0.17)
b) D^+	**F**	0.88	0.75	1.19	1.03
	FC	0.66	0.81	0.1	0.95
	T	0.82	0.91	0.99	1.16
	CP	0.82	0.86	0.88	1.1
	OP	0.63	0.48	0.76	0.53
Mean (SD)		0.76(0.11)	0.76(0.17)	0.78(0.41)	0.95(0.24)
c) D^-	**F**	0.56	0.52	0.71	0.64
	FC	0.49	0.43	0.68	0.67
	T	0.66	0.57	0.86	0.72
	CP	0.46	0.79	0.41	0.86
	OP	0.45	0.22	0.56	0.23
Mean (SD)		0.52(0.09)	0.51(0.2)	0.64(0.16)	0.62(0.23)

C- 5. Descriptive information such as mean and standard deviation across all groups (non-depressed (ND); depressed group who responded to the treatment (D+); and depressed group who did not respond to the treatment (D-), for both variables of the research (sites: frontal, temporal, frontocentral, centroparietal and occipitoparietal, and hemisphere: left and right) at T1 (before mindfulness training).

Descriptive					
Hem	**Sites**	**Group**	**Mean**	**SD**	**N**
Left	**Frontal**	ND	0.97	0.18	7
		D+	0.88	0.28	6
		D-	0.56	0.23	5
	Temporal	ND	0.95	0.27	7
		D+	0.83	0.22	6
		D-	0.65	0.31	5
	Frontocentral	ND	0.83	0.34	7
		D+	0.66	0.13	6
		D-	0.49	0.13	5
	Centroparietal	ND	0.68	0.30	7
		D+	0.83	0.18	6
		D-	0.46	0.14	5
	Occipitoparietal	ND	0.90	0.12	7
		D+	0.63	0.13	6
		D-	0.45	0.10	5
Right	**Frontal**	ND	1.07	0.22	7
		D+	0.75	0.22	6
		D-	0.53	0.07	5
	Temporal	ND	1.14	0.13	7
		D+	0.91	0.17	6
		D-	0.57	0.10	5
	Frontocentral	ND	1.02	0.15	7
		D+	0.81	0.15	6
		D-	0.43	0.17	5
	Centroparietal	ND	0.91	0.23	7
		D+	0.86	0.27	6
		D-	0.79	0.13	5
	Occipitoparietal	ND	0.63	0.17	7
		D+	0.48	0.46	6
		D-	0.22	0.09	5

C- 6. Descriptive information such as mean and standard deviation across all groups (non-depressed (ND); depressed group who responded to the treatment (D+); and depressed group who did not respond to the treatment (D-), for both variables of the research (sites: frontal, temporal, frontocentral, centroparietal and occipitoparietal, and hemisphere: left and right) at T2 (after mindfulness training).

Descriptive					
Hem	**Sites**	**Group**	**Mean**	**SD**	**N**
Left	**Frontal**	ND	1.24	0.17	7
		D+	1.19	0.20	6
		D-	0.70	0.21	5
	Temporal	ND	0.98	0.24	7
		D+	0.99	0.21	6
		D-	0.86	0.54	5
	Frontocentral	ND	0.99	0.15	7
		D+	1.00	0.18	6
		D-	0.68	0.14	5
	Centropareital	ND	0.72	0.14	7
		D+	0.88	0.19	6
		D-	0.41	0.09	5
	Occipitoparietal	ND	0.97	0.13	7
		D+	0.76	0.10	6
		D-	0.56	0.09	5
Right	**Frontal**	ND	1.44	0.09	7
		D+	1.03	0.22	6
		D-	0.64	0.13	5
	Temporal	ND	1.15	0.18	7
		D+	1.16	0.24	6
		D-	0.72	0.13	5
	Frontocentral	ND	0.95	0.12	7
		D+	0.95	0.15	6
		D-	0.67	0.14	5
	Centropareital	ND	1.12	0.18	7
		D+	1.11	0.34	6
		D-	0.86	0.22	5
	Occipitoparietal	ND	1.10	0.27	7
		D+	0.54	0.22	6
		D-	0.23	0.11	5

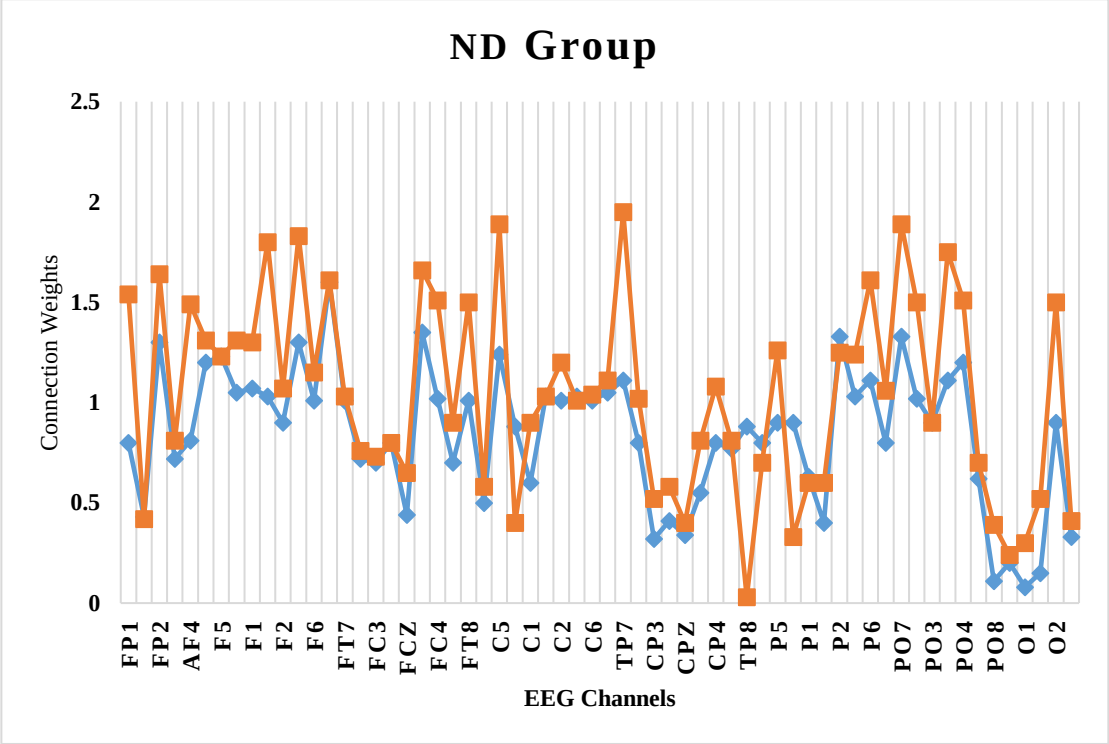

C- 7. The average of the connection weights created by each of the input neurons (representing an EEG channel) in the SNN models trained on EEG data related to non-depressed participants (ND) showing changes before and after the training. Blue line represents the connectivity values in the SNN model before the training (T1) and orange line represents the ones after the training (T2).

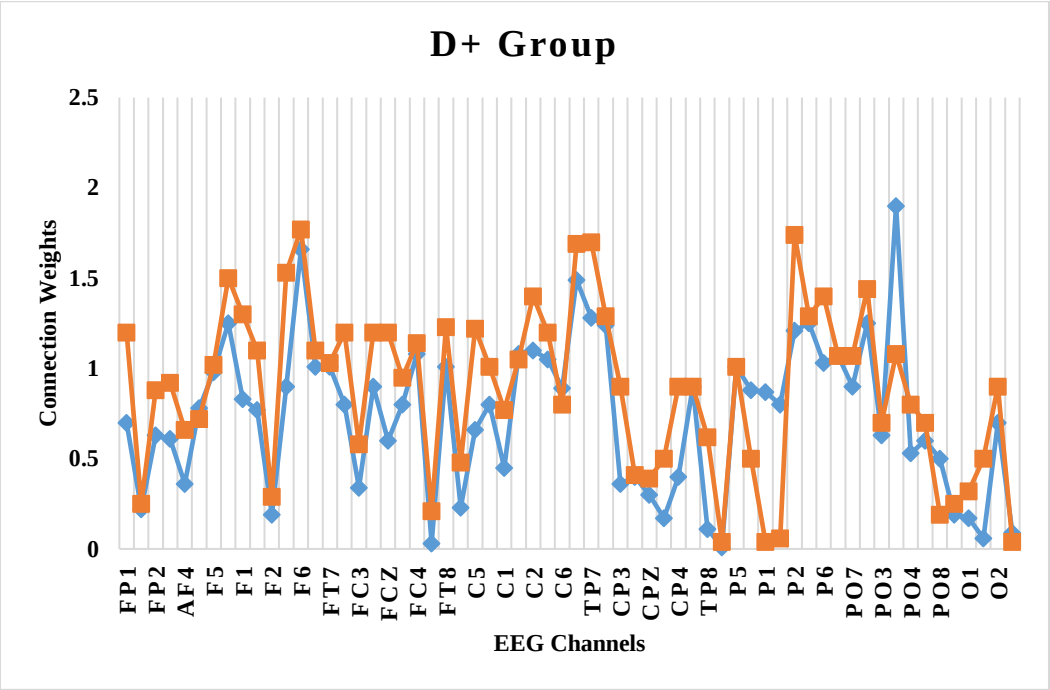

C- 8. The average of the connection weights created by each of the input neurons (representing an EEG channel) in the SNN models trained on EEG data related to depressed group who responded to the training (D^+) showing changes before and after the training. Blue line represents the connectivity values in the SNN model before the training (T1) and orange line represents the ones after training (T2).

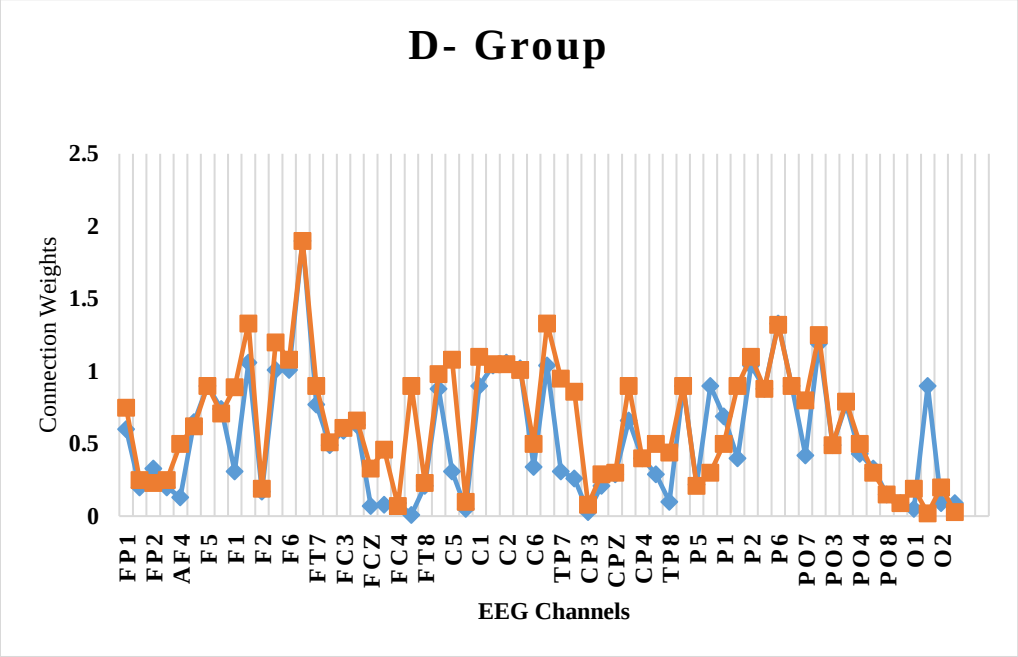

C- 9. The average of the connection weights created by each of the input neurons (representing an EEG channel) in the SNN models trained on EEG data related to depressed group who did not respond to the training (D^-) showing changes before and after the training. Blue line represents the connectivity values in the SNN model before the training and orange line represents the ones after training.